공학박사학위논문

고체산화물 연료전지-엔진 하이브리드 시스템 실험 및 열전달을 고려한 시뮬레이션 모델을 통한 시스템 설계 및 성능 개선에 대한 연구

Improvement of System Design and Performance of a SOFC-Engine Hybrid System with Integrated System Experiment and Simulation Model Considering Heat Transfer

2022 년 8 월

서울대학교 대학원

기계항공공학부

김 용 태

고체산화물 연료전지-엔진 하이브리드 시스템 실험 및 열전달을 고려한 시뮬레이션 모델을 통한 시스템 설계 및 성능 개선에 대한 연구

Improvement of System Design and Performance of a SOFC-Engine Hybrid System with Integrated System Experiment and Simulation Model Considering Heat Transfer

지도교수 송 한 호

이 논문을 공학박사 학위논문으로 제출함

2022 년 4 월

서울대학교 대학원
기계항공공학부
김 용 태

김용태의 공학박사 학위논문을 인준함

2022 년 6 월

위 원 장 : _____ (인)

부위원장 : _____ (인)

위 원 : _____ (인)

위 원 : _____ (인)

위 원 : _____ (인)

Abstract

Improvement of System Design and Performance of a SOFC-Engine Hybrid System with Integrated System Experiment and Simulation Model Considering Heat Transfer

Yongtae Kim

Department of Mechanical Engineering

The Graduate School

Seoul National University

The objective of the solid oxide fuel cell (SOFC)-engine hybrid system is to obtain additional power and improve system efficiency by combustion in the engine using the anode-off gas of SOFC. The research on the SOFC-Engine hybrid system has been conducted with proposing the system configuration, confirming the performance and operating range at various operating points, and demonstrating actual proof of operation, similar to the research methodology of the SOFC-Gas turbine hybrid system. In this process, prior studies were conducted by changing the configuration and the combustion method of the engine, expanding the

operating range of the system, and suggesting ways to improve performance.

The study of the SOFC-Engine hybrid system was started with the SOFC-HCCI (Homogeneous charge compression ignition) engine hybrid system at the beginning of the study, and the study was conducted in the order of simulation analysis, experimental analysis, and demonstration through hybrid system integration operation. However, as a result, it was difficult to control engine combustion in response to the changing operating point of the HCCI engine, and at the same time, it was confirmed through the demonstration operation that the system thermal self-sustainable operation was difficult. Therefore, the engine combustion method was changed from HCCI to spark-assisted auto-ignition (SAI) method to secure the ease of combustion control of the engine and to increase the thermal utilization of the system. Previous studies were conducted on the operability and performance of points.

In this study, using SOFC-SAI engine hybrid system, the performance and operation characteristics from the start-up to the design point operation were analyzed and a demonstration experiment was conducted to establish the start-up operation strategy. In addition, the limitation of the system (Impossibility of thermal self-sustainable operation) was analyzed and then a new system configuration diagram was suggested. Demonstration experiment capable of thermal self-sustainable operation was performed, and simulation model development and analysis were conducted with the new system configuration. Finally, through the simulation study, we aimed to analyze the heat loss of the system and to suggest and analyze the method to improve the heat loss and performance of the system.

As the first stage of the study, an experimental study through the integrated

operation of the SOFC-SAI engine hybrid system was performed. This is the first SOFC-Engine hybrid system demonstration operation using the spark-assisted auto-ignition method, and the experiment was carried out for the entire process from the start-up operation to the design point operation considering the actual commercialization operation. Since the engine is in the middle of the hybrid system, it was necessary to confirm the performance, operation characteristics, and controllability of the engine in the start-up operation. As a result, the system performed stable operation of both SOFC and engine for about 35 hours of operation time. In the whole process of start-up operation, the engine RPM was able to respond in real time considering the volume flow rate and temperature flowing into the engine for various operating points of the SOFC so that the engine intake pressure could be maintained at atmospheric pressure (1 bar). In addition, it was possible to appropriately control the spark timing to generate the maximum brake torque of the engine for various operating points. Also, it is necessary to burn the undiluted reformed gas in the engine. Stable combustion (COV < 5%) in the engine and the external reforming rate of 12% could be achieved through the two-step reforming process using the exhaust heat of the engine and the thermal energy of the anode-off gas was confirmed in this process. In operation at the design point, SOFC power was 5.2 kW, and the engine power was 530 W (Indicated net power), which was consistent with the results of the engine standalone test in the previous study. It was confirmed that the COV value indicating engine combustion stability increased by 12% as the dilution gas (H_2O, CO_2) increased. As a result, it was confirmed that the thermal efficiency of the system could be improved by 5%p through the engine. Although this performance could be secured, as a result of the experiment, a lot of heat loss occurred in the system, and in order to compensate for this and operate stably, electric heaters were added to the upper and lower parts

of the stack and electric heaters to the cathode air line. As a result, even at the design point, the system operation depended on the electric heater and the electric furnace to provide more than 3.4kW of heat, and about 600W of heat loss occurred even in the anode off-gas. In conclusion, the system thermal self-sustainable operation was impossible with the experimental setup of the configuration diagram.

As the second stage of the study, a modified system configuration diagram was proposed to enable thermal self-sustainable operation to solve the limitation of the previous configuration diagram. The configuration diagram of the existing SOFC standalone system was maintained, and a branch valve was additionally applied at the rear end of the anode so that the anode off-gas was branched and supplied to the engine and burner. Using the newly devised configuration diagram, a hybrid system was built, and a demonstration operation was performed to develop a system capable of thermal self-sustainable operation. However, it was unable to produce as much additional power as the stack added for system operation stability (Two stacks added compared to the existing system), and the operation was performed with the limited branching ratio under 23%. Accordingly, to predict the maximum branching ratio to the engine and to analyze the system improvement method, a simulation model that can simulate the hybrid system based on various operating points of the demonstration operation was developed. Previous studies developed a simulation model assuming that all pipe and equipment were adiabatic. In this study, a simulation model including a heat transfer model was developed to calculate heat loss in SOFC and pipe. In addition, the reliability and scalability of the model were secured by validating the developed simulation model to the four operating points of the demonstration operation. The convective heat transfer and radiative heat transfer between the system hot box and the outside can be considered through the heat transfer model

applied to the simulation model. Inside the hot box, the concept of "cavity gas" was introduced so that the cavity gas and the pipe and SOFC inside the hot box perform convective heat transfer. In addition, the number of Re, Pr, and Nu was calculated in consideration of the flow rates of fuel and air input to the system and thermodynamic properties in all pipes. Through this, convective heat transfer coefficient of the flow inside the pipe can change in response to changing operating conditions, so that the actual heat transfer physics can be simulated.

Finally, heat loss analysis was performed through the developed simulation model, and the system performance improvement was analyzed by suggesting a method to reduce heat loss and improve system performance. It was confirmed that the maximum engine branching ratio of 34% was calculated through several assumptions and constraints. And the system efficiency can be increased by 2.32%p at the maximum engine branching rate. To reduce heat loss and improve system performance, a method of increasing the power level in the current system and a system scale-up method were proposed. It was confirmed that the maximum engine branching ratio was 50% at maximum power level of present system and 60% at maximum scale-up system. The system efficiency can be increased by 3.22%p and 3.46%p, respectively. Therefore, it was possible to study system scalability through the model developed in this study, and it is expected to contribute to commercialization and efficiency improvement by suggesting the improvement direction of the SOFC-Engine hybrid system.

Keywords:

Solid oxide fuel cell, Spark ignition engine, SOFC-Engine hybrid system integrated operation, Engine branching ratio, System level heat transfer model and analysis, System scale-up

Student Number: 2015-20719

Table of Contents

List of Figures

Number *Page*

List of Tables

Number *Page*

Chapter 1. Introduction

1.1. Research background

Recently, as environmental destruction due to global warming has accelerated, environmental regulations around the world are being strengthened. Particularly, the regulations to reduce carbon dioxide emissions have been strengthened, which have a high impact on global warming [1-2]. According to the EIA, in 2021 the transportation, industrial and electric power sector is the main cause of carbon dioxide emissions as shown in Figure 1.1 so that research and development are needed to develop new energy sources or improve efficiency of energy conversion equipment [3]. Also, considering that many internal combustion engine vehicles are being replaced by electric vehicles in transportation sectors, minimizing carbon dioxide emissions in electric power sectors is crucial to prevent more environmental destruction. As a result, new and renewable energy is being spotlighted by replacing fossil fuels previously used in the energy industry [3].

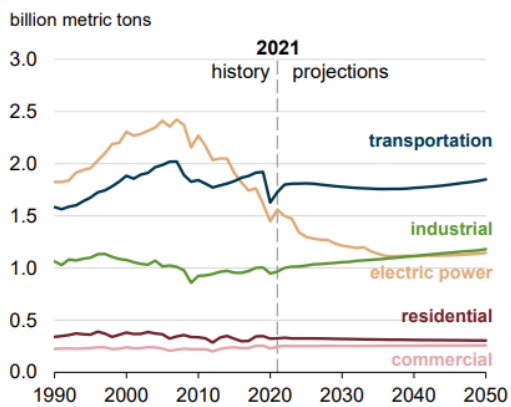

Figure 1.1. Energy related CO_2 emissions by sector [3]

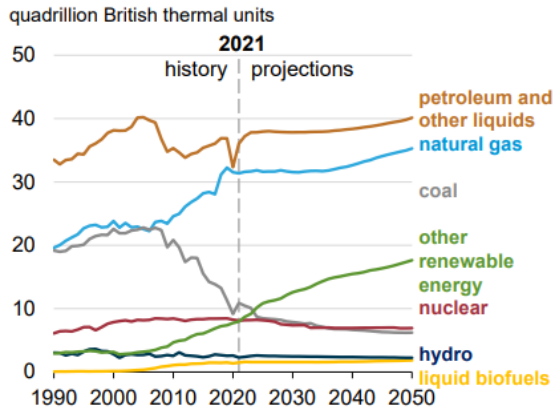

Figure 1.2. Energy consumption by fuel [3]

Among new and renewable energy, solid oxide fuel cell (SOFC) is in the spotlight in the energy industry to reduce the energy industry's carbon dioxide emissions. A fuel cell is a technology that converts chemical energy of fuel into electrical energy through a direct chemical reaction without burning it so has the advantage at its efficiency and emission characteristics [4]. Among several types of fuel cell, SOFC has the advantage that does not require an expensive catalyst unlike other fuel cells, and it can be used by reforming various hydrocarbons by operating at a high temperature of 700~800 °C, in particular [5]. In addition, in that on-site reforming can be performed using existing natural gas infrastructure facilities, the initial cost can be greatly reduced, which has great marketability. Furthermore, on-site natural gas reforming has the effect of reducing carbon dioxide emissions throughout the entire process because the amount of carbon dioxide emissions per unit of hydrogen production is also small [6].

SOFC cannot convert 100% of the energy of the input fuel due to the problem of performance and durability degradation result from fuel depletion at the anode outlet in case of using 100% of fuel. Hence, it uses only about 70~75% of fuel and emits the remaining 25~30% of thermochemical energy [7]. A typical SOFC standalone system burns these anode off-gas through a catalytic combustor at the rear end of the anode to provide heat necessary for the system operation and to recover waste heat [7]. The SOFC hybrid system has been researched to increase efficiency by using this unused fuel to obtain additional power and heat by replacing the catalytic combustor with other energy conversion device.

Particularly, many researchers have been researching a hybrid system combining SOFC and gas turbine [8-10], and in fact, Siemens of the US and Mitsubishi Heavy Industries of Japan have also conducted research to demonstrate this [8-9]. Most SOFC-GT hybrid systems have been studied by being applied to large-scale power generation systems [10], but there are relatively few studies on SOFC-Engine hybrid systems with power generation capacity suitability at smaller scales. Although experiments and modeling studies on SOFC-Engine hybrid systems are increasing recently, there are very few studies that demonstrate the integration of the two systems. Therefore, study of SOFC-Engine hybrid system starts from this background to develop high efficiency and less adverse effects on the environment of SOFC-Engine hybrid system,

1.2. Concept of SOFC-Engine hybrid system

As mentioned above, the SOFC-Engine hybrid system is a concept to obtain additional power output by burning 25-30% of anode off-gas through the internal combustion engine by replacing catalytic combustor. We selected the internal combustion engine as the HCCI (Homogeneous charge compression ignition) engine and proposed the SOFC-Engine concept for the first time by organizing a consortium consists of universities, research institutes and a corporation and registered the concept as a patent in the US and Korea [11].

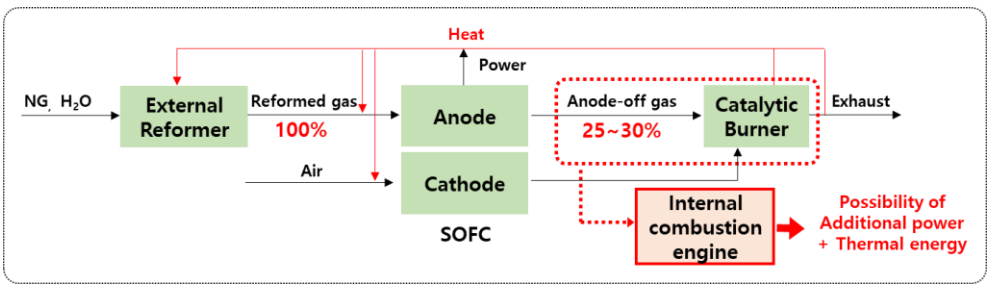

Figure 1.3. Concept of SOFC-Engine hybrid system

Figure 1.3 shows the concept of the SOFC-Engine hybrid system. As shown in the figure, the internal combustion engine has replaced the catalytic burner. The internal combustion engine, which has replaced the catalytic burner, must produce additional power output and, at the same time, use the exhaust gas to provide the amount of heat required for the system operation such as steam production, external reforming and other heat exchanging processes. If insufficient heat is provided by engine, the SOFC-Engine hybrid system cannot be meaningful. Therefore, the SOFC-Engine hybrid system requires research on system performance, operability, and operation region, as well as system heat distribution.

1.3. Previous studies of SOFC-Engine hybrid system

For a long time, SOFC hybrid system has been mainly studied as SOFC-gas turbine (GT) hybrid system. For the SOFC-GT hybrid system, several studies have been conducted on the system configuration, operation characteristics, and control method using various methods such as simulation, experiment, and demonstration [8-10].

Accordingly, like the SOFC-GT hybrid system study, many studies have been conducted on the SOFC-Engine hybrid system, such as the system configuration diagram, operating characteristics, and modeling, through simulation and experimental verification methods. As an early study on the SOFC-Engine hybrid system, studies comparing the SOFC standalone system, the SOFC-GT hybrid system, and the SOFC-HCCI engine hybrid system were performed from a thermo-economic point of view [12-15]. Through the study, it was found that the SOFC-HCCI engine hybrid system is superior to the SOFC standalone system and the SOFC-GT hybrid system in terms of system power efficiency and economic feasibility through system output analysis and levelized cost of electricity (LCOE) analysis.

As for the SOFC-Engine hybrid system, the HCCI engine was adopted as a combustion method, and many studies on the SOFC-HCCI engine hybrid system were conducted first. Kang et al. developed SOFC-HCCI engine hybrid system dynamic modeling and conducted a study on dynamic characteristics and control strategy establishment according to load transition [16]. In addition, as an experimental study on the SOFC-HCCI engine hybrid system, a study on the HCCI engine experiment using emulated anode off-gas was also conducted. Choi et al. performed a study showing the performance of the HCCI engine for various

air/fuel ratios and various SOFC fuel utilizations [7,17]. This is the first study to secure combustion stability and power output by combusting emulated SOFC anode off-gas using an HCCI engine. Besides, a study was conducted to show the operation performance for various operating points of the design point by combining the 1-D SOFC simulation model and the HCCI engine test results [18]. Moreover, through simulation studies, Choi. analyzed that the heat loss of the HCCI engine was calculated to be excessively large. The Woschni heat transfer correlation, which is generally used for calculating the heat loss of the engine [19], was modified to be adjusted to the SOFC anode off-gas composition, and composition-considered Woschni heat transfer correlation was developed [20]. Furthermore, a study was conducted to demonstrate the integrated operation of the SOFC-HCCI engine hybrid system. Kim et al. established the SOFC-HCCI engine hybrid system and conducted a study to analyze the operation characteristics and performance that occurred during long-term operation of about 200 hours [21]. This is the first study to establish and demonstrate SOFC-HCCI Engine. Also, using the same system experiment results, Koo et al. performed energy and exergy analysis, and found that exergy destruction occurs a lot through heat loss [22]. As a result, it was confirmed that the large heat loss in the HCCI engine caused the greatest exergy destruction.

A study was also conducted using other engine combustion methods different with the SOFC-HCCI engine hybrid system. In general, HCCI engine has advantages of lean burn, high efficiency, and low NOx emission characteristics, so it was adopted in the SOFC-Engine hybrid system and research has been preceded. However, the HCCI engine has disadvantages in that it is difficult to control combustion timing because there is no direct ignition control input and is sensitive to the intake temperature of the engine because it depends on the auto-ignition of

the fuel [23,27]. As a method to improve this, a study was conducted that adopted spark ignition as the combustion method. Kim et al. performed spark ignition combustion under various engine intake temperature conditions using emulated anode off-gas and studied operation performance and operable range for various operating conditions [24-25]. And the difference between the HCCI combustion method and the general spark ignition was confirmed, and the spark assisted HCCI combustion method was confirmed.

Another study was also conducted to analyze the heat loss in each BOP components and pipe by performing thermal modeling for the SOFC standalone system [26]. The heat loss was calculated by applying the resistance model as a heat transfer model for a total of three system diagrams. However, this study was not validated for system experiments.

Although studies on various SOFC-Engine hybrid systems have been conducted, there has been no study on the problem of system heat distribution caused by the engine replacing the catalytic burner. Consequently, it is necessary to analyze the heat distribution of the SOFC-Engine hybrid system.

1.4. Research motivation and objectives

In the initial study of the SOFC hybrid system, only the study of the SOFC-GT hybrid system was mainly performed. However, as interest in the SOFC-Engine hybrid system has grown in recent years, many related studies have been conducted. Most of the studies were conducted in experimental and simulation methods, and various operating conditions were explored.

However, in case of simulation studies, there were few studies on heat loss in system pipe and components, and most calculations were conducted using adiabatic assumptions. In Kattke K. et al.'s study, heat loss was calculated through thermal modeling, but there is a limit to examine heat loss in an actual system because validation of the experiment was not performed [26].

In addition, in experimental studies, experiment of actual proof of concept have been performed on the SOFC-HCCI engine hybrid system, but it is difficult to analyze the heat loss because electric heaters were used for system operation stability, and it is difficult to understand the possibility of thermal self-sustainable operation of the system.

In the case of the SOFC-SAI engine hybrid system, a spark-assisted auto-ignition (SAI) engine alone experiment using emulated anode off-gas was performed, and a simulation study was also performed. However, an integrated system operation combining the SOFC and SAI engine was not performed.

Starting from this motivation, in this paper, the SOFC-SAI engine hybrid system demonstration experiment operation and simulation model development, considering heat transfer between system component and environment, was performed. Although the integrated operation in the design point operation of the

SOFC-Engine hybrid system has been performed before, the system integration operation including the start-up operation has never been experimented. In the start-up operation, the fuel cell is operated at a lower fuel flow rate, lower fuel utilization rate, and lower external reforming rate compared to design point operation, and accordingly, the temperature, composition, and flow rate of fuel flowing into the engine are significantly different. Therefore, control variables and performance such as the optimum spark ignition timing, engine rotation speed, combustion stability, and power output of the engine could be significantly different, and it is necessary to analyze the operation characteristics and control strategy for optimal operation. Through this study, the entire operation of the SOFC-SAI engine hybrid system including the start-up operation was performed and analyzed. In addition, as a result, since the SOFC-SAI engine hybrid system was unable to operate thermally self-sustainable, we proposed a new SOFC-Engine hybrid system with a new configuration that can improve the system thermal balance and conduct experiments. Through the experiments and simulation model development, off-design point was explored, and system design improvement method was suggested to improve system performance, and to analyze it in terms of heat and performance. Based on this, this dissertation has two objectives, which are summarized as follows.

The first objective of this dissertation is to verify and analyze the operation characteristics, performances, and possibility of thermal self-sustainable operation of each process from start-up operation to design point operation of the SOFC-SAI engine hybrid system.

The second objective of this dissertation is to secure the experimental results of the new hybrid system that operates by thermally self-sustainable, and to develop a simulation model in which the heat loss is considered that is validated to the experimental results. Therefore, this dissertation aims to conduct heat loss analysis through the developed simulation model and propose a system design and operating point to improve system performance and predict its performance.

1.5. Organization of the dissertation

This dissertation consists of a total of 5 chapters and the main contents of the dissertation is dealt in chapter 2 to 4.

Chapter 2 explains the history of the SOFC-Engine hybrid system configuration changes and the two configuration diagrams covered in this dissertation. Since two diagrams are introduced and studied in this dissertation, in order not to cause confusion about the configuration diagrams covered in each chapter, the characteristics and limitations of the SOFC-SAI engine hybrid system configurations are briefly explained, and the improved configuration diagram is presented. The difference between the two diagrams covered in this dissertation is also explained.

Chapter 3 shows the results of the system integration operation of the SOFC-SAI engine hybrid system. From start-up operation to design point, the characteristics, control parameters, and performance of system operation are examined. By calculating the amount of additional heat energy provided to the system and the amount of heat loss at the location where the main heat loss occurs, the feasibility of thermal self-sustainable operation of the actual SOFC-SAI engine hybrid system is analyzed.

Chapter 4 shows newly changed system configuration: SOFC standalone system with SI engine hybrid system. According to the analysis in chapter 3, a new system for thermal self-sustainable operation should be suggested, and a new system configuration based on SOFC standalone system configuration is suggested. First, chapter 4 briefly shows the results of the system integration operation experiment for the newly changed system configuration diagram. Then the SOFC

system simulation model development method, which consider the heat loss of pipe and some components, and the validation results, which is validated to the experimental data are shown. With this simulation model, heat loss is analyzed for several proposals of designs that can improve system heat loss and performance. In addition, the system performance and heat loss of the system is predicted by applying the proposed design, such as varying of pipe diameter or length, system power level up, and scale up of system, into the developed simulation model.

Finally, in Chapter 5, a summary and conclusions of the study are discussed.

Chapter 2. History of SOFC-Engine hybrid system development: configuration change

2.1. History and description of configuration change: previous studies of SOFC-Engine hybrid system

SOFC-Engine hybrid system has been studied for several years. As mentioned earlier, the detailed SOFC-HCCI engine hybrid system configuration diagram was first proposed in our group. Starting from this configuration concept, Lee et al. studied and proposed the possibility of SOFC-HCCI engine hybrid system from the thermo-economic point of view [13-15]. Experiments and simulation studies using the first SOFC-HCCI engine hybrid system configuration diagram were conducted for 3 years after forming a consortium in 2014. Since there was no empirical study on the SOFC-Engine hybrid system, a lot of time was needed to study the limiting factors of the system. The limitations of the system were analyzed through various experiments and simulation studies, and accordingly, the subsequent studies were conducted by suggesting new diagrams that improved the limitations of the previous system. Through these studies, a total of 4 diagrams including two diagrams used in this dissertation were developed. The configuration to be introduced in the chapter 2.1 is the three configuration diagrams studied before. The SOFC-SAI engine hybrid system, which is the third configuration diagram, was introduced in chapter 2.1 because it was studied in the previous study. However, since the integrated operation of the SOFC-SAI engine hybrid system has never been performed before, this configuration is also dealt with in chapter3 to show the results of the integrated operation.

2.1.1. SOFC-HCCI engine hybrid system configuration (with one external reformer)

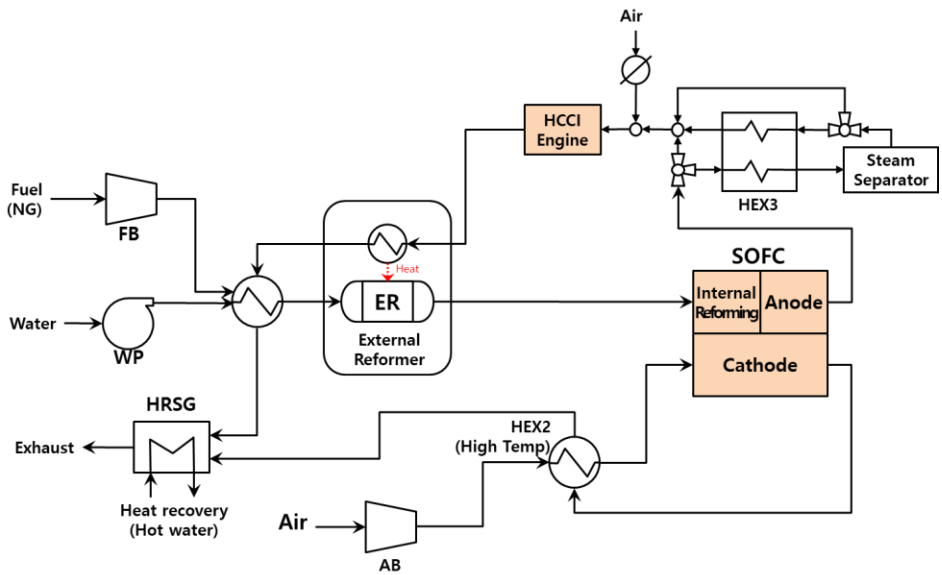

Figure 2.1. SOFC-HCCI engine hybrid system configuration (with one external reformer) [7]

The first configuration diagram is shown in Figure 2.1. This configuration is dealt with in SOFC-HCCI engine hybrid system study that adopts HCCI engine as the bottoming cycle. The first SOFC-HCCI engine hybrid system consist of three main components: SOFC, HCCI engine, and one external reformer.

First, the fuel, usually selected as methane or natural gas, is mixed with steam, and reformed in the external reformer using steam-methane reforming reaction. The heat required for external reforming is provided through the heat of exhaust gas of HCCI engine. Partially reformed gas passed through the external reformer is then entrained to the SOFC anode to generate power. The remainder of reforming

process is completed by internal reforming in the SOFC anode using the heat generated by electrochemical reactions at the anode and the electric power is also generated. The SOFC anode off-gas is discharged from the SOFC anode, and the discharged anode off-gas is used as fuel for the HCCI engine combustion to obtain additional power. On the other hand, the air is supplied to the SOFC cathode passing through heat exchanger to increase the temperature of air until proper temperature (700 ~ 750 °C) level for operating SOFC.

The anode-off gas consists of H_2O, CO_2, CO, and H_2, of which H_2 and CO are used as fuel for the engine, and H_2O and CO_2 act as diluent gases. The anode-off gas is generally disadvantageous for combustion because the ratio of diluent gas is almost 4 times higher than that of fuel, and it is a highly diluted gas [7]. In general, when a fuel with a high ratio of diluent gas is used in the engine, the flame propagation speed is slowed, so it may be difficult to combust with the spark ignition method [19]. Due to this characteristic, research was conducted by selecting the HCCI combustion strategy, which is generally capable of proper combusting of highly diluted fuel.

Simulation studies and engine-alone experimental studies were conducted using this configuration diagram. SOFC and engine performances were explored such as power output, combustion efficiency, CO and NOx emissions, engine intake and exhaust temperatures, external reforming rate. These performances were confirmed under various operating conditions such as fuel utilization rate of SOFC, equivalence ratio of engine, fueling rate of system and combustion timing. Design point and off-design point of system operation was also confirmed. In addition, another essential parameter for thermal self-sustainable system operation was engine exhaust temperature because the engine exhaust enthalpy was used for

providing heat to external reformer. Hence, various improvement methods, such as delaying engine combustion timing and thermal barrier coating on engine cylinder, were proposed and applied to secure more engine exhaust energy. Nevertheless, the engine exhaust temperature required to secure a sufficient external reforming rate was not secured, so the dependence on SOFC internal reforming increased. This could increase the heat loss of the SOFC and decrease the anode off-gas temperature. This also could lower the engine intake temperature so that adequate HCCI combustion was difficult and eventually became a factor to reduce the durability and thermal self-sustainability of system operation.

The first SOFC-HCCI engine hybrid system demonstration operation was performed by combining the SOFC and HCCI engine with the configuration of Figure 2.1. External reformer developed by Chungnam National University, 5kW-class SOFC of MiCo corporation, BOPs set up by Korea Institute of Machinery and Materials (KIMM), and HCCI engine set up by Seoul National University were installed and combined. 200-hour continuous operation was conducted to prove feasibility of SOFC-HCCI engine hybrid system concept with the experimental setup. The heat loss in the pipe from the engine exhaust valve to the external reformer and the heat loss in the anode off-gas were large, making it difficult to operate thermally self-sustainable without additional heat supply. Therefore, furnace at the upper and lower side of SOFC, 2 electric heaters at anode inlet and engine exhaust line, and additional burner for providing heat to entrained cathode air were added for stable operation. As a result, the amount of heat provided through the furnace, electric heater, and burner was very large, almost 5.88kW [7], and as a result, the thermal self-sustainable operation of the system was impossible without additional heat sources. This was confirmed by the study of Choi. [7] and Kim et al. [21].

2.1.2. SOFC-HCCI engine hybrid system configuration (with two external reformer)

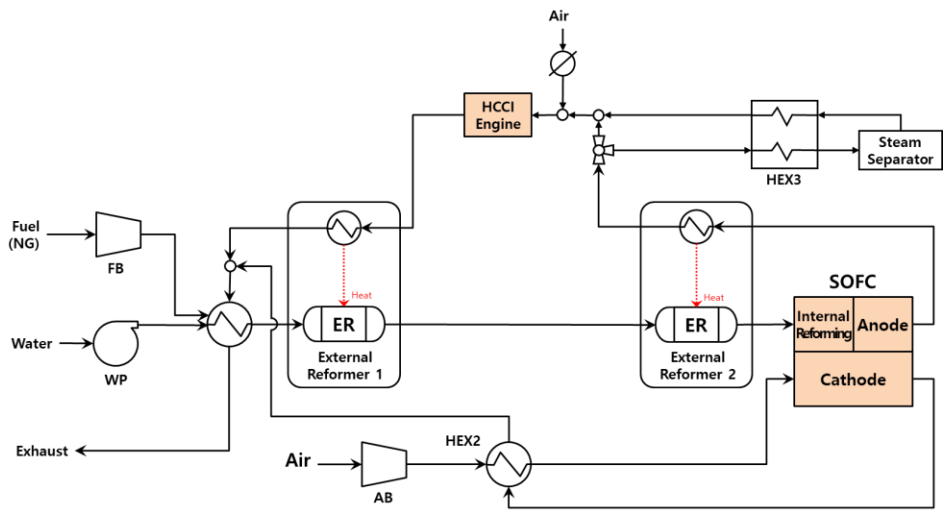

Figure 2.2. SOFC-HCCI engine hybrid system configuration (with two external reformer) [17]

The second configuration diagram is shown in Figure 2.2. In the second configuration diagram, an external reformer was added to improve the limitations of the first configuration. The main limitation of the first SOFC-HCCI engine hybrid system was lack of heat at engine exhaust. This limitation cause lowering external reforming rate and temperature of anode inlet gas so that heat distribution was not optimized. Therefore, newly modified configuration was suggested to solve the limitation.

The maximum temperature of gases in the SOFC system are anode off-gas and cathode off-gas. Since the cathode off-gas provides the amount of heat required to heat the air supplied to the cathode, heat of the cathode off-gas could not be used for other heat exchanging. Therefore, the maximum available system hot gas is

anode off-gas, and it was attempted to additionally provide heat to the external reformer using this. In previous studies, it was difficult to secure the exhaust heat energy of the HCCI engine and the heat loss in the pipe was large, so it was difficult to secure sufficient external reforming rate and anode inlet gas temperature with only one external reformer. As the external reformer was added, it was confirmed that the external reforming rate increased from the study of Choi. [7].

However, since the HCCI engine has combustion characteristics in which pre-mixed fuel and air are auto-ignited by engine compression, so combustion is sensitive to engine intake temperature conditions. Accordingly, there is a disadvantage in that it is difficult to control combustion when the temperature of the engine intake air is not sufficiently secured or the change in the intake air temperature is large. In the demonstration operation using the previous configuration diagram, when a sufficient intake air temperature was secured, the operating point of the system did not change significantly, so the combustion of the HCCI engine occurred stably. On the other hand, the combustion of the HCCI engine could become unstable due to changes in engine intake air temperature. In the case of the improved configuration, although it was not verified through demonstration operation, the intake air temperature of the HCCI engine had to be lowered because the high-temperature heat of the anode off-gas was used for external reforming (External Reformer 2). As a result, engine intake temperature margin was reduced, which causes difficulties in HCCI engine combustion control. In addition, the heat loss in the engine exhaust gas pipe and the anode off-gas pipe was still high, so an additional improvement method was needed.

2.1.3. SOFC-SAI engine hybrid system configuration

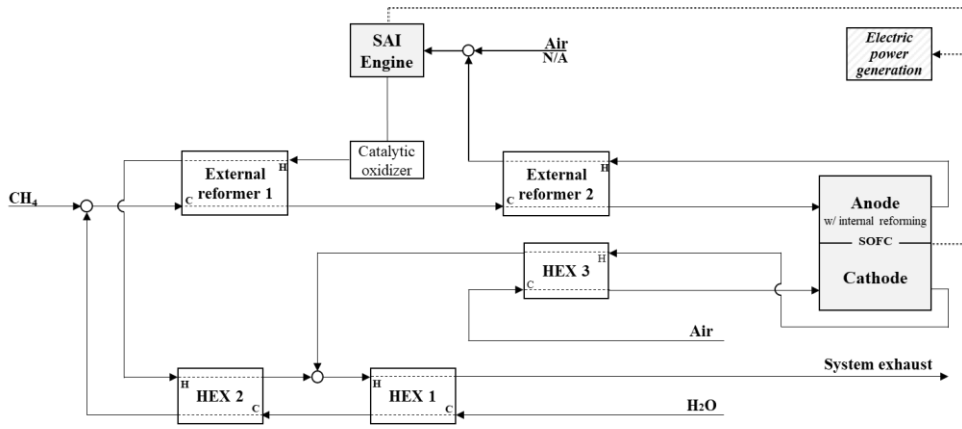

Figure 2.3. SOFC-SAI engine hybrid system configuration [25]

Third, the SOFC-SAI engine hybrid system was proposed and studied to improve the limitations of the SOFC-HCCI engine hybrid system. SOFC-SAI engine hybrid system configuration is shown in Figure 2.3. In the SOFC-HCCI engine hybrid system with two external reformers studied previously, due to the combustion characteristics of the HCCI engine, it was difficult to control engine combustion when the engine intake temperature margin was insufficient. If the engine combustion becomes unstable due to this, the pressure of the SOFC anode becomes unstable due to the pulsation, which may cause problems in the durability of the SOFC. In addition, it cannot provide uniform and sufficient heat to the external reformer 1, which reforms by using the exhaust heat of the engine, thus reducing the stability and durability of the system operation. Therefore, the spark ignition combustion method was suggested as a method that could make stable combustion even at a lower engine intake temperature and ensure combustion stability and power output for various operating conditions.

Since the spark ignition engine uses spark as a combustion trigger, it has the advantage of being able to operate in response to various operation conditions by controlling the spark timing. Unlike the HCCI engine, which uses enough chemical energy of anode off-gas to cause combustion, but cannot control the start of ignition, so that engine combustion may become unstable, a spark can be used to provide a small amount of energy to control the start of ignition. This allows combustion even at low intake temperatures. In the SOFC-HCCI engine hybrid system with two external reformers, the external reforming rate could be increased, but the HCCI combustion could become unstable due to the decrease in engine intake air temperature. Through spark ignition, it was possible to secure the stability of engine combustion in response to the decrease in engine intake air temperature while taking advantage of the high external reforming rate.

Therefore, an engine independent experiment was performed at various operating points in response to the engine intake temperature changing according to various external reforming rates of external reformer 2 and various SOFC operating conditions. The fuel flow rate and steam carbon ratio of SOFC were fixed as target design values, and power output, emissions, combustion stability, energy and exergy analysis were performed on various fuel utilization rate of anode, intake air temperature of engine, equivalence ratio, and spark ignition timing. As a result, it was confirmed that the HCCI engine combustion changed to the spark assisted HCCI combustion while lowering the engine intake temperature, and power output similar to that of the HCCI engine under SOFC-HCCI engine hybrid system could be secured at various operating points. In addition, emissions, combustion stability (COV: 5-7%), and improvement of exergy efficiency were confirmed, and feasibility of SAI operation in engine was confirmed in the end [24]. The SOFC system was studied through simulation, unlike the engine. For the

efficient heat distribution of system, an additional heat exchanger and an external reformer were added to the configuration diagram and this optimized configuration diagram is shown in Figure 2.4.

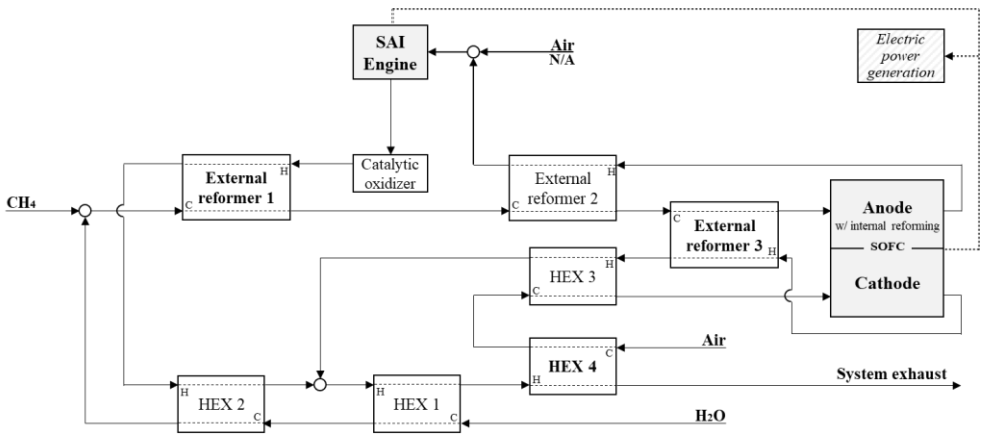

Figure 2.4. Optimized SOFC-SAI engine hybrid system configuration [24]

As a result, the optimized system configuration and operating area capable of thermal self-sustainable operation were confirmed through a simulation study. This can be confirmed by the research of Kim. [24].

However, the SOFC-SAI engine hybrid system was not demonstrated through the system integration operation combining SOFC and engine. It is necessary to confirm whether real-time combustion control is possible and sufficient performance can be secured under various operating conditions. In addition, it is also essential to confirm whether thermal self-sustainable operation of the system can be secured through system integration operation demonstration. In this dissertation, SOFC-SAI engine hybrid system integration operation results and analysis were covered in chapter 3.

2.2. Description of SOFC-Engine hybrid system configuration in the dissertation

This dissertation deals with the configuration diagram of two SOFC-Engine hybrid systems. First, the SOFC-SAI engine hybrid system configuration diagram is dealt with, and secondly, a new configuration, SOFC standalone system with SI engine concept hybrid system configuration, which improved the limitations of the SOFC-SAI engine hybrid system is dealt with.

As mentioned earlier, the SOFC-SAI engine hybrid system study was conducted only through simulation studies and engine-alone experiments. In consideration of the system thermally self-sustainable operation, the system configuration diagram was optimized, and the operating area where the system thermal self-sustainable operation is possible was examined. However, since the system simulation did not consider the heat loss of system components and pipe, there is a possibility that the system may not operate under the same operating conditions in the actual demonstration operation. Therefore, it is necessary to perform system integration operation by combining SOFC and engine, to confirm whether system thermal self-sustainable operation is possible, and whether the operating conditions and performance of the system are consistent with the simulation study results.

In addition, additional considerations are required for actual system integration operation. In the case of SOFC, since they operate at a high temperature of about 700 to 800°C, a start-up operation process is essential to create high-temperature operating conditions. However, as shown in Figure 2.3, the engine is located between SOFC and system BOP due to the characteristics of the system configuration. Therefore, when SOFC starts operation, the engine must also operate.

If the engine does not operate, back pressure is generated in the engine intake, which increases the pressure of the anode and may cause a leak in the SOFC. In order not to operate the engine during SOFC starting operation, anode off-gas can be bypassed by installing an electronic switching valve at the rear end of the hot side of external reformer2 and the front end of the hot side of external reformer1. However, since the gas temperature at the rear end of the hot side of external reformer2 is too high, it is difficult to secure an electronic switching valve that can operate stably under these conditions, and system complexity and cost increase. Therefore, the engine operates necessarily even in the starting operation of the SOFC.

Accordingly, the integrated operation of the SOFC-SAI engine hybrid system needs to be studied from starting operation to design point operation. In the case of start-up operation, the flow rate of fuel supplied to the SOFC and the temperature of the SOFC are different, and since the load operation of the SOFC is not performed, the flow rate, temperature, and composition of the anode off-gas supplied to the engine are all significantly different from the design point operation. It is necessary to confirm whether combustion of the spark ignition engine can stably occur under these starting operating conditions. In addition, it is necessary to confirm whether external reforming can occur sufficiently by securing the engine's power output and exhaust temperature, and as a result, thermally self-sustainable operation of the system is possible. Hence, chapter 3 deals with the study on the integrated operation of the SOFC-SAI engine hybrid system and the configuration diagram that is dealt with in chapter 3 is shown Figure 2.3.

Pre-viewing at the results of Chapter 3, as a result, thermal self-sustainable operation of the integrated operation of the SOFC-SAI engine hybrid system was impossible. The temperature of the SOFC was not sufficiently secured, and accordingly, the composition and flow conditions of the anode off-gas at the design point were different from the results of the engine-alone test. In addition, the electric furnace was operated to secure the temperature of the SOFC during the entire operation process, and the electric heater was operated to pre-heat the cathode air, making it impossible to operate the system by thermally self-sustainable. Therefore, it was necessary to devise a method capable of thermally self-sustainable operation, and an improvement method was proposed using the burner of the SOFC standalone system. The internal configuration of the hot box of the new system is the same as that of the SOFC standalone system. However, it is different with SOFC standalone system by installing a branching valve at the rear end of the SOFC, a part of the anode off-gas is branched to the engine. This configuration is shown in Figure 2.5.

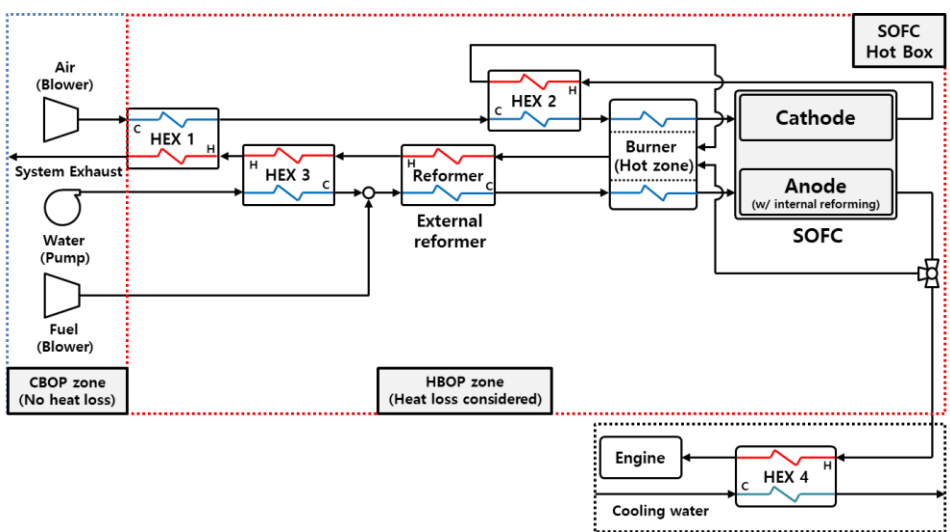

Figure 2.5. New configuration: SOFC standalone system with SI engine concept hybrid system

A part of the branched anode off-gas is supplied to the burner, mixed with the cathode out air, and combusted, and provides heat necessary for the system BOPs, anode inlet gas, and cathode inlet gas. The remaining anode off-gas, not the anode off-gas branched to the burner, is supplied to the engine to get additional power output. In addition, in order to increase the load on the engine, a heat exchanger was placed in front of the engine intake to cool the anode off-gas entrained to the engine and condensed moisture to reduce the dilution component. Therefore, the anode off-gas entrained to the engine was cooled to room temperature(~25°C), and the engine combustion method became a complete spark ignition, not a spark assisted HCCI.

In this dissertation, Chapter 4 shows the experimental results of the final system configuration, and using this, a simulation model was developed, and validation was conducted. A study was performed to suggest and analyze heat loss and design methods to improve system performance through the developed simulation model. As a result, a method of reducing the heat loss of the system and maximizing the branching ratio of anode off-gas branching to the engine was suggested through a simulation model, and a study was conducted to analyze the performance accordingly.

Chapter 3. Operation characteristic and performance of the integrated SOFC-SAI engine hybrid system operation

3.1. System configuration and control parameters

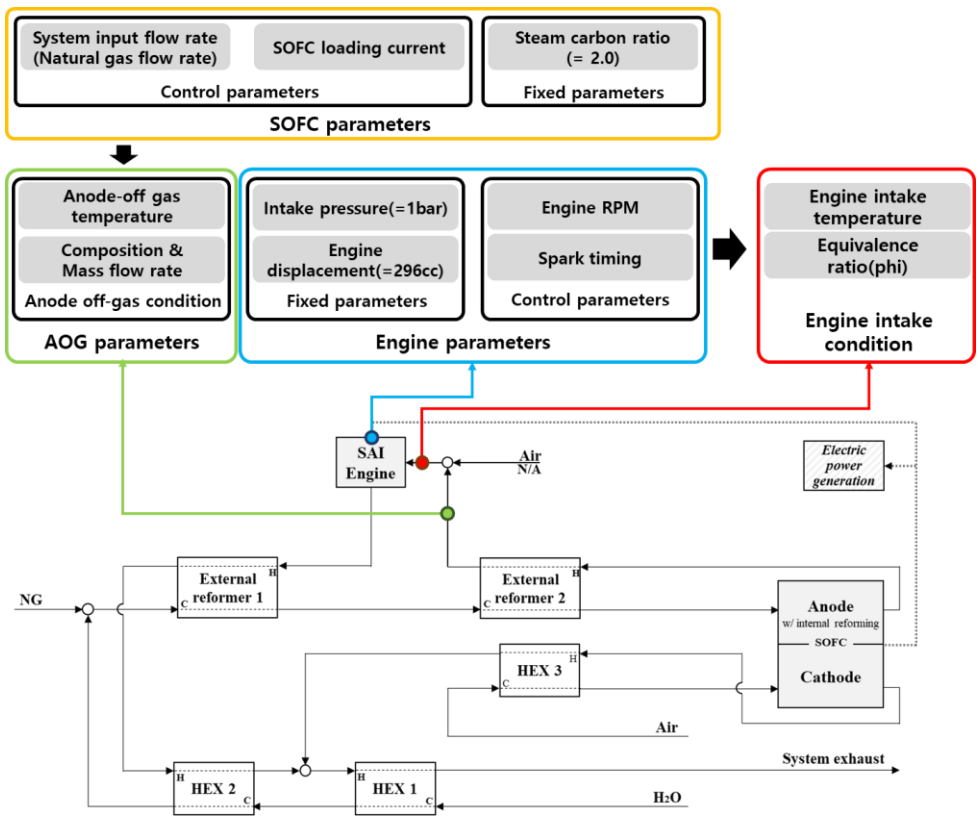

Figure 3.1. SOFC-SAI engine hybrid system engine parameters

Figure 3.1 shows the schematic of SOFC-SAI engine hybrid system and parameters of system that is related to system operation.

SOFC parameters

SOFC-SAI engine hybrid system has several fixed and control parameters each of SOFC and engine. SOFC input variables that affect operating performance and characteristics include fuel type, fuel flow rate, S/C ratio (steam to carbon ratio), air flow rate, and SOFC loading current, and operating conditions including SOFC operating temperature. In this study, only natural gas was used as the fuel type and the S/C ratio was fixed to 2.0, which is the minimum value considering preventing carbon coking of the reformer and SOFC. For the composition of natural gas, KOGAS gas was used, and the composition is shown in Table 3.1 [7, 14, 28]. Since Korea's natural gas import sources are diversified, the composition ratio of natural gas has not just one value. Therefore, a data obtained by averaging the composition of various natural gas import sources was used based on the KOGAS data. However, Cantera and GRI 3.0 mechanism were used as the analysis program and chemical reaction mechanism, but the GRI 3.0 mechanism did not deal with butane, so the composition was newly calculated form KOGAS data and used in this study. This is shown in Table 3.2.

Table 3.1. Mole fraction base natural gas composition of KOGAS

Mole fractions of natural gas composition (%)	
CH_4	91.3
C_2H_6	5.4
C_3H_8	2.1
C_4H_{10}	1.0
N_2	0.2

Table 3.2. Mole fraction of natural gas composition in this study

Mole fractions of natural gas composition (%)	
CH_4	92.22
C_2H_6	5.45
C_3H_8	2.12
N_2	0.2

Fuel flow rate, air flow rate, SOFC loading current and SOFC operating temperature were controlled and SOFC voltage was determined according to the design performance of 2.5kW-class stack of MiCo corporation used in this demonstration experiment. The air flow rate was controlled for only controlling SOFC operating temperature with monitoring cathode inlet air temperature and SOFC operating temperature. The fuel flow rate and SOFC loading current were controlled during the start-up process before reaching the design point and were maintained at almost constant values at the design point. However, as SOFC was operated together with the engine, the fuel flow rate and SOFC loading current were also controlled within a certain range to secure the engine power output and exhaust gas temperature.

AOG parameters

In the case of the engine, the input variables of the engine were determined according to the input variables of the SOFC and operating conditions. Anode off-gas was used as fuel for the engine, and the anode off-gas was determined by the SOFC's operating temperature, loading current, and fuel flow rate. The temperature condition of the anode off-gas was changed as it passes through the external reformer 2. Anode off-gas, the highest temperature gas in the system, was used to provide the heat required for reforming the partially reformed gas supplied to the SOFC anode, and the heat provided is determined according to the design performance of the external reformer 2. It is discharged to the rear end of the hot side of external reformer 2. Accordingly, the mass flow rate, temperature, and composition of the anode off-gas supplied to the engine are determined. The pressure is maintained at atmospheric pressure because the stack of MiCo corporation used in the experiment is a planar type of anode-supported stack.

Engine parameters

Considering the engine-alone parameters, the engine displacement should be matched at various operating points of the system design point by considering the composition and temperature of various anode off-gas supplied to the engine, and the temperature and flow rate of engine intake air. As a result, a commercial engine, Yamaha MZ 300, was selected. A brief specification of the Yamaha MZ 300 is shown in Table 3.3 of chapter 3.3.

The engine intake pressure was maintained at 1 bar to maintain the atmospheric pressure condition of the anode, and for this, a throttle was not applied.

In order to control the operation of the engine, two parameters can be considered: the engine RPM (engine rotation speed) and the spark ignition timing. Since an engine is a device with a constant displacement, it has a constant volume inside the engine cylinder. Therefore, in order to control the volume flow rate of the engine under the fixed engine displacement, it is necessary to control the engine RPM so that more or less volume flow rate is supplied to the engine per unit time. First, the volume flow rate of the anode off-gas was determined because the composition, temperature, and mass flow of the anode off-gas were determined already. Under this condition, if the RPM of the engine was controlled, the volume flow rate of air inhaled to the engine could be controlled. These air and anode off-gas mixed at the front of the engine, and a temperature of the mixture could be determined according to the mixing ratio of mixture because the engine intake air was fixed at room temperature. The engine RPM was controlled continuously to maintain the engine intake pressure at 1 bar.

Accordingly, the engine intake air temperature and the equivalence ratio (phi), which means the fuel-air mixing ratio, was determined. Therefore, the RPM control of the engine could determine the condition of engine intake, and the description is shown in Figure 3.2. Since the temperature, mass flow rate, and composition of the anode off-gas were determined, increasing the engine RPM increased the volume flow rate of air flowing into the engine. As the inhaled room temperature air increases, the temperature of the mixture gas flowing into the engine decreases and the ratio of air components increases, resulting in a decreasing of equivalence ratio (phi). Conversely, if the engine RPM is reduced, the temperature of the mixture gas flowing into the engine increases and the equivalence ratio (phi) increases.

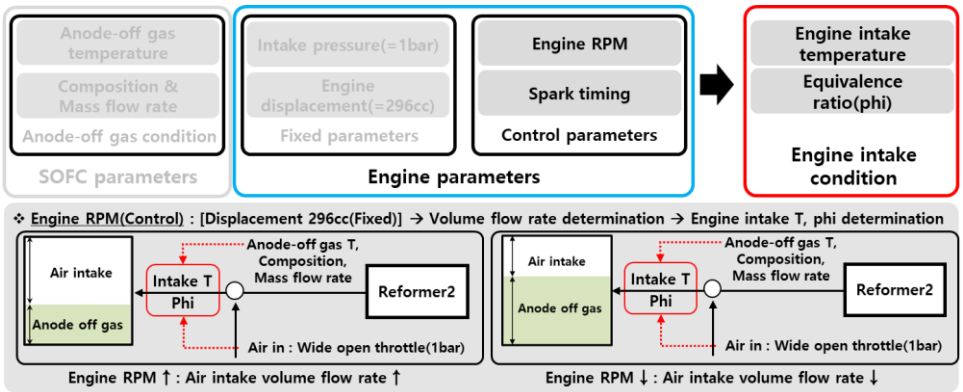

Figure 3.2. Control parameter of engine: Engine RPM control

Second, the spark ignition timing could be controlled. In a spark ignition engine, the spark ignition timing determines the starting timing of combustion of a mixture of fuel and air inhaled into the engine. Considering the engine intake gas condition determined through engine RPM, if the engine intake temperature was low or the fuel utilization rate of SOFC was relatively high, the dilution component of anode off-gas was increased. Under this condition, the spark ignition timing should be advanced because it was an unfavorable condition for engine combustion. The spark ignition timing can be advanced or retarded based on the crank angle degree of the engine. If the anode off-gas with favorable conditions for engine combustion was inhaled, the spark ignition timing could be retarded. In this experimental study, the spark ignition timing was controlled by calculating the anode off-gas condition in real time. If the system is operated at various operating points, automatic control through mapping can also be applied in the future.

3.2. Process description of hybrid system operation from start-up to design point

As mentioned earlier, in the system integration operation, the engine was operated together from the start-up operation of the SOFC. In general, the SOFC-Engine hybrid system is used for power generation, so unlike a fuel-cell vehicle, the range of operation conditions does not change much, so it maintains relatively constant operating conditions. Therefore, since the composition, temperature, flow rate of the anode off-gas flowing into the engine are relatively constant, there are not many cases in which the RPM of the engine is changed in real time. However, when the engine was operated together from the start-up operation of the SOFC, it was more often operated in the transient state compared to the operation at the design point. Hence, it is necessary to control the engine RPM and spark ignition timing in real time because the operation condition change more often compared to design point operation.

Figure 3.3 is a diagram showing the operation process of the SOFC-SAI engine hybrid system in three stages from start-up operation to design point on the diagram: Pre-heat process, heating with engine combustion process and SOFC loading process.

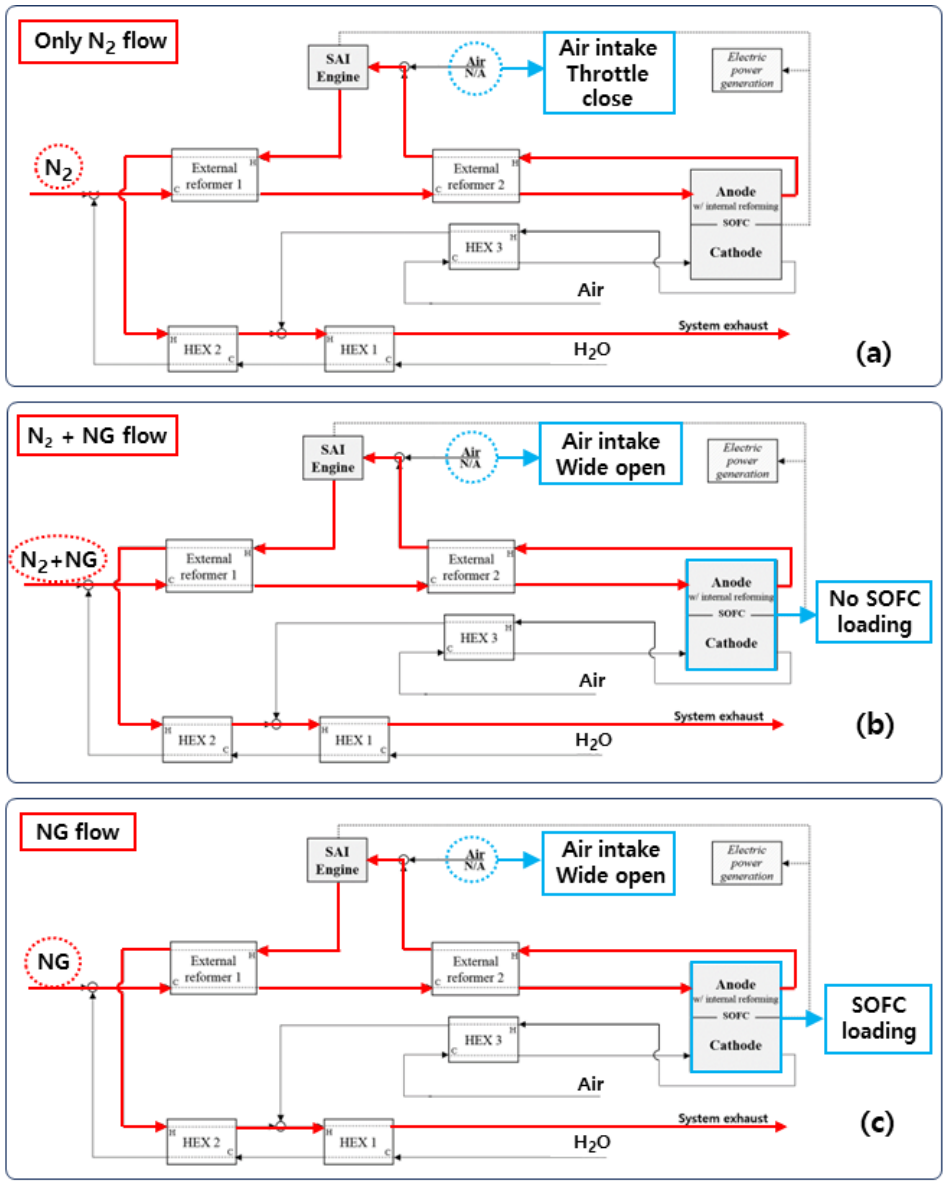

Figure 3.3. Process description of 3 steps of system operation:

(a) Pre-heat process (b) Heating with engine combustion process

(c) SOFC loading process

(a) Pre-heat process

1) Figure 3.3 (a) shows the pre-heat process of the initial start-up operation. The red line shown in the figure is a flow path of the gas supplied to the anode, and how the preheated gas exchanges heat inside the system is shown. In the initial start-up process, all BOPs and SOFCs are at room temperature. In order for fuel to be reformed, sufficient temperature conditions are essential, but the reforming rate of the fuel cannot be secured at room temperature. If fuel is entrained into SOFC in an unreformed state, carbon coking may occur, so natural gas (NG) cannot be supplied during the initial start-up process. Therefore, nitrogen, which has a considerably low reactivity, is supplied to the fuel supply line of the SOFC and undergoes a preheating process. Since there is no amount of heat generated by the system, in the initial start-up process, electric furnaces are placed at the upper and lower parts of the SOFC to perform preheating. The nitrogen gas preheated in the SOFC anode passes through the external reformer 2, preheats the nitrogen gas supplied to the anode, and flows into the engine. Since nitrogen gas is not a combustible gas, combustion reaction doesn't occur in the engine, and no engine power output and exhaust heat energy are generated. Therefore, nitrogen gas is bypassed only through the engine, and the heat is discharged through the system exhaust line after distributing the heat in the order of external reformer 1, HEX2, and HEX1. At the external reformer 1, the heat of nitrogen which exhausted from engine gives heat to newly supplied nitrogen from the system inlet. At this time, the engine repeats compression and expansion during operation, and since it has the same compression ratio and expansion ratio, there is no temperature change in

intake and exhaust if it is an ideally adiabatic condition engine. However, since heat loss exists through the engine cylinder wall, the thermal energy of nitrogen gas is lost through bypassing the engine. Therefore, in order to reduce heat loss as much as possible, the intake throttle located at the intake air of the engine is closed to prevent lowering the temperature of the preheated nitrogen gas by inhaled room temperature air. This preheating process proceeds until the temperature of the SOFC stack reaches 700°C and the temperature of the external reformer 2 reaches 300°C.

(b) Heating with engine combustion process

2) Figure 3.3 (b) shows the heating with engine combustion process after the initial pre-heat process. Since the external reformer and SOFC have been sufficiently preheated by the electric furnace, carbon coking does not occur even when natural gas is supplied to the fuel line. Therefore, the flow rate of nitrogen supplied to the fuel line is reduced, the flow rate of natural gas is increased, and water is supplied according to the S/C ratio (steam to carbon ratio) 2.0. The supplied water becomes steam in a super-heated vapor state as it passes through HEX1 and HEX2, and it flows into the external reformer together with the supplied natural gas to proceed with the steam methane reforming (SMR) reaction. The partially reformed gas through the external reformer 1 and 2 is supplied to the anode, undergoes internal reforming reaction and water gas shift reaction, and is discharged as anode off-gas. In this second start-up process, the supply of fuel is insufficient, so when SOFC load operation is performed, a sudden

voltage loss (concentration loss) and durability problems may occur due to the depletion of fuel inside the anode. Therefore, in this process, only the internal reforming reaction and water gas shift reaction occurs without load operation of the SOFC, and the fully reformed anode off-gas is supplied to the engine. The anode off-gas supplied to the engine after passing through the external reformer 2 is pre-mixed with the air inhaled through the engine intake throttle and burned inside the engine. The air intake throttle is fully opened to maintain 1 bar at the intake manifold of engine. Through this, the engine obtains power output and exhaust heat energy, and the exhaust heat energy provides heat to the external reformer 1 and steam heat exchanger 1 and 2 located at the rear of the engine. In this process, the engine RPM is controlled to match the proper equivalence ratio and volume flow rate in response to the increasing fuel supply and decreasing nitrogen supply and the temperature of mixture gas inhaled to the engine. Additionally, the engine spark ignition timing is also controlled to control the engine combustion stably and generate maximum power output.

(c) SOFC loading process

3) Figure 3.3 (c) shows the SOFC loading process performed at the last process of the start-up operation as well as the design point operation. The nitrogen supply is completely shut off and the natural gas supply is increased. As the natural gas supply increases, the current is also increased to perform the SOFC loading operation to generate electric power. The heat energy exhausted from SOFC increase according to the increased fuel

supply and current because the electrochemical reaction is exothermic reaction. With the exothermic electrochemical reaction, the temperature of the SOFC reaches a design point of 750°C. In this process, the engine RPM is controlled to match the proper equivalence ratio and volume flow rate in response to the increasing fuel supply and temperature, and the composition of the anode off-gas that changes according to the operation of the SOFC loading. In addition, as the SOFC loading current increases, the dilution composition ratio of the anode off-gas increases, making it more unfavorable for engine combustion. Therefore, in order to secure stable engine combustion and power output, it is necessary to control the spark ignition timing, and overall operation is performed while advancing the spark ignition timing. The air intake throttle is also fully opened to maintain 1 bar at the intake manifold of engine.

3.3. Experimental setup

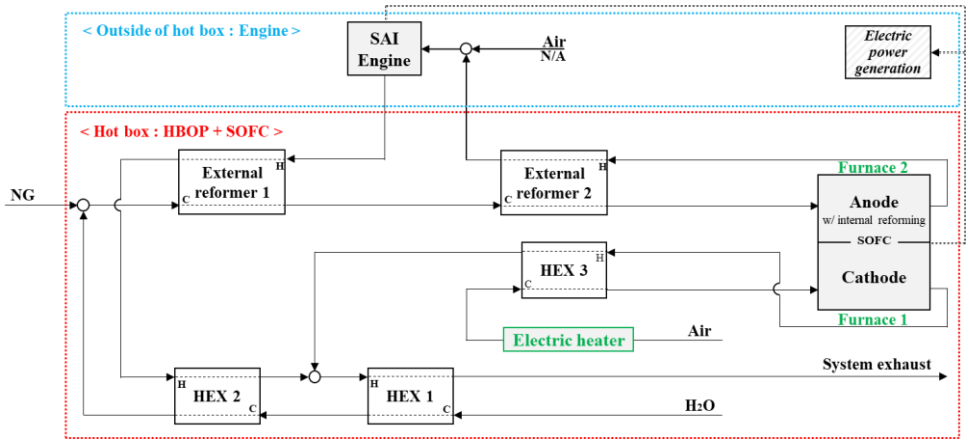

Figure 3.4. Schematic of the SOFC-SAI engine hybrid system conducted for the experiment

Figure 3.4 shows the schematic of the SOFC-SAI engine hybrid system conducted for the experiment. The catalytic oxidizer at the rear end of SAI engine was eliminated because of back pressure issue at the engine exhaust manifold. All the BOPs and SOFC was located in the hot box, and the engine was located at the outside of hot box. In order to provide thermal energy for the system start-up operation, an electric heater was installed at the air supply line and two furnaces were installed at upper part and lower part of the SOFC, respectively.

The main components of the experimental setup were the SOFC and engine. A 5kW-class SOFC system was constructed using two parallelly-connected 2.5kW-class stacks developed by MiCo corporation, which conducted the experiment together. Each 2.5kW-class stack consists of 80 cells which were serially connected. As mentioned above, a Yamaha MZ 300 commercial engine was selected as the engine, and the engine specifications are presented in table 3.3.

Table 3.3. Specifications of an engine: Yamaha MZ 300

Yamaha MZ 300 specifications	
Bore	80mm
Stroke	59mm
Compression ratio	8.4
Displacement	296cc
Number of cylinders	Single cylinder

In order to control the engine RPM to a desired target RPM, a motor and an inverter that could control the engine torque were required. A commercial air filter was used for engine intake to prevent foreign substances from entering. In addition, it was necessary to control the engine oil temperature because the temperature of the engine oil may rise excessively when excessive fuel was inhaled into the engine or engine operation with a high load continuously occurs. In consideration of commercialization, an engine oil cooling system was set up with an oil tank, an oil fan, and an oil pump outside the engine. The engine oil was circulated using an oil pump and cooled using an oil fan to maintain proper viscosity and lubrication performance, and controlled to 90±5℃. Since the temperature of the anode off-gas supplied to the engine was 280~300℃, which was relatively high compared to room temperature, a lot of heat loss may occur in the pipe. To prevent this, the pipe between the external reformer 2 and the engine intake valve was reinforced with insulation materials with a radius of about 100mm. Lastly, the spark plug controlling the combustion of the engine used Kistler's spark plug integrated in-

cylinder pressure sensor to give a spark ignition signal and measure the in-cylinder pressure at the same time. Data such as temperature, current, and voltage inside the SOFC system were measured using the data acquisition system built by MiCo corporation. Engine data acquisition such as in-cylinder pressure, intake/exhaust pressure and temperature, engine oil temperature, and equipment control such as spark timing signal and engine RPM control signal were performed through Simulink and xPC target and NI DAQ board. The equipments used in the experiment are shown in Figure 3.5-Figure 3.8.

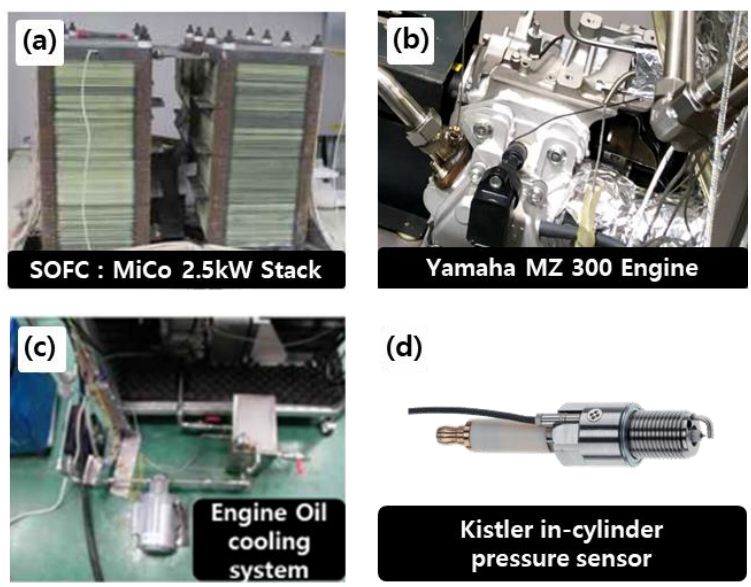

Figure 3.5. Experimental apparatus:

(a) 2 set of 2.5kW stack of MiCo corporation (b) Engine (Yamaha MZ 300) (c) In-house engine oil cooling system (d) Kistler spark plug integrated in-cylinder pressure sensor

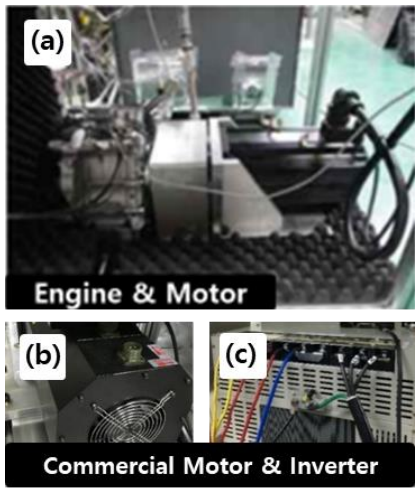

Figure 3.6. Experimental apparatus:

(a) Engine integrated with motor (b) Commercial motor (c) Commercial inverter

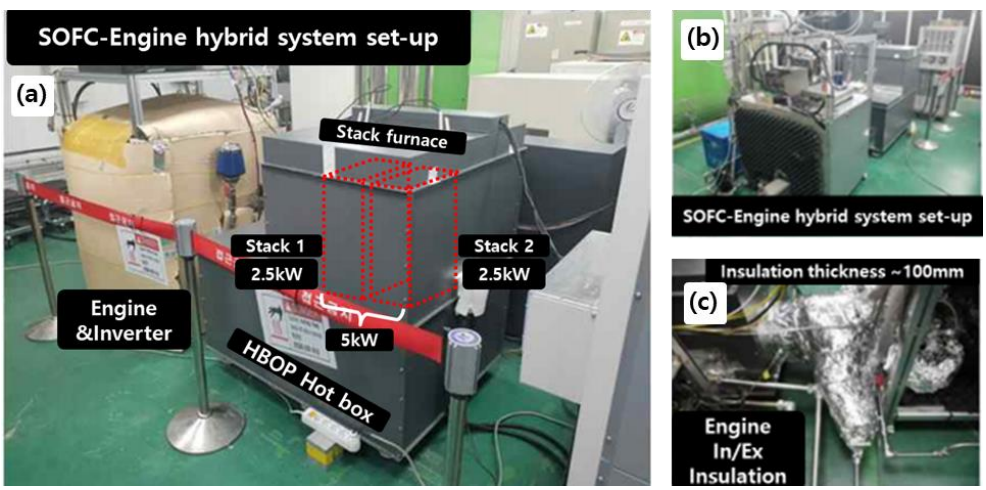

Figure 3.7. Experimental apparatus:

(a), (b) SOFC-SAI engine hybrid system set-up

(c) Engine Intake/Exhaust pipe insulation

3.4. Results: operation characteristics and performance

3.4.1. Pre-heat process

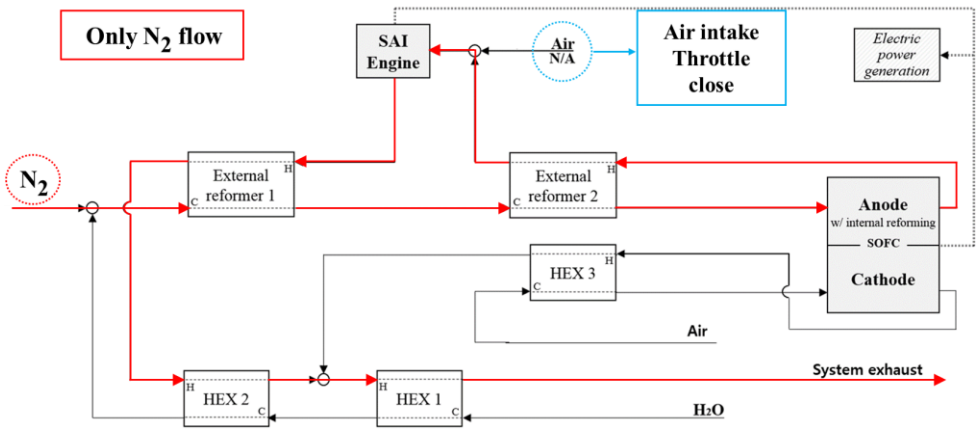

Figure 3.8. Hybrid system start-up process 1: Pre-heat process

The schematic diagram and flow path of the pre-heat process, the first process of the system integration operation, is shown in Figure 3.8. The first process was the longest operating process among the start-up operating processes, and it was operated for about 27 hours. In this process, neither the SOFC nor the engine produced power output, and only the pre-heat process using nitrogen gas occurred. As the SOFC system heated up, the temperature of the external reformer and stack increased, and the temperature of nitrogen gas passing through this equipment also increased. This is shown in Figure 3.9.

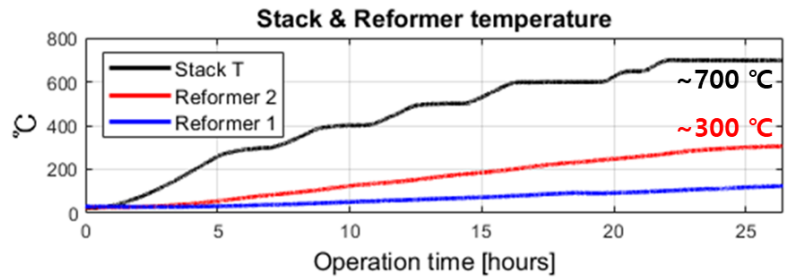

Figure 3.9. Stack & external reformer temperature of pre-heat process

In order to preheat the system faster, the mass flow rate of nitrogen supplied to the system was increased, and accordingly, the volume flow rate of nitrogen gas supplied into the engine was also increased. The volume flow rate of nitrogen gas increased due to two factors: temperature and mass flow rate. During the initial 18 hours of the system, the temperature of the stack and external reformer increased a lot, but the temperature of nitrogen gas discharged to the anode did not rise that much because of heat capacity of nitrogen. After 18 hours of start-up operation, the temperature of nitrogen gas discharged from the anode increased faster due to the mass flow rate of nitrogen gas increased to increase the preheating rate, and the temperature of nitrogen gas entrained into the engine also increased rapidly. The volume flow rate of nitrogen gas in the engine intake was rapidly increased due to the effect that the mass flow rate and temperature of nitrogen gas increased together, and the engine RPM was increased to maintain the pressure of the engine intake air at 1 bar. This is shown in Figure 3.10-Figure 3.11.

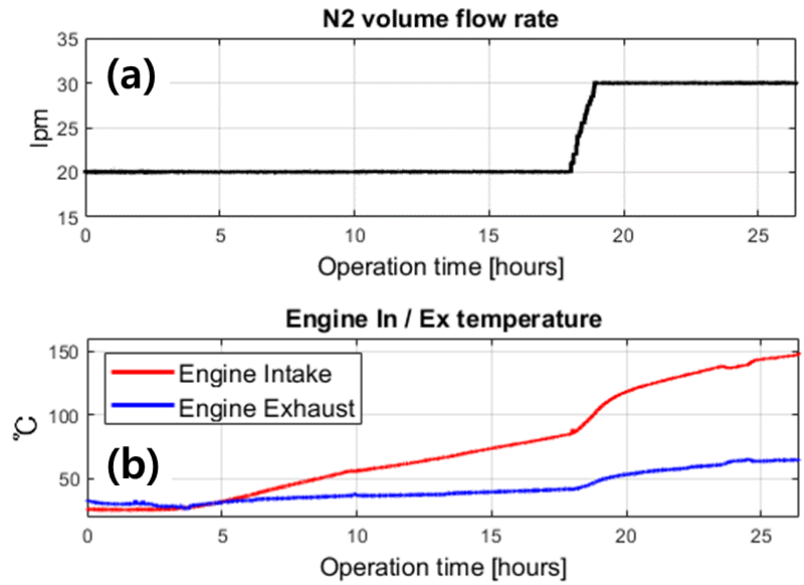

Figure 3.10. Engine intake condition change: (a) Supplied nitrogen volume flow rate change (b) Engine intake/exhaust temperature change

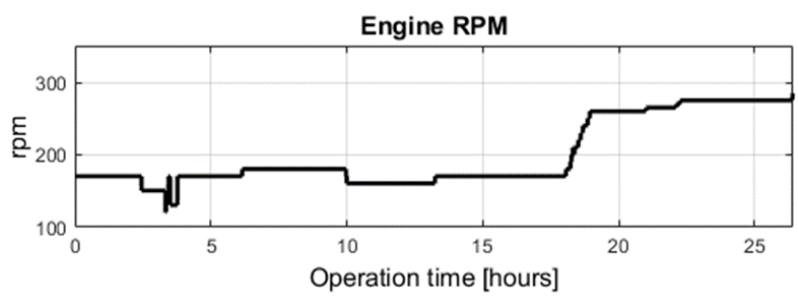

Figure 3.11. Engine RPM control response to engine intake temperature and flow rate

Since the throttle of the engine intake air was closed to reduce heat loss during the preheating process, if the volume flow rate inhaled to the engine and the volume flow rate of nitrogen gas to the engine did not match, the engine intake air pressure might rise or fall. This affected the pressure of the anode, and if excessive negative pressure or back pressure was created, it adversely affected the durability of the anode. Therefore, it was necessary to maintain a stable pressure during the start-up operation through engine RPM control. This process was carried out until a sufficient reforming temperature was secured, which is the stack temperature was 700°C and the temperature of the external reformer 2 was 300°C.

3.4.2. Heating with engine combustion process

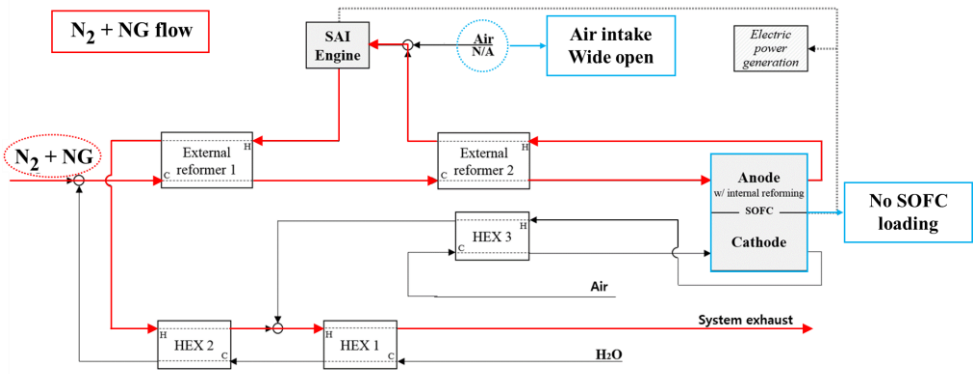

Figure 3.12. Hybrid system start-up process 2: Heating with engine combustion process

The schematic and flow path diagram of the heating with engine combustion process is shown in Figure 3.12. In this process, natural gas was supplied as system input to proceed with fuel reforming because the external reformer and SOFC had been sufficiently preheated. Since a sudden change in flow rate could induce engine intake back pressure, the flow rate of natural gas was increased by a small amount and maintained at the 4LPM (liter per minute) level while maintaining the flow rate of nitrogen gas. This is shown in Figure 3.13.

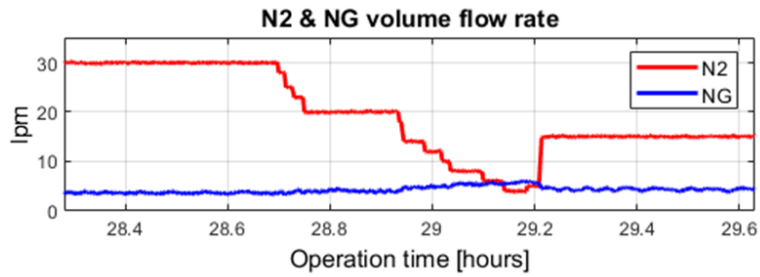

Figure 3.13. System input condition variation: Nitrogen & natural gas flow rate

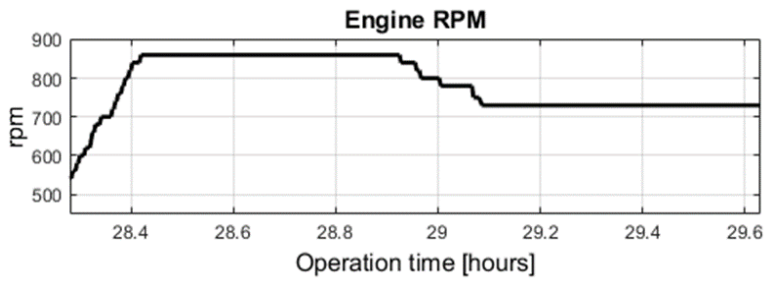

Figure 3.14. Engine RPM control response to system input variable variations

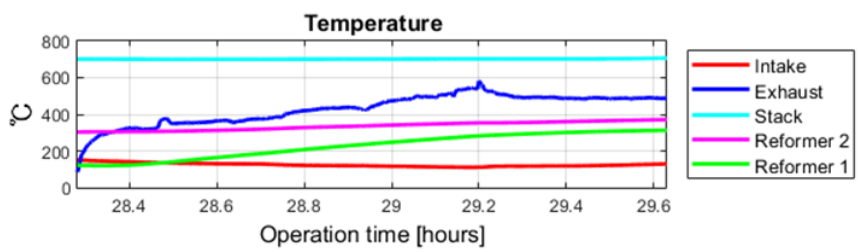

Figure 3.15. System main component temperature variation during the heating with engine combustion process

In Figure 3.14, the engine RPM rapidly increased from 550RPM to 850RPM with natural gas supply. However, the engine intake temperature was maintained relatively constant or slightly decreased, which is shown in Figure 3.15. As shown in Figure 3.12, the air throttle of the engine intake air was fully opened from the second start-up process. As a result, even if the engine RPM was increased, the engine intake pressure was always maintained at the atmospheric pressure of 1 bar. In the second start-up process, since combustion occurred in the engine using reformed gas, air as an oxidizer for fuel was required. Accordingly, the engine intake air was inhaled from fully opened throttle. At this time, if the throttle was partially opened, the pressure of the pipe at the rear end of the anode could be lowered, so it was fully opened to secure the durability of the anode. Therefore, the engine RPM increased along with the natural gas supply was to secure the proper equivalence ratio by inhaling the engine intake air. During the process, engine intake equivalence ratio was maintained almost 0.85.

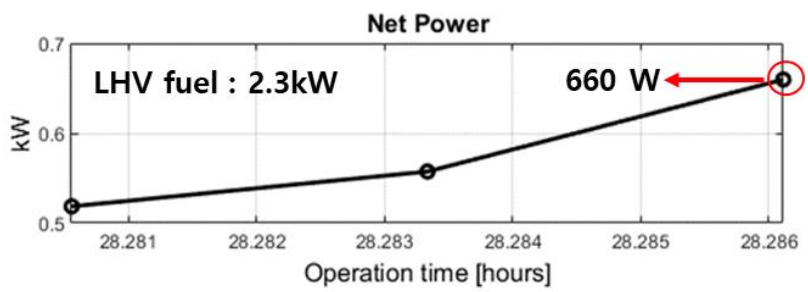

Figure 3.16. Engine net power during reformed gas combustion process

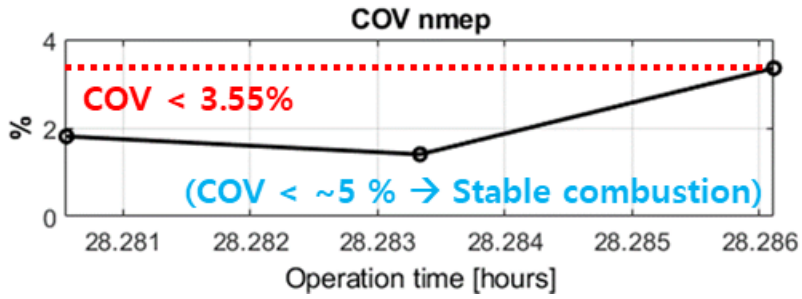

Figure 3.17. Engine combustion stability (COV) during reformed gas combustion process

Combustion successfully occurred through the engine spark ignition after supply of natural gas. This is the first successful combustion in the start-up process of the SOFC-Engine hybrid system. Even in combustion using reformed gas, the engine performed stable combustion, and significant power output was secured in the process.

The engine cycle is formed by a total of four stroke stages: intake, compression, expansion, and exhaust, and the pressure inside the engine cylinder changes at each stage. The pressure inside the engine cylinder is transmitted to the piston to produce power, and the volume inside the cylinder can be calculated for each crank angle degree (CAD). Therefore, for each CAD, the pressure can be calculated integrals with respect to the internal volume of the cylinder, and if divided by the time taken per cycle, the net indicated power of the engine is obtained. That is, the net indicated power of the engine means the net power before transmission to the shaft power [19]. The maximum indicated net power output of engine was 660 W, and the indicated efficiency of engine was 28.7%. In addition, it was confirmed that the COV, which means the combustion stability of the engine,

came out as low as less than 5% in the reformed gas combustion process. This can be seen in Figure 3.17. The definition of indicated efficiency and coefficient of variation (COV) in net mean effective pressure (NMEP) used in Figure 3.16 and Figure 3.17 is described in Eq. (3.1) and Eq. (3.2) [19]. The COV is standard deviation divided by mean NMEP over 60 cycles and indicated efficiency is efficiency based on input fuel LHV.

$$COV_{NMEP}(\%) = \frac{\sigma_{NMEP}}{NMEP} \times 100 \quad (3.1)$$

$$Indicated\ efficiency(\%) = \frac{W_{indicated,Engine} + W_{indicated,SOFC}}{LHV_{fuel,system\ in}} \times 100 \quad (3.2)$$

$$Reforming\ rate(\%) = \frac{LHV_{partial\ reformed\ gas} - LHV_{non-reformed\ gas}}{LHV_{fully\ reformed\ gas} - LHV_{non-reformed\ gas}} \times 100 \quad (3.3)$$

In figure 3.15, the temperature of external reformer 2 was increased to 350°C, and thus the external reforming rate was increased up to 11.9%. The definition of reforming rate is described in Eq. (3.3). This external reforming rate value meant a rather low external reforming rate, and since the rest of the reforming must be secured through the internal reforming of the SOFC. Therefore, there was a possibility that the temperature gradient inside the SOFC or heat loss might increase. In order to secure the external reforming rate, more heat was required, which was attempted to be solved by inducing heat generation through SOFC loading in the following process.

3.4.3. SOFC loading process

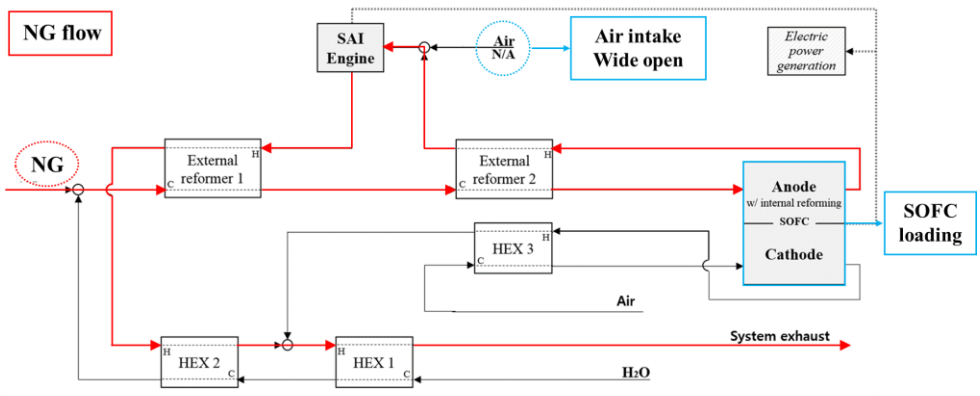

Figure 3.18. Hybrid system start-up process 3: SOFC loading process

The schematic and flow path diagram of the SOFC loading process, which is the last process of the start-up process, is shown in Figure 3.18. In this process, the nitrogen gas supply was completely stopped and the SOFC was operated increasing the load while increasing the supply amount of natural gas. As the natural gas supply increased, the flow rate into the engine also increased. Since the engine was operated while increasing the SOFC load, the ratio of fuel composition among anode off-gas flowing into the engine decreased and the ratio of the dilution composition among anode off-gas increased. A significant proportion of the hydrogen and carbon monoxide compositions of the reformed gas from external reformer were converted into steam and carbon dioxide by the electrochemical reaction, internal reforming reaction, and water gas shift reaction of SOFC. Therefore, the volume flow rate of gas flowing into the engine increased due to an increase of temperature and fuel flow rate and composition transition of anode off-gas by SOFC loading, and the engine performed a control to increase the RPM to keep the equivalence ratio constant. This is shown in Figure 3.19-3.20.

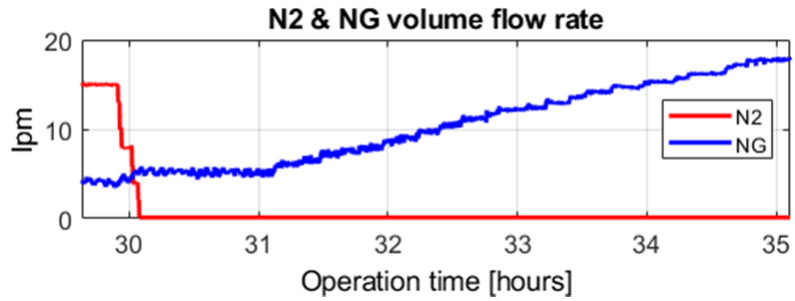

Figure 3.19. System input condition variation: Nitrogen & natural gas flow rate

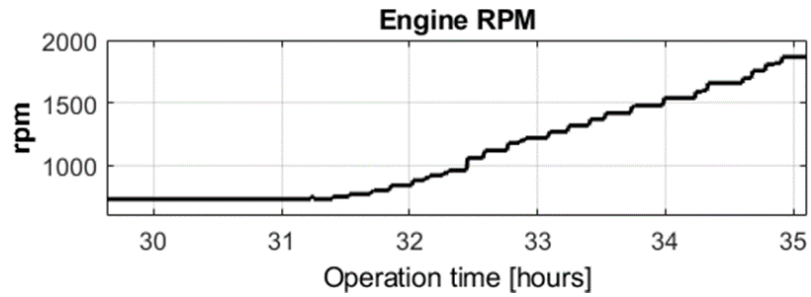

Figure 3.20. Engine RPM control response to system input variable variations

Increasing the load of the SOFC means increasing the operating current of the SOFC at the same amount of fuel and it means increasing the fuel utilization rate of SOFC. The SOFC load per unit amount of fuel can be defined as the fuel utilization rate, which can be defined as Eq (3.4).

$$Fuel\ utilization(\%) = 1 - \frac{LHV_{anode\ out}}{LHV_{fully\ reformed\ gas\ @\ T_{SOFC}}} \times 100 \quad (3.4)$$

When the operating current of the SOFC increases, the hydrogen composition constituting the fully reformed gas undergoes more electrochemical reactions to increase the power output of the SOFC. However, due to the characteristics of the i-V curve of a typical SOFC, the ohmic loss increases and the voltage per unit cell decreases. As a result, the SOFC can produce more power output as the fuel utilization rate increases, and a higher SOFC temperature can be secured through an electrochemical reaction that is an exothermic reaction. Accordingly, the temperature of the anode off-gas supplied to the engine also increases, thereby increasing the engine intake gas temperature. This can be seen in Figure 3.21-3.23.

Table 3.4. Design point operation conditions of SOFC

SOFC operation conditions	
NG input [kW]	10.49
S/C ratio	2.0
SOFC current [A]	81.48

Table 3.5. Design point operation conditions of engine

Engine operation conditions	
RPM	1800
Equivalence ratio (phi)	0.85
Engine intake temperature [°C]	280

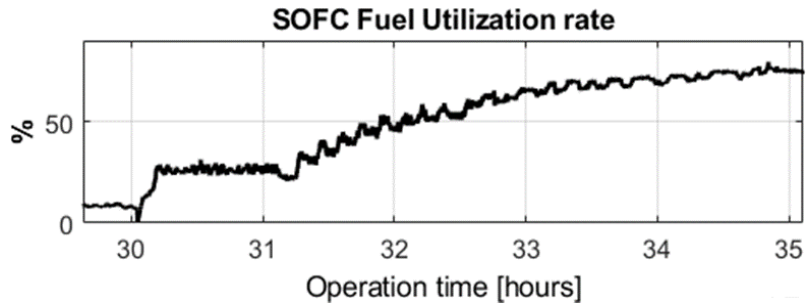

Figure 3.21. SOFC fuel utilization rate variation during SOFC loading process

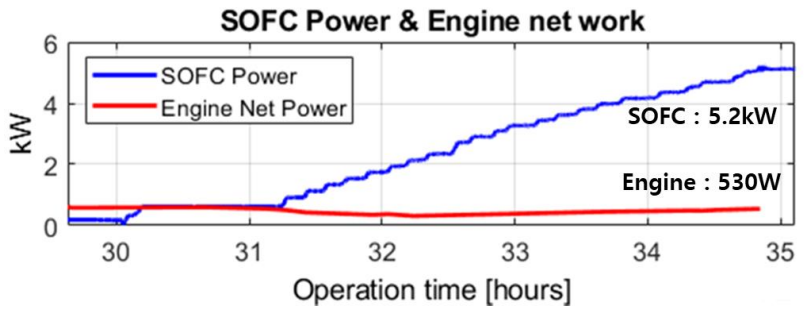

Figure 3.22. SOFC & engine power output during SOFC loading process

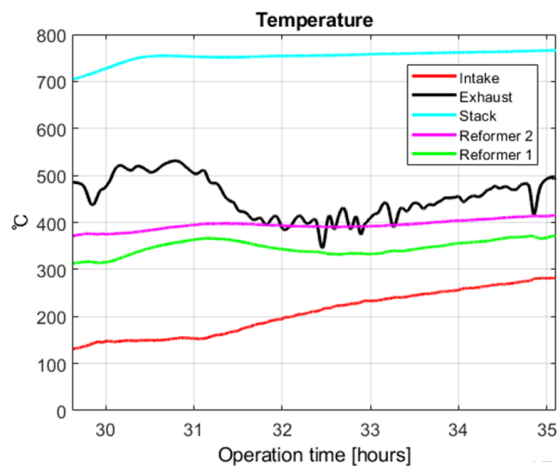

Figure 3.23. System main component temperature variation during SOFC loading process

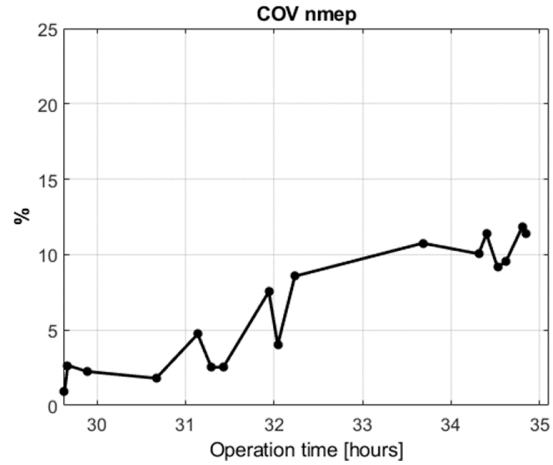

Figure 3.24. Engine combustion stability (COV) during SOFC loading process

As a result, it was possible to reach the final design point through the SOFC loading process, and the power output at the design point was 5.2kW for SOFC and 530W for engine. It could be confirmed that this result was consistent with the results of previous studies by Kim. [24]. The final design point condition of this experiment is shown in Table 3.4-3.5 and the results is shown in Figure 3.21-3.23.

In the case of the COV value, which means the combustion stability of the engine, continued to increase as the SOFC fuel utilization rate increased because the dilution composition flowing into the engine increased. In general, the standard for stable combustion is a COV value of 5%, but when the fuel utilization rate increased, the COV increased from 5% to 12%, confirming that there was some difficulty in securing stable combustion. This is shown in Figure 3.24. In terms of engine control, the higher the SOFC fuel utilization rate, the more unfavorable to combustion due to the dilution composition flows into the engine. As a result, the flame propagation speed of the engine was slowed, and to compensate for this, advanced spark ignition timing was able to respond.

3.5. Discussion

3.5.1. Limitation of operation: insufficiency of heat

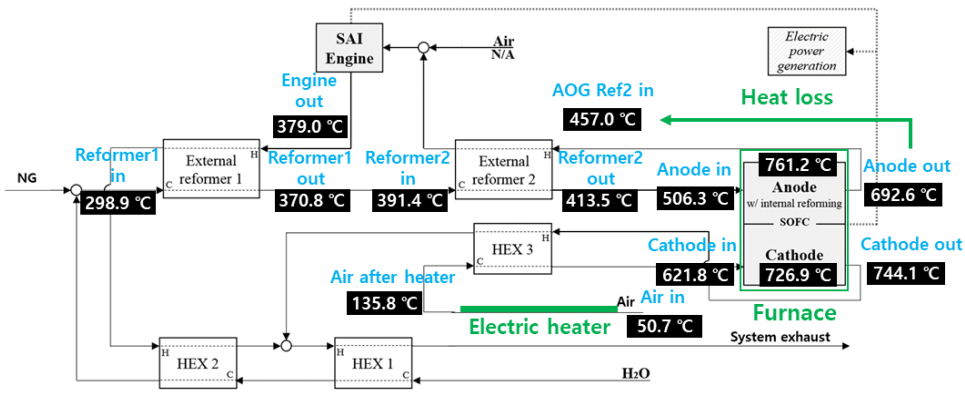

Figure 3.25. Temperature of each point at design point operation

Through the experiment, the SOFC-SAI engine hybrid system demonstration operation was performed for the first time, and it was confirmed that meaningful performance was secured and control according to variations in system operating conditions was possible. However, the electric furnace providing heat to the SOFC and the electric heater preheating the cathode air were operated in the entire operation from start-up operation to even at design point operation. As a result, it was confirmed that both the furnace and heater could not shut off the power even during operation at the design point, and the thermal self-sustainable operation was impossible.

Figure 3.25 shows the temperature at each point of the system in design point operation. Using this, the limitations were analyzed that made the system thermal self-sustainable operation impossible.

First, there was the furnace that provided the largest amount of heat to the system. Since the furnace used in the experiment was located at the upper and lower part of the stack, two sets were used, and each furnace consumed a minimum of 2.91kW of power. Using the temperature of the SOFC, the anode in/out, and the cathode in/out temperature, and the amount of fuel and current input to the system measured in the experiment, the endothermic reforming reaction, electrochemical reaction, and heat transfer due to difference of temperature was calculated. Also, the enthalpy in/out input to the SOFC was calculated through the SOFC in/out condition. Assuming that there was no heat loss of SOFC, it was possible to calculate the minimum amount of heat transferred from the electric furnace, which was calculated to be 2.91 kW. Accordingly, it should be minimum value because it didn't consider the heat loss from SOFC body to the environment, so the amount of heat provided by electric furnace should be larger than 2.91kW.

Second, it was possible to calculate the amount of heat provided by the electric heater for preheating the cathode air. Since the temperature of air before and after the electric heater was measured in the experiment, the minimum heat transfer amount supplied through the electric heater could be calculated by the enthalpy difference, which was calculated as 483W.

A total of 3.39kW of heat was provided by adding only the two heat sources, which was a large amount of heat accounting for 65.5% of SOFC Power. Since this value was calculated just based on enthalpy, the actual power consumption of electric heaters was expected to be greater. If heat loss was also considered, a larger amount of heat would have been provided, and if such a large amount of heat was provided, the thermal self-sustainable operation of the system would inevitably be impossible. In addition, it can become a meaningless system by reducing the

efficiency significantly.

Additionally, the heat loss in the pipe between the anode out and the external reformer 2 was also calculated as the difference in enthalpy using temperature and composition data, and heat loss of 600W occurred.

As a result, although a large amount of heat was provided, the temperature of the anode inlet and the cathode inlet could not be sufficiently secured, showing a temperature difference of 100°C or more with the SOFC. If the inlet temperature of anode and cathode is different with the stack temperature by more than 100°C, a large temperature gradient may occur inside the stack, which may cause a durability problem. In addition, large temperature gradients result in large heat losses, reducing system efficiency.

In order to solve this limitation, a solution may be suggested by small change of the system configuration. However, in order to increase the temperature of the anode inlet and the cathode inlet, heat exchanging is required through a fluid having a higher temperature than this. However, the cathode out air cannot be used for heat exchanging because the amount of heat is insufficient even though heat exchanging with the cathode in air is already performed. Even in the case of the anode out temperature, it is difficult to sufficiently increase the temperature of the anode inlet through heat exchanging because it is not as high as the stack temperature. In addition, it is difficult to increase sufficient temperature of the anode inlet because heat loss in the pipe of anode out gas is large and heat exchanging at a lower temperature is inevitable. For this reason, in the next chapter, a new configuration diagram is going to be suggested, and research using the new configuration is going to be introduced.

3.6. Conclusions

In this chapter, the operation characteristics and performance of the integrated SOFC-SAI engine hybrid system operation, and the operation strategy in start-up operation were investigated. The start-up operation was divided into three stages and analyzed, and it was confirmed how the control variables of the engine were controlled according to the changes of the system input variables in each process. Furthermore, the possibility of thermal self-sustainable operation of the integrated SOFC-SAI engine hybrid system operation was analyzed, and as a result, the necessity of a new system configuration capable of thermal self-sustainable operation was suggested.

The detailed results can be summarized into the following three points.

1) ***Engine control:***

   By determining the type and flow rate of supply gas suitable for each stage of the start-up operation, and controlling engine RPM in real time, the engine intervened in the entire start-up operation process and was successfully operated. Through engine RPM control, the engine was able to operate while maintaining the engine intake pressure at 1 bar and at a constant equivalence ratio (phi: ~0.85). In addition, the spark ignition timing that can produce the maximum indicated net power of the engine was found through spark ignition timing control, which can be utilized for spark control in the future.

2) ***System performances:***

   The undiluted fully reformed gas, which was not performed in the engine-alone experiment of previous study, was successfully combusted through

the engine. It was confirmed that spark-assisted auto-ignition was possible to perform stable combustion with a COV of 3.55% or less, and it was confirmed that the engine could produce significant power of 660W with net indicated power and 28.7% with net indicated efficiency during the start-up process. In the SOFC loading process, as the fuel utilization rate increased, the engine spark ignition timing was advanced, so that the net indicated power of the engine was constantly secured at 530W, and combustion stability was also secured at a certain level. However, it was confirmed that the COV of the engine increased from 2% to 12% as the dilution composition ratio of the anode off-gas increased, and the combustion stability of the engine was slightly decreased. Therefore, it is necessary to control the dilution composition ratio of the anode off-gas in order to secure combustion stability of the engine. As a result, the possibility of increasing the system efficiency by 5.05%p (based on engine net indicated power) was confirmed through the engine.

3) Limitation:

An electric furnace and heater, which was used to provide the thermal energy required for start-up operation, was also used for design point operation. As a result of calculation through the experimental data, it was confirmed that at least 3.39 kW of thermal energy was provided and considering all the heat loss not reflected in the calculation, it was confirmed that the thermal energy provided to the system was significantly large. This could lower the system efficiency from 54.6% to 41.3%, thus fading the meaning of system development. Nevertheless, the inlet temperature of the anode and cathode was lower than that of the SOFC

stack by more than 100°C, possibly causing a temperature gradient inside the stack. As a result, it means that the thermal self-sustainable operation of the SOFC-SAI engine hybrid system is impossible, and the need to propose a new system configuration diagram capable of self-heat operation was confirmed.

Chapter 4. Alteration of SOFC-Engine hybrid system configuration and system level analysis for improving performance & design of system

4.1. Alteration of system configuration for thermal self-sustainability

As analyzed in Chapter 3, the system integration operation was impossible without an additional electric heater and furnace in the experiment using the SOFC-SAI engine hybrid system configuration diagram. Previous study of Kim. [24] tried to find the operating area and conditions for system's thermal self-sustainable operation by adding a reformer and heat exchanger to the previous system configuration through simulation model. However, it was model that did not consider the heat loss of the system, and the operable range of the system was narrowed. Therefore, by changing the system configuration diagram, a simple SOFC-Engine hybrid system was suggested in which a part of anode off-gas was branched to the engine from the SOFC standalone system configuration diagram. Since the thermal self-sustainable operation of the existing SOFC standalone system has been proven, the component of the SOFC standalone system was maintained as it was, and the added engine used only the energy remaining in the SOFC standalone system, so using only the residual chemical energy of the branched anode off-gas was the main concept. Hence, it can be called the SOFC standalone system with SI engine hybrid system.

4.1.1. Description of the new system configuration concept: SOFC standalone system with SI engine concept hybrid system

There are three differences between the new system configuration diagram and the previous system configuration diagram. First, a burner used in a SOFC standalone system was adopted to provide the necessary heat to the system. Unlike the previous configuration diagram, only one reformer was used because it could be provided the sufficient heat required for reforming reaction from the heat produced by the burner. Second, a branching valve was applied so that the anode off-gas was branched to the burner and leftover part of the anode off-gas into the engine. Third, unlike in previous studies, not all anode off-gas flowed into the engine, but only branched anode off-gas flowed, so the chemical energy flowing into the engine was reduced. Therefore, the power output per time could be inevitably reduced compared to the previous system's engine, and a method to increase combustion efficiency and engine load (net power per engine cycle) was needed. In addition, the anode off-gas was generally composed of a large amount of diluent gas, H_2O, and CO_2, which lowers the flame propagation speed inside the engine and could be a factor that makes engine combustion difficult. Therefore, in order to reduce the dilution composition of the anode off-gas flowing into the engine, a heat exchanger was installed in front of the engine to condense moisture. Lastly, since the purpose of this system configuration was to establish and demonstrate a thermally self-sustainable operation system, additional electric heaters and furnaces were not used. The new system configuration diagram of the SOFC standalone system with SI engine hybrid system including BOPs, SOFC, and engine is shown in Figure 4.1.

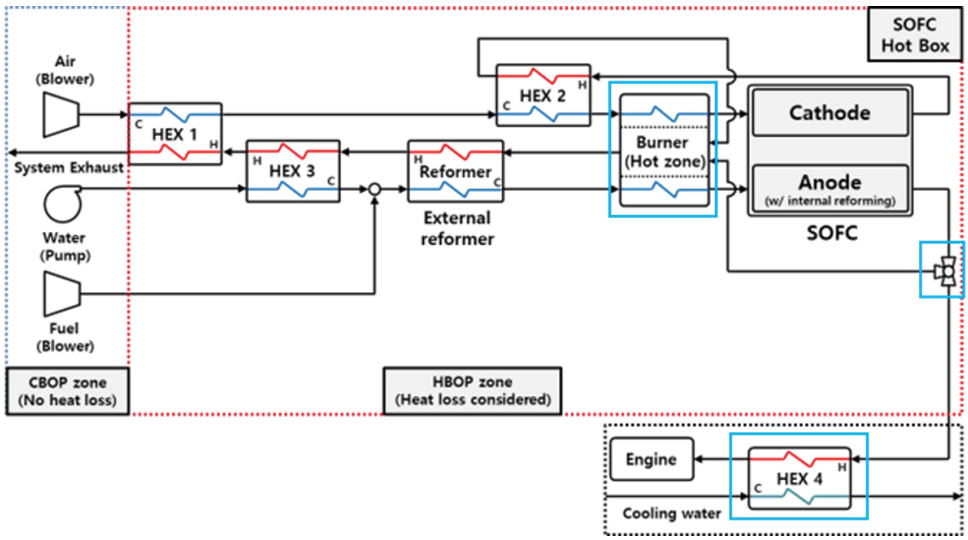

Figure 4.1. New configuration of SOFC-Engine hybrid system: SOFC standalone system with SI engine hybrid system

Various hydrocarbon fuels can be used as fuel for the SOFC standalone system, but methane or natural gas is commonly used. In this experiment and analysis through simulation model, natural gas was used as the fuel of the system. An external reformer of the shell and tube heat exchange type was placed inside the system hot box and as a method of external reforming, steam methane reforming (SMR) method was adopted which could increase the hydrogen fraction. Since the steam methane reforming reaction is an endothermic reaction, the heat required for the reaction must be provided. Cathode air and anode off-gas discharged from the rear end of SOFC were burned in a burner to provide heat required for external reforming in the form of heat exchanging. For the steam methane reforming reaction, steam must be supplied along with natural gas as fuel, and to prevent carbon coking inside the reformer and SOFC, steam must be supplied at an

appropriate steam-carbon ratio (S/C ratio). Therefore, city water was supplied to make the steam required for the reforming, and the heat required for making steam was provided by remaining system exhaust heat after using at external reformer.

Other BOPs consist of heat exchangers (HEX 1 ~ HEX 4) for heat distribution and blowers and a pump to supply fuel, air, and water. First of all, the air supplied to the system was supplied by a blower and flowed into the SOFC cathode after three stages of heat exchanging (HEX1, HEX3, burner). First, heat exchanging with the system exhaust gas was conducted (HEX1), secondly, heat exchanging with the cathode out air (HEX2), and finally heat exchanging with the combusted gas of the mixture between cathode out air and anode off-gas in the burner, and eventually the air was entrained to the cathode. Next, since the water supplied to the system must be heated as super-heated vapor before being supplied to the external reformer, heat was provided by remaining system exhaust heat after using at external reformer (HEX3). The supplied steam was mixed with the natural gas supplied through the fuel blower and flowed into the external reformer. The partially reformed gas in the external reformer was entrained to the anode after heat exchanging with the combusted gas of the mixture between cathode out air and anode off-gas in the burner.

The anode off-gas discharged from the anode was branched through the branching valve and part of it was burned in the burner and remainder of it was supplied to the engine and combusted to produce additional power output. The anode off-gas supplied to the engine was cooled by heat exchanging with city water, and the water was discarded in the experiment. However, the discarded water can be later recovered as waste heat or used to heat water provided for reforming in the system.

The engine combustion method was adopted as the spark ignition. Because the anode off-gas branched to the engine was cooled to room temperature, the combustion phenomenon was appeared as full flame propagation due to complete spark ignition, unlike spark assisted HCCI in previous studies.

In this study, the SOFC-Engine hybrid system which have the configuration diagram of Figure 4.1 was constructed and demonstrated, and validation data was obtained. An SOFC consisting of 4 stacks with a 10kW level as the target power capacity was used, and for the stability of the system operation, a demonstration experiment was performed under the partial load condition of 5kW level. The data obtained through the experiment were used for validation of the simulation model for system level analysis.

4.1.2. Definition of related term: engine branching ratio

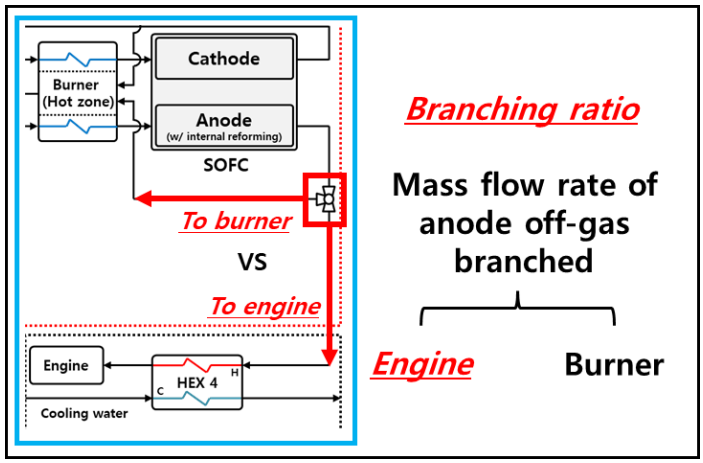

Figure 4.2. Description the definition of engine branching ratio

As mentioned earlier, the main concept of the SOFC standalone system with SI engine hybrid system is to use the anode off-gas as much as necessary for thermal self-sustainable operation of the SOFC standalone system, and to branch the residual chemical energy of anode off-gas to the engine. Therefore, it was necessary to define the ratio of branching anode off-gas to the engine, and through this concept, it was possible to analyze the maximum branching ratio that can branch to the engine in this study. The branching ratio concept is defined as Eq. (4.1) and described in Figure 4.2.

$$Branching\ ratio = \frac{Mass\ flow\ rate\ of\ AOG\ branched\ to\ Engine}{Mass\ flow\ rate\ of\ Total\ AOG} \quad (4.1)$$

4.2. Experimental setup and experiment results for simulation model validation

The experimental setup for the demonstration operation was constructed using the changed configuration diagram for the system's thermal self-sustainable operation. The purpose of the demonstration experiment was to confirm whether operation was possible at the design point without additional heat source supply, and to secure data for simulation model development. An experiment was performed to find the maximum branching ratio by increasing the branching ratio from 0%. By changing all of the fuel flow, air flow, and SOFC current, experiments were performed at various points, which became a validation point for simulation modeling.

The equipment used in the experimental setup was similar to the previous experiment, but there were some changes to the equipment. The engine was selected as an engine with a lower displacement because it inhaled a lower flow rate of anode off-gas than in the previous configuration diagram and the intake air temperature was also lower. As a result, a 120cc Honda GX 120 engine was selected and applied to the experiment. A brief specifications of Honda GX 120 engine is shown in Table 4.1. SOFC increased the number of stacks twice compared to the previous configuration in consideration of power level up. Therefore, four 2.5kW-class stacks were connected in parallel and applied to the system. The demonstration system setup using this is shown in Figure 4.3.

Table 4.1. Specifications of an engine: Honda GX 120

Yamaha MZ 300 specifications	
Bore	60mm
Stroke	42mm
Compression ratio	8.5
Displacement	118cc
Number of cylinders	Single cylinder

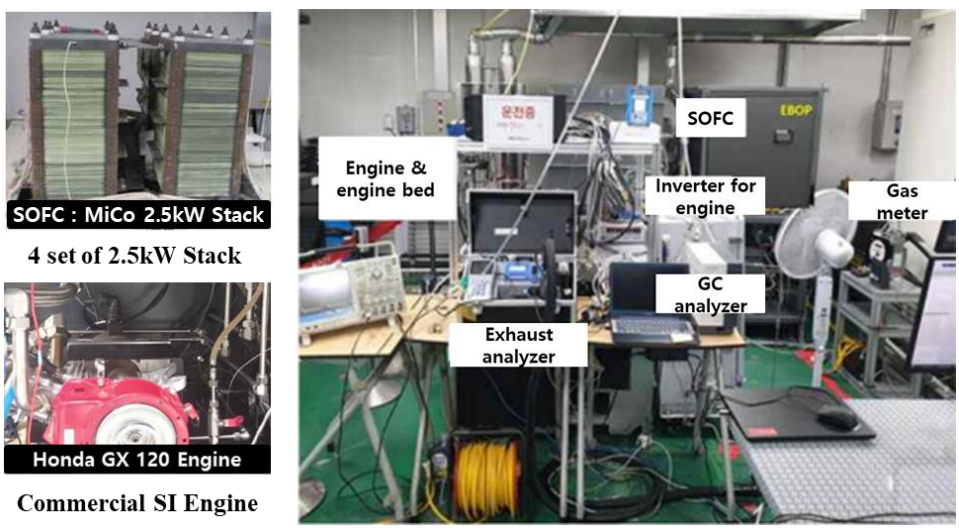

Figure 4.3. Experimental setup for demonstration operation of new hybrid system

The experiment was operated for a total of 30 hours. Steady state operation was performed with a total of four operation points with different operating conditions of the system. The results are shown in Table 4.2-4.5.

Table 4.2. Operation condition of operation point 1 (Validation point 1)

SOFC input condition	
NG input [lpm/kW]	17.71/10.4
Air input [lpm]	846.79
SOFC current [A]	85.37
Engine branching ratio (%)	0
SOFC & Engine performance	
SOFC DC Power [kW]	5.812
Engine Power [W]	0
Engine COV [%]	0

Table 4.3. Operation condition of operation point 2 (Validation point 2)

SOFC input condition	
NG input [lpm/kW]	18.11/10.6
Air input [lpm]	658.19
SOFC current [A]	85.37
Engine branching ratio (%)	19.12
SOFC & Engine performance	
SOFC DC Power [kW]	5.808
Engine Power [W]	159
Engine COV [%]	5.32

Table 4.4. Operation condition of operation point 3 (Validation point 3)

SOFC input condition	
NG input [lpm/kW]	18.03/10.6
Air input [lpm]	622.38
SOFC current [A]	85.41
Engine branching ratio (%)	20.58
SOFC & Engine performance	
SOFC DC Power [kW]	5.811
Engine Power [W]	207
Engine COV [%]	5.56

Table 4.5. Operation condition of operation point 4 (Validation point 4)

SOFC input condition	
NG input [lpm/kW]	22.02/12.9
Air input [lpm]	790.75
SOFC current [A]	104.13
Engine branching ratio (%)	23.01
SOFC & Engine performance	
SOFC DC Power [kW]	7.005
Engine Power [W]	288
Engine COV [%]	5.05

It was confirmed that the engine power output increased as the branching ratio was increased, and accordingly, it was confirmed that the system efficiency increased by 1.5%p, 1.95%p, and 2.23%p sequentially by the engine. The COV based on NMEP, which shows the combustion stability of the engine, all showed a value of about 5%, and it was found that the engine combustion occurred stably. As a result, it was confirmed that the branching to engine contributed to the system efficiency, and that the built system was capable of thermal self-sustainable operation. This was the first case of establishing an integrated operation system capable of thermal self-sustainable operation among several SOFC-Engine hybrid systems. However, for the safety of the experimental equipment, the branching ratio to the engine could not increase more than 23%. As the branching ratio was increased, the temperature of each component decreased, and the system could be shut down by the SOFC system internal control logic, so it was not possible to perform additional branching ratio increase experiments. Therefore, by developing a simulation model using four operation points as validation points, a study was conducted to analyze the maximum branching ratio and heat loss of the system.

Since the four validation points have some variation, they were suitable as validation points of the simulation model. Between validation points 1 and 2, there were fuel flow rate and engine branching ratio variation, between validation points 2 and 3, there was cathode air flow rate variation, between validation points 3 and 4, there were fuel flow rate and air flow rate, and SOFC loading current variation.

4.3. Simulation model

4.3.1. Outline of simulation model

This chapter deals with SOFC system modeling considering heat transfer. Most SOFC simulation studies perform modeling by considering only the SOFC heat transfer model, or modeling both SOFC and BOPs with adiabatic assumptions. However, according to previous experiments and previous studies, the heat loss generated from each component or pipe in the SOFC-Engine hybrid system is quite large. Therefore, in order to study methods to reduce heat loss and improve system performance, a model was needed to develop that can simulate the actual system properly by performing modeling considering heat loss.

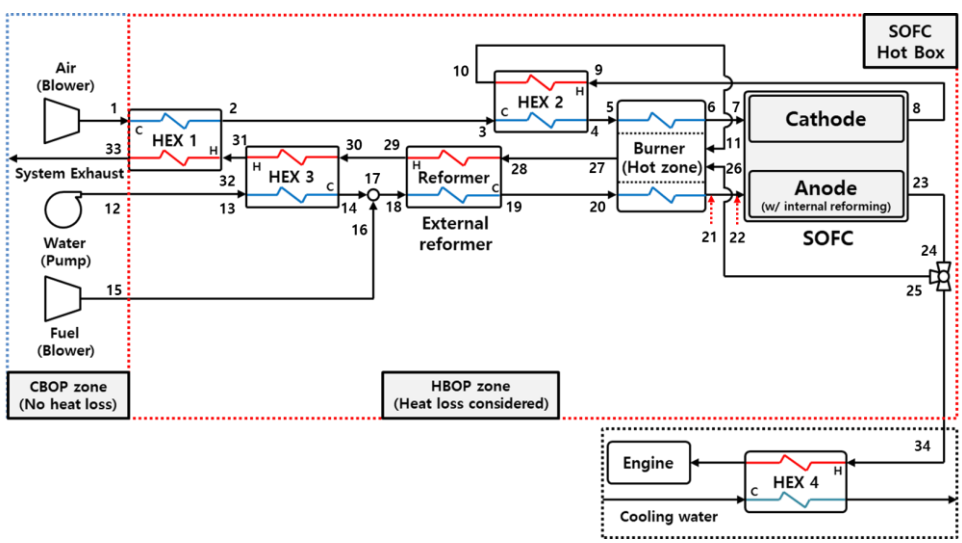

Figure 4.4. SOFC standalone system with SI engine hybrid system numbering of each point

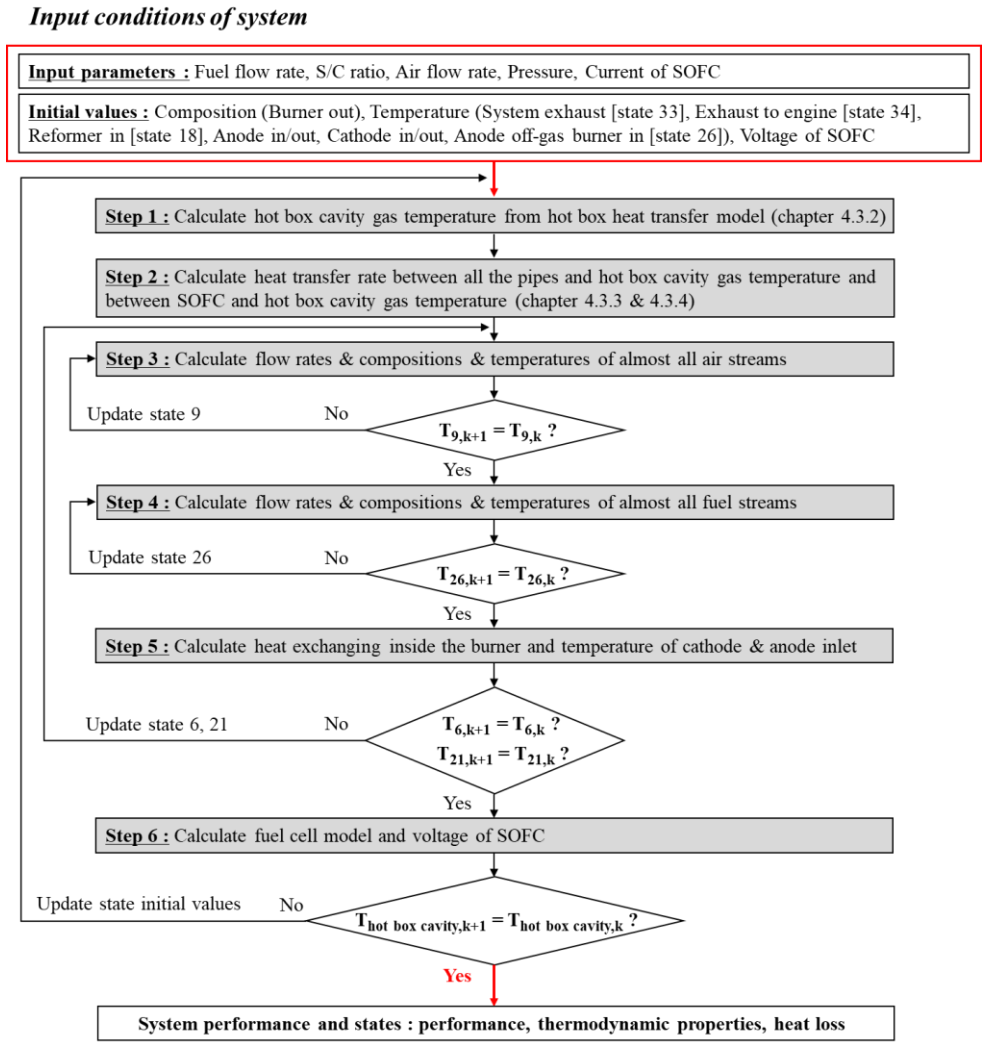

Figure 4.5. Iteration sequence of system simulation model

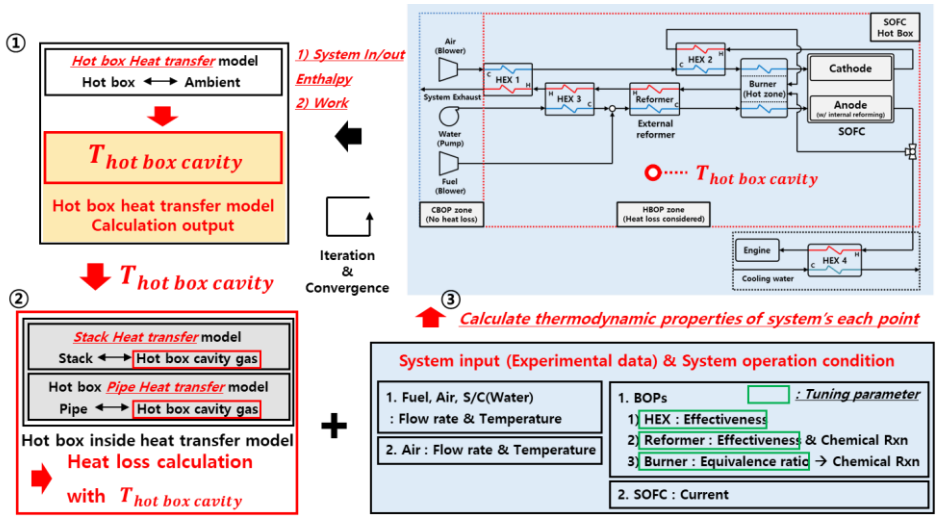

Figure 4.6. Schematic of iteration sequence of system simulation model

An iteration sequence of the simulation model calculation is shown in Figure 4.5-4.6 and the numbering of each point of system is represented in Figure 4.4. In the simulation model, the heat transfer model was divided into three categories. The first was the heat transfer from the hot box, the second was the SOFC heat transfer, and finally, the heat transfer in the pipe located between the BOPs was considered. The gas temperature of the empty space inside the hot box was the target to calculate in the heat transfer model of the hot box, and this was called the hot box cavity temperature. The hot box cavity temperature could be determined by calculating the cavity temperature inside the hot box and the heat transfer between the inner wall of the hot box, and the heat transfer between the outer wall and ambient of the hot box. The calculated hot box cavity temperature was then used to calculate the heat transfer of the SOFC and the heat transfer of the pipe. The thermodynamic properties at each point of the system were calculated by considering the system input conditions and the operating conditions, and the heat

transfer with the hot box cavity temperature was also calculated in this calculation. If the same calculation method was repeated several times and the convergence value was found, it became a steady-state property value under a given operating conditions.

The developed simulation model was validated on the four validation points of the experimental results introduced in chapter 4.2, and the effectiveness value of each heat exchanger and reformer was tuned to validate to the experimental data.

The simulation model did not include the detailed engine model. Since engine experiment was not performed for various operating points, the engine model could not be matched, so that the engine model was used as a model considering only indicated efficiency. The LHV of branched ratio of anode off-gas to the engine was calculated in the SOFC simulation model, and this value was multiplied by the engine indicated efficiency to calculate the engine output. Engine indicated efficiency was used as a fixed value of 25% using the engine efficiency confirmed from the experiment results. Since this study focused on analyzing the heat loss of the SOFC system and suggesting a performance improvement method, the engine model was considered as a simple efficiency model. The engine indicated efficiency confirmed from the experiment was shown in Figure 4.7.

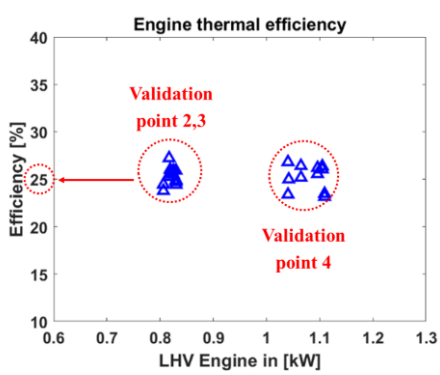

Figure 4.7. Engine indicated efficiency from experiment results

4.3.2. Hot box heat transfer model

The hot box heat transfer model was calculated through two processes. First, the system hot box was set as a black box, and the amount of heat loss to the outside from the hot box was calculated using the system input condition, output condition, SOFC power output, and the first law of thermodynamics. The system input condition was fixed value because it was an input value of system. On the other hand, firstly, the output condition of the system and the power of the SOFC was given as the initial condition, and then all thermodynamic properties of each component of the system were calculated. With these values and the first law of thermodynamics, the heat loss of hot box to the surround was calculated. This is shown in Figure 4.8.

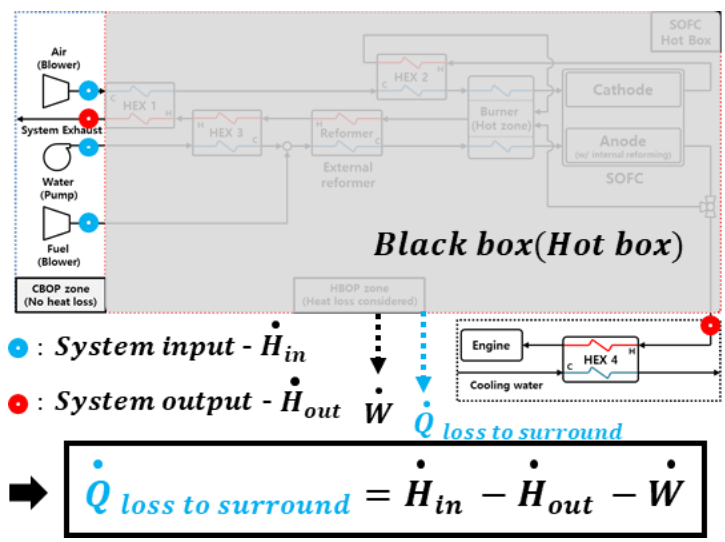

Figure 4.8. Hot box heat loss calculation model: black box model

The heat transfer at the outside of the hot box was considered as radiation and convective heat transfer. First, the hot box outer wall temperature was calculated using the previously calculated heat loss. Then, the hot box inner wall temperature was calculated considering conduction, and finally, the hot box cavity gas temperature was calculated using the hot box inner wall temperature and convective heat transfer in the hot box. Inside the hot box, only convection heat transfer was considered, excluding radiation. In addition, for the convective heat transfer coefficient outside the hot box, the value from general natural convection was used as a fixed value, and the convective heat transfer coefficient inside the hot box was determined by Kattke K. et al. values [26]. A detailed description is shown in Figure 4.9 and the coefficient values related to the heat transfer used in this study are represented in Table 4.6-4.7.

Table 4.6. Hot box dimension and information of SOFC standalone system

Hot box dimension	
Width [m]	1.845
Depth [m]	0.93
Height [m]	1.86
Hot box wall material	SUS 316
Insulation material	Cerakwool (KCC corporation)
Hot box wall thickness [m]	0.002
Insulation thickness [m]	0.125

Table 4.7. Heat transfer coefficient related to the hot box heat transfer model

Thermal conductivity & emissivity of hot box wall (SUS 316) [31]					
Temperature [K]	300	400	600	800	1000
Thermal conductivity [W/m-K]	13.4	15.2	18.3	21.3	24.2
Emissivity	0.17	0.17	0.19	0.23	0.30
Thermal conductivity of Cerakwool [32]					
Temperature [°C]	204		427		649
Thermal conductivity [W/m-K]	0.049		0.088		0.146
Convective heat transfer coefficient (h_{amb} [W/m^2-K])					10
Convective heat transfer coefficient ($h_{cavity\ gas}$ [W/m^2-K]) [26]					2

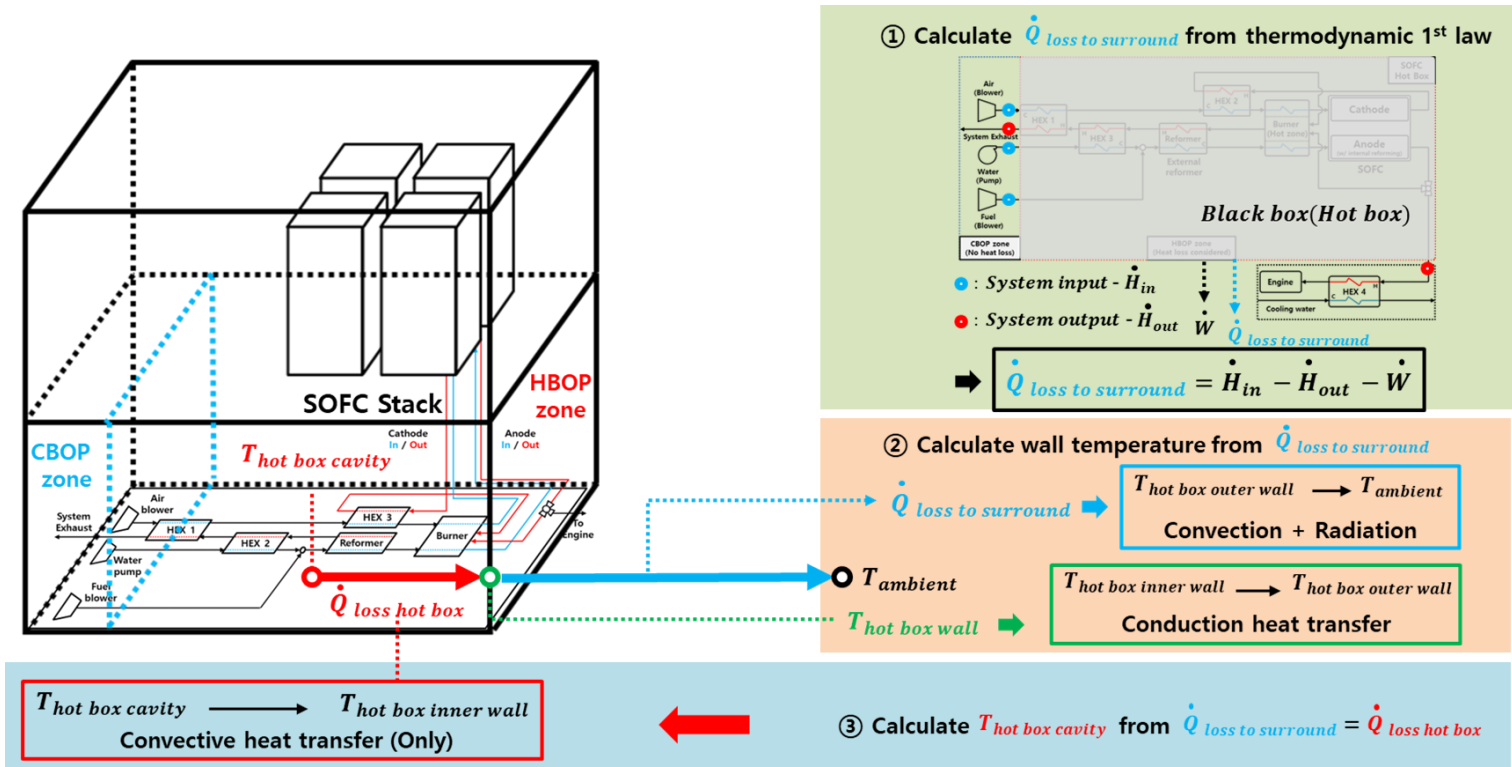

Figure 4.9. Hot box heat loss calculation model description

4.3.3. Fuel cell model with heat transfer

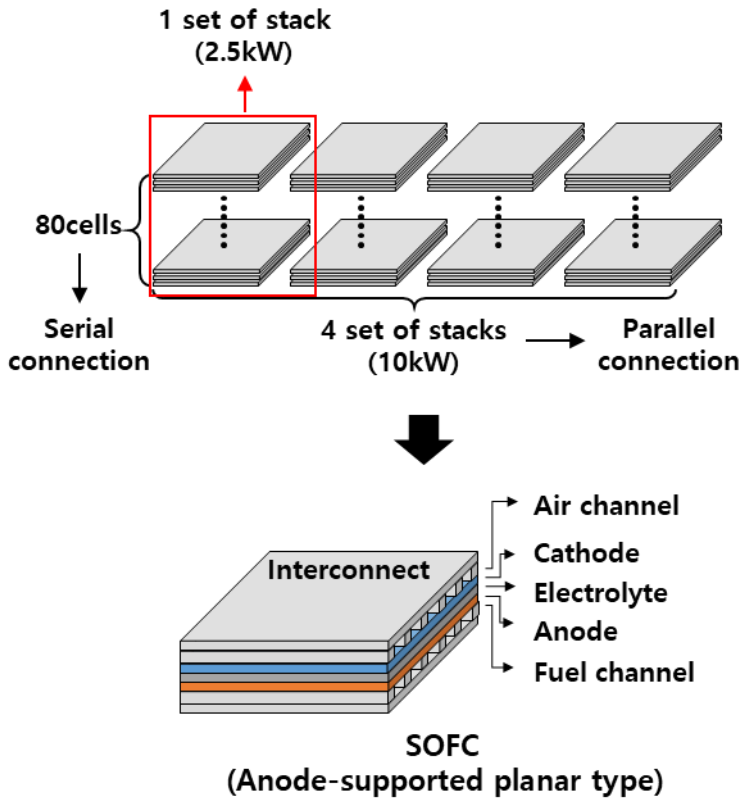

Figure 4.10. Detailed description of SOFC model

Figure 4.10 shows how the SOFC was modeled. The SOFC model was modeled to simulate the 2.5kW-class stack of the MiCo corporation. In a 2.5kW-class SOFC stack, a total of 80 cells were connected in series, and this constituted one stack. In this experiment, a total of 4 stacks were connected in parallel to obtain a total nominal power of up to 10kW.

One cell constituting the stack was again divided into six regions: air channel, fuel channel, cathode, anode, electrolyte, and interconnect. For SOFC heat transfer model, it was assumed that all solid parts of SOFC were one body. Accordingly, the electrode, electrolyte, and interconnect were composed of one body to form the SOFC body. Therefore, it was possible to calculate the heat transfer of the SOFC by dividing it into three control volumes. The SOFC heat transfer model was developed considering mass balance, energy balance, chemical reaction, heat transfer, and mass transfer, divided into SOFC body, air channel, and fuel channel. The convective heat transfer coefficients of the air and fuel channels were calculated using the Reynolds number, Prandtl number, and Nusselt number considering the internal flow velocity and channel shape. All thermodynamic calculations were performed using MATLAB and Cantera [29], and chemical reactions were calculated using the GRI 3.0 mechanism [30]. A detailed SOFC modeling is introduced in appendix A.

4.3.4. Flow pipe heat transfer model

Pipe heat transfer modeling of SOFC system was performed considering both actual component arrangement and dimension. The pipe diameter and the physical properties of the pipe used the specification of the 1-inch SUS pipe actually used. The pipe length was set close to the actual length considering the actual arrangement and dimension. Only the convective heat transfer between the pipe and the hot box cavity gas temperature mentioned above was considered, and the convective heat transfer coefficient was used the same as the value used to calculate the hot box cavity gas. Assuming fully developed flow, it was assumed that there was no change in the pipe flow velocity profile passing through the pipe. It was assumed that the flow velocity in the pipe cross-section was constant by simplifying the velocity profile, so the flow velocity was calculated using the system input volumetric flow rate and the pipe cross-sectional area which is shown in Eq (4.2). In order to calculate the convective heat transfer coefficient of the internal flow at each point of the pipe, the thermodynamic and flow properties at each point were calculated using the temperature, composition, and pressure values of the point. Using this, the convective heat transfer coefficient was calculated considering the Reynolds number, Prandtl number, and Nusselt number which is shown in Eq (4.3) - (4.5) and Table 4.8 [31]. The heat transfer coefficient of pipe wall was calculated using properties of Table 4.9 considering the wall temperature.

$$\boldsymbol{Flow\ velocity} = \frac{\boldsymbol{Volume\ flow\ rate}}{\boldsymbol{Pipe\ area}} \quad (4.2)$$

$$Re = \frac{4 * Mass\ flow\ rate * \pi}{Pipe\ diameter * \mu} \quad (4.3)$$

$$Pr = \frac{Cp_{gas} * \mu}{k_{gas}} \quad (4.4)$$

$$h_{convective\ pipe\ flow} = Nu * \frac{k_{gas}}{pipe\ diameter} \quad (4.5)$$

Table 4.8. Nondimensional number related to heat transfer coefficient [31]

Laminar flow		**Turbulent flow**	
Re	**$\leq$ 3000**	**Re**	**$3000 < Re \leq 5 \cdot 10^6$**
		Pr	**$0.5 \leq Pr \leq 2000$**
Nu	**4.36**	**f**	**$(0.790 \cdot \log(Re) - 1.64)^{(-2)}$**
		Nu	**$(f/8) \cdot (Re-1000) \cdot Pr/(1+12.7 \cdot ((f/8)^{0.5}) \cdot Pr^{(2/3)}-1))$**

Table 4.9. Heat transfer coefficient related to the pipe heat transfer model

Thermal conductivity & emissivity of hot box wall (SUS 316) [31]					
Temperature [K]	300	400	600	800	1000
Thermal conductivity [W/m-K]	13.4	15.2	18.3	21.3	24.2
Emissivity	0.17	0.17	0.19	0.23	0.30
Convective heat transfer coefficient ($h_{cavity\ gas}$ [W/m^2-K]) [26]					2

4.3.5. BOP model

There were heat exchanger, reformer, and burner in the BOP of the system. In the case of the burner, adiabatic flame temperature was calculated by oxidizing the fuel components of anode off-gas branched to burner with cathode out air to reach equilibrium-state under isobaric and adiabatic process. The energy balance equation is shown in Eq (4.6). The cathode air was branched in the burner, so part of cathode air only participate in reaction and the branching ratio of cathode air was turned so that the calculated adiabatic flame temperature matched the burner internal temperature measured in the actual experiment. The remainder of branched cathode air was merged at the burner outlet and the thermodynamic state of burner outlet was calculated with adiabatic mixing process between the remainder of branched cathode air and oxidized mixture. The branched ratio value of air inside the burner was tuned and fixed at 45.5%.

$$h_{burner\ in}(T_{in}, x_{in}) = h_{burner\ out}(T_{adiabatic}, x_{out}) \quad (4.6)$$

Additionally, the air entrained to cathode and the reformed gas entrained to anode was provided heat by heat exchanging with the adiabatic flame temperature of combusted gas inside the burner. The heat exchanging inside the burner was modeled using effectiveness method.

Heat exchangers, reformer, and heat exchanger inside the burner were all assumed to be counter flow type heat exchangers and modeled using effectiveness method. The formula for effectiveness is expressed in Eq (4.7) [31].

$$\varepsilon = \frac{q_{HEX,real}}{\min(C_h, C_c) \cdot (T_{h,i} - T_{c,i})} \quad (4.7)$$

In the case of the reformer, the endothermic reforming reaction and water gas shift reaction were also taken into consideration under equilibrium-state. The effectiveness was tuned so that the simulation data and the experimental result were matched. The energy balance equation of external reformer is shown in Eq (4.8).

$$h_{RFM\ in}(T_{RFM\ c,in}, x_{c,in}) = h_{RFM\ out}(T_{c,out}, x_{partially\ reformed}) \quad (4.8)$$

4.4. Simulation model validation to experimental data

4.4.1. Methodology of simulation model validation

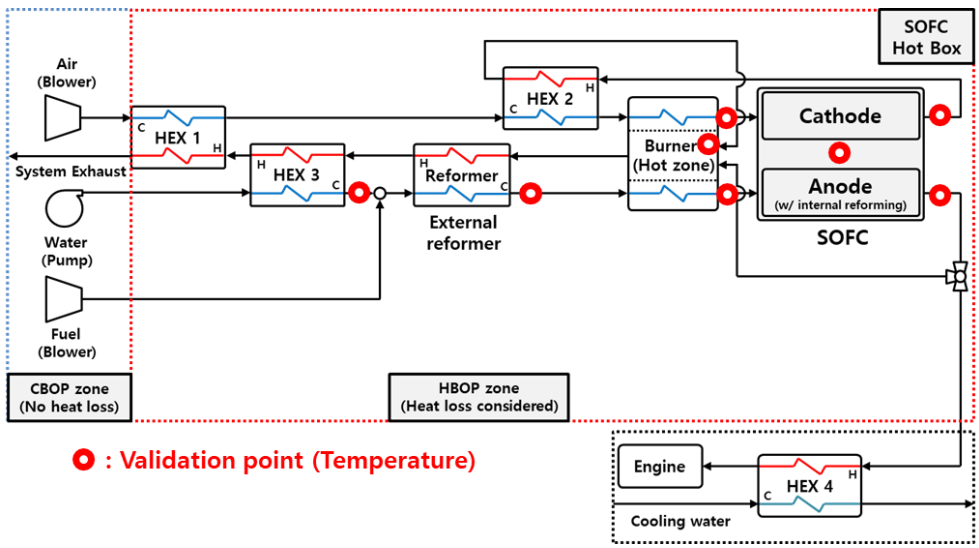

Figure 4.11. Validation points description

For simulation model validation, a total of 8 points of temperature were measured inside the hot box. In addition, for validation, 4 validation points with different system input variables such as fuel flow rate, air flow rate, engine branching ratio, and SOFC current were selected, which are shown in Table 4.2-4.5. It is the same as the point selected as the operation point of the experiment introduced in chapter 4.2.

As mentioned earlier, the effectiveness of HEXs, reformer and heat exchanger inside the burner was determined as the tuning parameter, and the temperature of 8 validation points was matched by adjusting the tuning parameter. Effectiveness was not allowed to exceed 0.85, and since the reformer was a shell and tube type heat

exchanger, it was considered to have a lower value than a plate type heat exchanger. In addition, in the case of heat exchanging between a high-temperature fluid with a large flow rate and a low-temperature fluid with a small flow rate, the effectiveness of heat exchanger is relatively high value [31]. Similarly, the effectiveness of heat exchanger which use water as a heat exchanging fluid is generally high value [31]. With these considerations, the effectiveness was tuned to match temperatures of validation points and eventually the effectiveness was considered to be a large value in HEX3. The effectiveness values used in the simulation model is shown in Table 4.10.

Table 4.10. Effectiveness values of each HEXs, reformer, and heat exchanger inside the burner

Effectiveness of HEX	
HEX 1	0.80
HEX 2	0.65
HEX 3	0.808
Effectiveness of external reformer	0.47
Effectiveness of heat exchanger inside the burner	
Cathode line heat exchanger inside the burner	0.733
Anode line heat exchanger inside the burner	0.85

4.4.2. Validation results

As mentioned above, the validation result was confirmed whether the modeling result was consistent with the experimental result at the validation point for temperature data and stack voltage at a total of 8 points. As a result, the SOFC stack temperature, voltage, anode in/out, cathode in, and steam mixing in were validated to a considerably high degree. Although the temperature at the external reformer and burner cathode out showed a small difference from the experimental results, it was confirmed that it did not deviate significantly from the trend. In the case of burner, since it was calculated using adiabatic flame temperature, even a slight deviation between the ratio of anode off-gas and air could cause a temperature difference, showing the largest difference. However, it showed a sufficient level of matching to simulate the physical phenomena of the system. The validation result is shown in Figure 4.12-4.14.

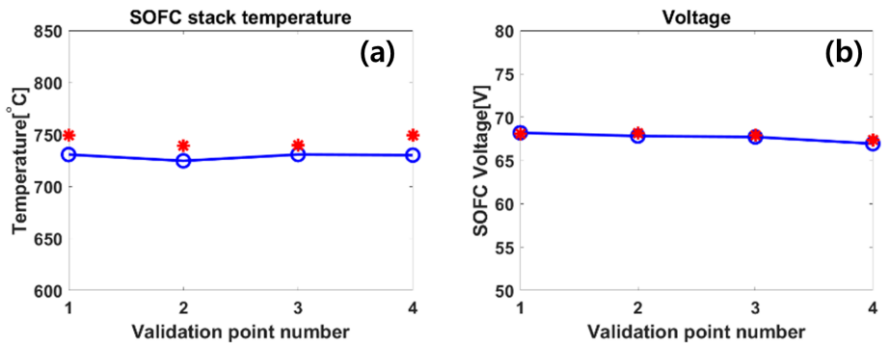

Figure 4.12. Validation results: SOFC Stack

(a) SOFC stack temperature (b) SOFC voltage

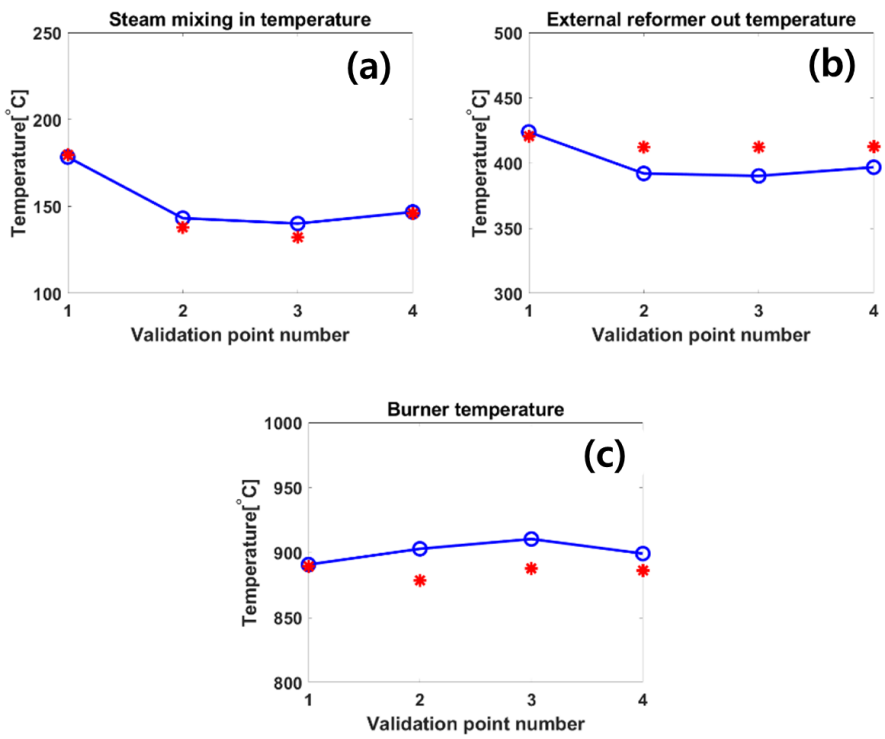

Figure 4.13. Validation results: BOPs

(a) Temperature of steam mixing in (state 14) (b) Temperature of external reformer out (state 19) (c) Burner adiabatic flame temperature

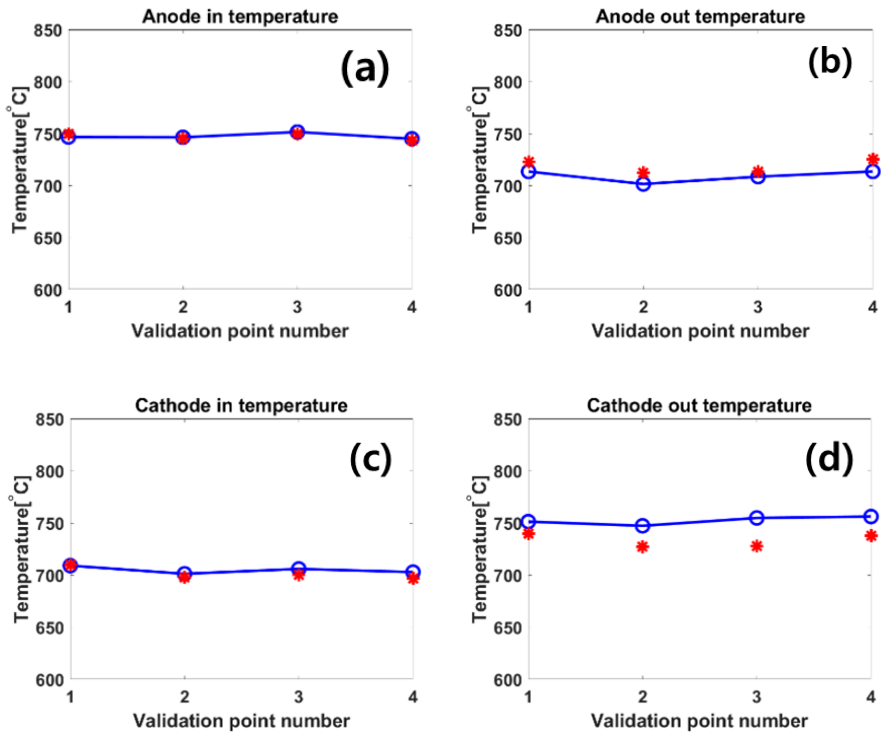

Figure 4.14. Validation results: Stack in/out

(a) Anode in (state 22) (b) Anode out (state 23) (c) Cathode in (state 7) (d) Cathode out (state 8)

4.5. Results: system level analysis with simulation model

4.5.1. System heat balance: heat loss ratio of each point

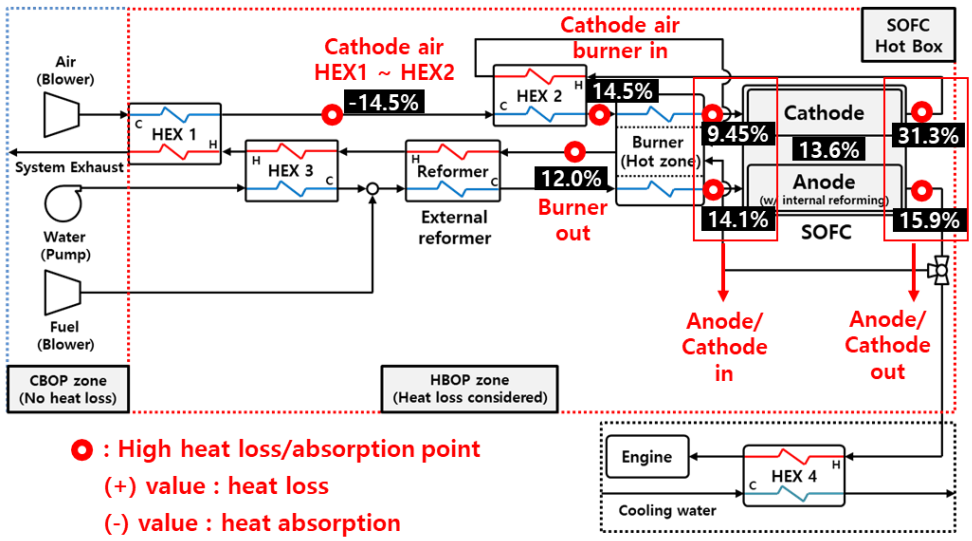

Figure 4.15. High heat loss points of validation point 1 in Table 4.2

$$Heat\ loss\ ratio(\%) = \frac{Pipe\ heat\ loss}{System\ Total\ heat\ loss} \tag{4.9}$$

Figure 4.15 shows the heat loss ratio in the pipe where the main heat loss occurs at validation point 1. The heat loss ratio shown in Eq. (4.9) is the ratio of the heat loss in each pipe to the system total heat loss. This means that the heat loss or absorption at which point is whether dominant or not in the total heat loss. For pipes not shown in the figure, heat loss was all calculated, but the heat loss ratio was not high, so it was not displayed in the Figure 4.15 and the heat loss ratio deals with in later chapter also will show only the main heat loss.

In the Figure 4.15, the heat loss ratio of the cathode air out pipe was the most dominant. In addition, it was confirmed that the higher the flow rate and the higher the temperature, the higher the rate of heat loss, such as anode in/out, cathode in, and burner out. Comparing the anode in (state 22) and out (state 23), even though the anode in (state 22) was hotter, the flow rate of the anode out (state 23) was larger, so the convective heat transfer inside the pipe was large and the heat loss increased at the anode out (state 23) pipe. On the other hand, when comparing the anode in (state 22) and the cathode in (state 7), even though the flow rate of the cathode in (state 7) was much larger, the temperature of the anode in (state 22) was much higher, so the rate of heat loss at anode in (state 22) was higher. Comparing the cathode air burner in (state 5) and the cathode in (state 7), the cathode in (state 7) was a hotter gas and the rate of heat loss was low even though the flow rate was the same, which was caused by the difference in pipe length. It meant that heat loss could be reduced through pipe length optimization even for high-temperature gas in the system.

As a result, since the heat loss ratio in the high temperature part was large, it was expected that it would be effective to reduce the total heat loss by reducing the heat loss in the high temperature part. On the other hand, between HEX 1 and HEX 2, the heat loss ratio showed a negative value, which meant that heat was absorbed. Therefore, in the case of the low temperature part of the system, if the pipe length was increased and optimized, it could be used as a source to absorb the heat loss of the system.

4.5.2. Maximum engine branching ratio

In the system demonstration operation, the maximum possible engine branching ratio could not be confirmed to ensure the safety of the SOFC standalone system. Accordingly, using the simulation model, validation point 1 of Table 4.2 was used as a reference point to research the maximum engine branch ratio.

As the anode off-gas was branched to the engine, the amount of heat remaining in the system was reduced, so the temperature of each component decreased, which also reduced the operating temperature of the SOFC. Hence, the SOFC operating temperature was fixed at 730°C, which was the SOFC temperature of the reference point, while the anode off-gas branching ratio increased because it could cause power output loss when voltage loss occurred due to the SOFC operating temperature decrease. Also, when the temperature of the components decreased, the first place where a problem could occur was the steam line supplied to the reformer. If steam was condensed into moisture in the supply line, the steam could not be supplied properly, and carbon coking issue might occur in the reformer and SOFC. Therefore, the system constraint that maximizes the engine branching ratio was considered as the point at which the temperature of steam mixing in became 100°C.

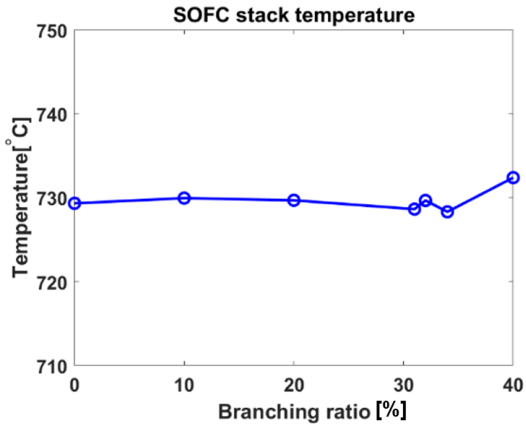

Figure 4.16. SOFC stack temperature with engine branching

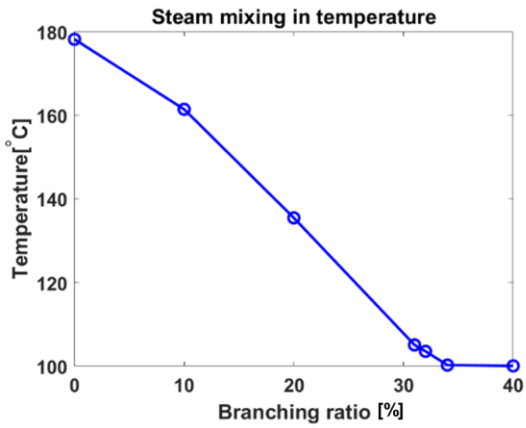

Figure 4.17. Steam mixing in (state 14) temperature with engine branching

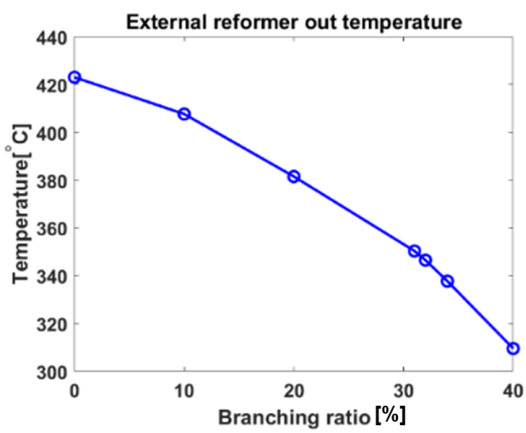

Figure 4.18. External reformer out (state 19) temperature with engine branching

As the engine branching ratio increased, the simulation was performed while the temperature of the SOFC was fixed, and as expected, the temperature of most components decreased. It is shown in Figure 4.16-4.18. As a result, when the engine branching ratio reached 34%, the temperature of steam mixing in (state 14) reached 100℃ with steam quality equal to 1. As mentioned above, since the engine model was considered as a simple efficiency model, if the engine efficiency is fixed at 25% and the power output when the engine branching ratio reaches 34% was calculated, the power of 344W was generated. It is shown in Figure 4.19.

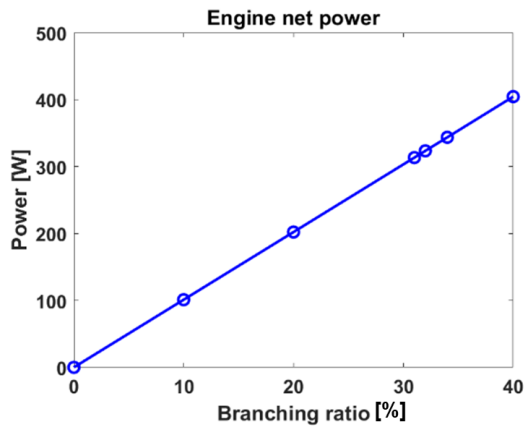

Figure 4.19. Engine net power expectation with engine branching

On the other hand, as the temperature of the external reformer decreased, the external reforming rate decreased and the internal reforming rate of the SOFC increased. As a result, the voltage loss of SOFC increased and the SOFC power output decreased. Therefore, as the engine branching ratio increased, the engine power increased while the SOFC output decreased. Finally, it was necessary to analyze the system power and efficiency. As a result, the system power and efficiency were increased because the power increased due to engine branching was larger than that of the SOFC power was decreased. Efficiency was increased by 2.2%p at 34% of engine branching ratio. It is shown in Figure 4.20-4.21.

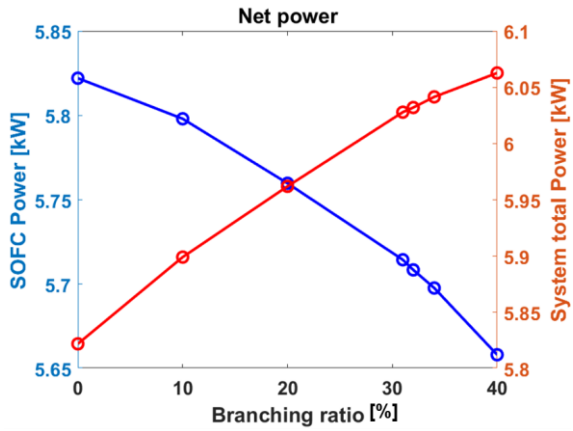

Figure 4.20. SOFC & system total power predictions with engine branching

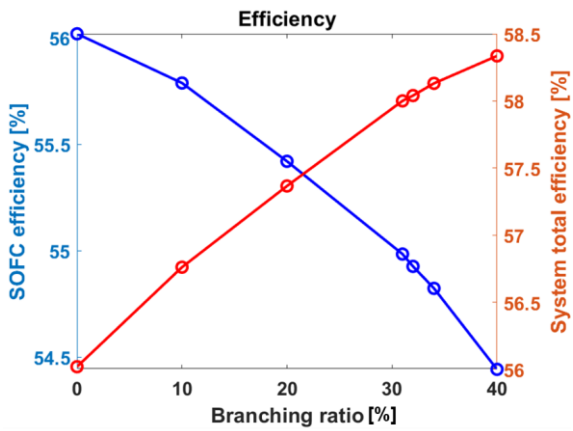

Figure 4.21. SOFC & system efficiency predictions with engine branching

The system heat loss according to the increase of the engine branching ratio was also analyzed. As a result, it was confirmed that the heat loss ratio to LHV fuel (heat loss ratio divided by LHV fuel of system input) decreased as the engine branching ratio increased. Since the LHV of the system input fuel was in a fixed value at 10.4kW, this meant that the total heat loss was reduced. It was analyzed that this was because the heat loss to the outside of the hot box was reduced due to the decrease in the cavity gas temperature of the system. This was shown in Figure 4.22-4.23.

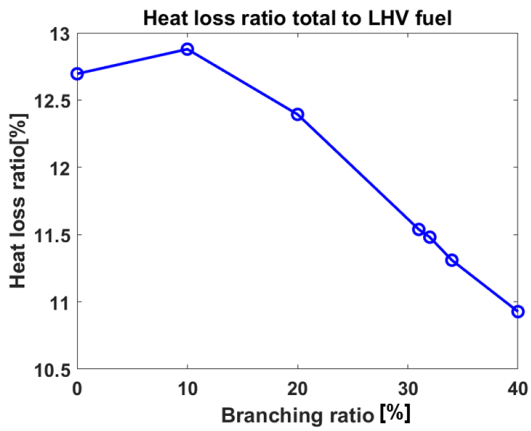

Figure 4.22. Total heat loss ratio to LHV fuel with engine branching

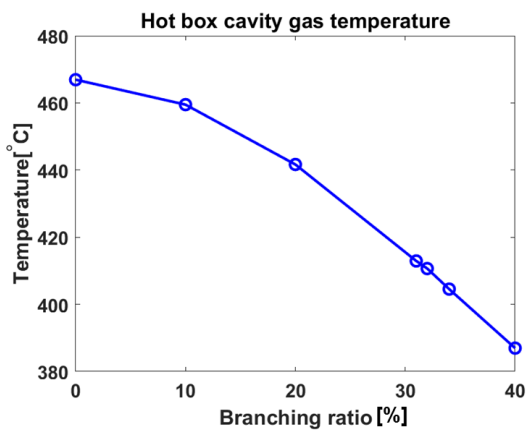

Figure 4.23. Hot box cavity gas temperature with engine branching

Considering the heat loss in the high temperature part of the system analyzed previously, the heat loss increased as the engine branching ratio increased. This is because the temperature decrease of the cavity gas was larger than that of the high temperature part of the system. On the other hand, the heat absorption of the low temperature part of the system increased significantly, comparing the absolute value, it was the amount that compensates all the heat loss in the high temperature part. This was because the temperature decrease in the high temperature part of the system was relatively small while the air flow rate was lowered to fix the temperature of the stack. In addition, the temperature decrease in the low temperature part of the system was relatively large, so that the heat was distributed properly. This is shown in Figure 4.24-4.25. The sum of main heat loss increment is about 2.1% of LHV fuel in Figure 4.24 and the sum of main heat absorption increment is about 2.25% of LHV fuel in Figure 4.25.

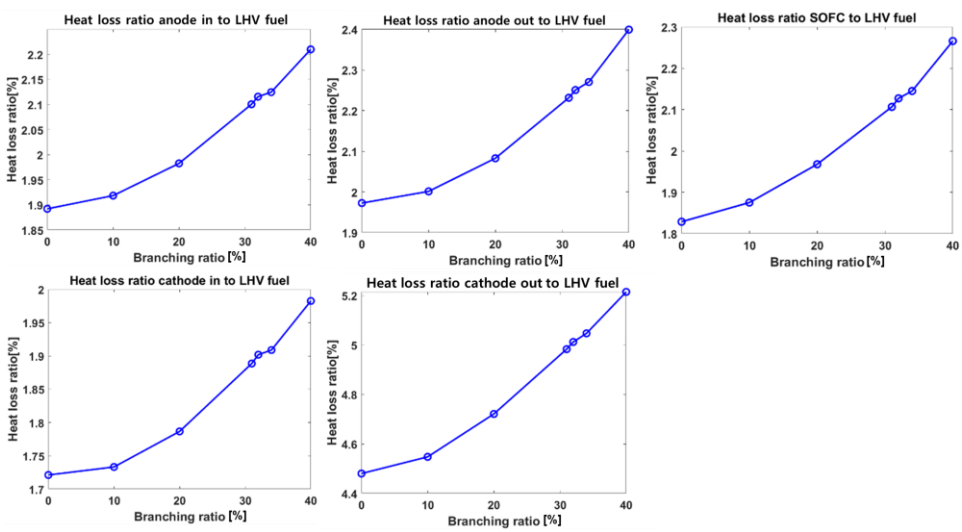

Figure 4.24. Heat loss ratio to LHV fuel of high temperature point with engine branching: heat loss increase

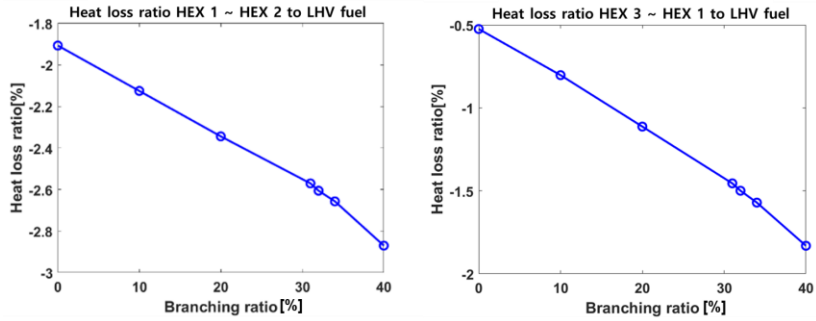

Figure 4.25. Heat loss ratio to LHV fuel of low temperature point with engine branching: heat absorption increase

4.5.3. Methodology of system performance improvement: power level up, scale-up

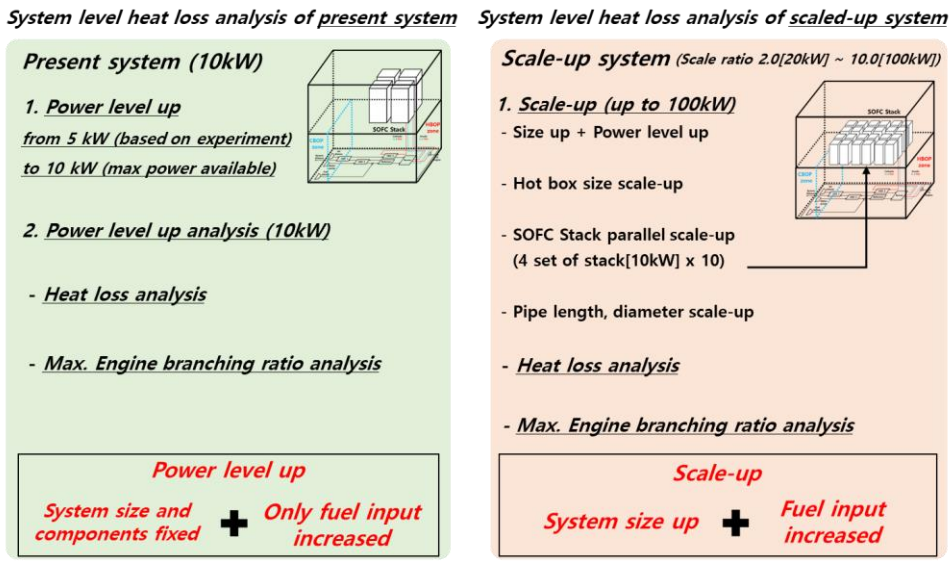

Figure 4.26. Difference description of power level up and scale up

In this chapter, power level up and scale up methods are presented to improve system performance. Figure 4.26 is a figure that briefly introduces the differences between these two methods. The biggest difference between the two methods is the presence or absence of size-up of the system hot box and the stack. The description of each method and the research results are introduced in detail from the following chapter.

4.5.3.1. Power level up

4.5.3.1.1. Assumptions and methodology for power level up

In the experiment, although four 2.5kW-class stacks were used, only 5kW of SOFC power was produced. In order to secure the safety of the equipment, it was not possible to proceed with the full power level (10kW) experiment, and the experiment was performed only under partial load conditions (5kW). Therefore, it was necessary to analyze the performance and heat loss when the power level of the SOFC was increased to the maximum point. Based on this, it was necessary to analyze how much the branching ratio to the engine could be increase when the power level was up and how much it could contribute to the increase in system efficiency.

Accordingly, power level up analysis was performed by increasing fuel input from the operating conditions of validation point 1 while completely maintaining the configuration and dimensions of the system. System input fuel flow and current were increased by 25% on the same scale to produce up to twice the power. Since the fuel flow and current were increased on the same scale, the SOFC fuel utilization rate was kept constant. In addition, the pipe diameter and length, which were maintained which was system design parameters. However, the air flow rate was adjusted differently from the power level up scale. As in the previous analysis, air was supplied at a larger flow rate than the power level up scale to fix the SOFC operating temperature.

Table 4.11. Power level up scale ratio (reference point: validation point 1)

Fuel input scale ratio	(Ref. point) 1.0 (17.71 [lpm])	1.25	1.5	1.75	2.0
LHV of fuel [kW]	10.4	13	15.6	18.2	20.8
Current scale ratio	(Ref. point) 1.0 (85.37 [A])	1.25	1.5	1.75	2.0
Air input scale ratio	1.0 (846.76 [lpm])	1.41	1.84	2.3	2.77

4.5.3.1.2. Improvement in heat loss

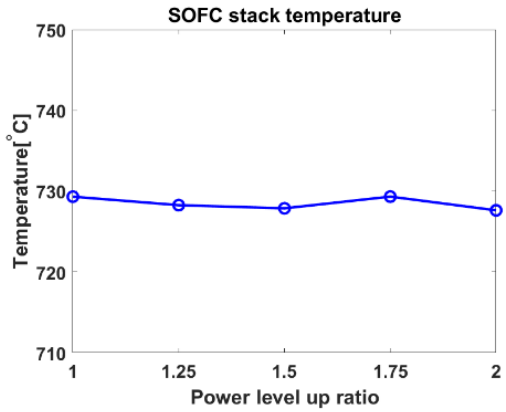

Figure 4.27. SOFC stack temperature with power level up

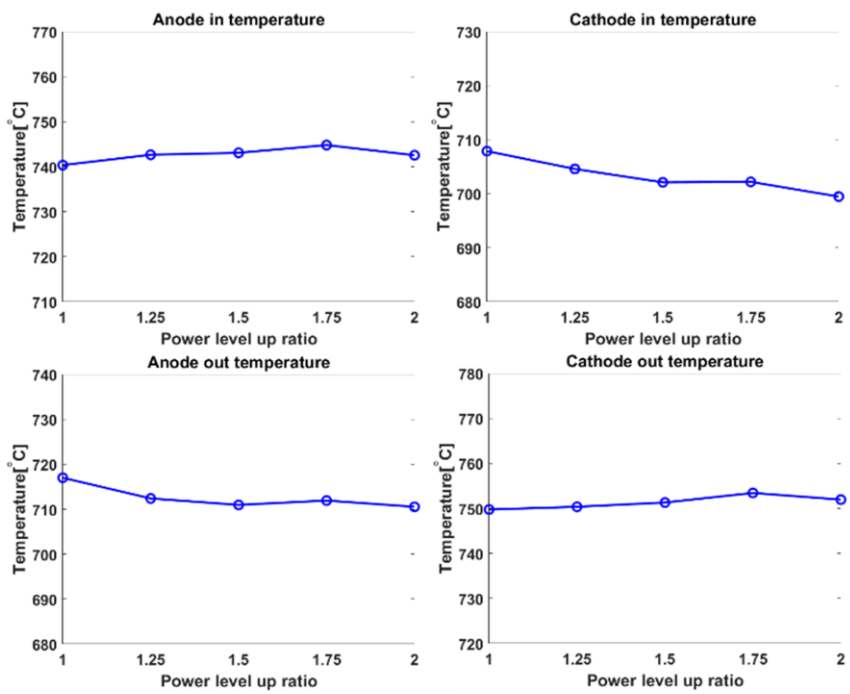

Figure 4.28. SOFC anode in/out (state 22, 23), cathode in/out (state 7, 8) temperature with power level up

Figure 4.27 shows the stack temperature according to the power level up ratio. Since the air flow rate was adjusted to fix the temperature of the SOFC stack, the temperature of the SOFC stack was kept constant. Unlike the previous engine branching, since there was no branching of anode off-gas, the temperatures of anode in and out and cathode in and out were also kept relatively constant. This is shown in Figure 4.28.

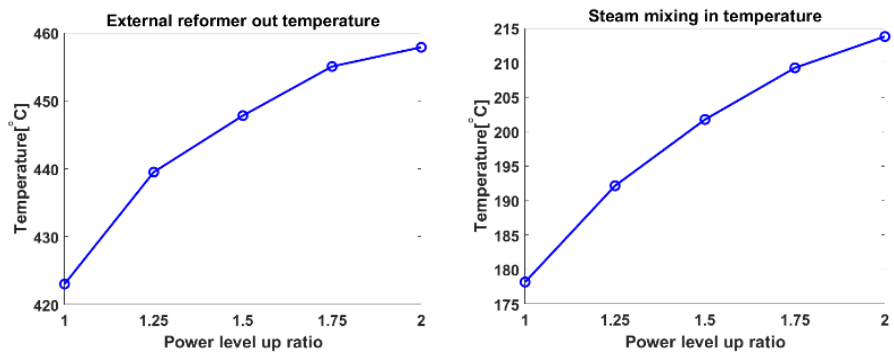

Figure 4.29. System low temperature part: external reformer out (state 19) & steam mixing in (state 14) temperature with power level up

However, it can be seen from Figure 4.29 that the temperature of the low-temperature part of the system increased, because as the air flow rate increased, the enthalpy discharged to the system exhaust increased, which could provide more heat to the low-temperature part. Therefore, as the power level was up, the amount of heat remaining in the system increased, and there was a possibility that the engine branching ratio could be increased. In addition, the increment in the amount of heat discharged to the system exhaust meant that the heat loss through the system hot box could be reduced. This was because, instead of increasing the heat

loss through the hot box surface, the amount of heat that the fluid took away increased. This can be confirmed through the decrease in the total heat loss ratio to LHV fuel in Figure 4.30.

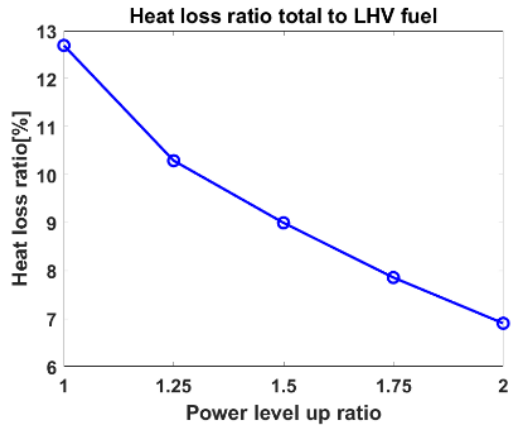

Figure 4.30. Total heat loss ratio to LHV fuel with power level up

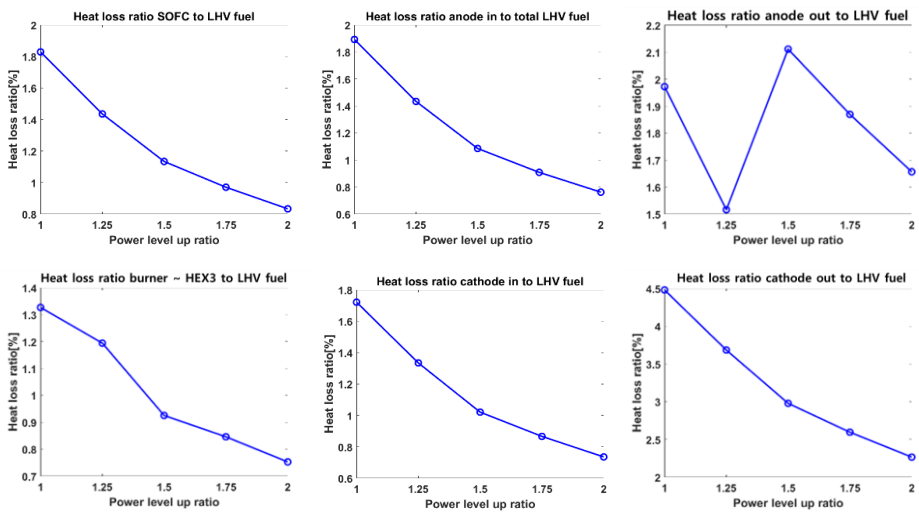

Figure 4.31. Heat loss ratio to LHV fuel of high temperature point with power level up: heat loss decrease

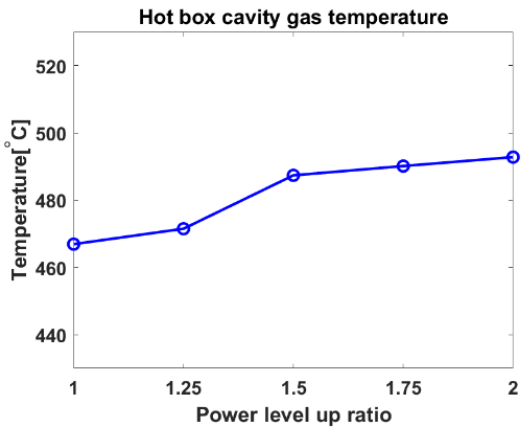

Figure 4.32. Hot box cavity gas temperature with power level up

As the total heat loss of the system also decreased, the heat loss of the high temperature part of the system also decreased as the power level increased, which can be seen in Figure 4.31. All of the heat loss in the high-temperature part of the system decreased as shown in the figure. As shown in Figure 4.32, as the hot box cavity gas increased, the temperature difference with the high-temperature part of the system decreased because the temperature of high-temperature part was maintained. Accordingly, the heat loss in the high-temperature pipe was reduced by power level up method.

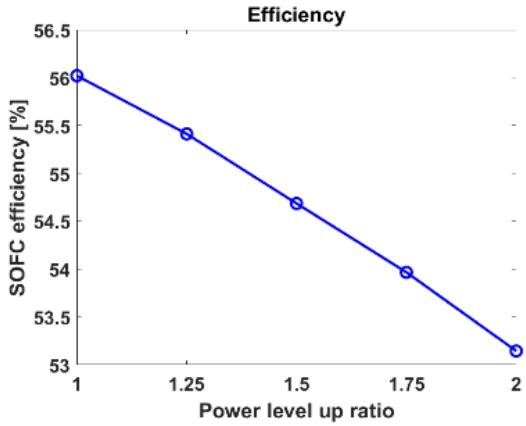

Figure 4.33. SOFC efficiency with power level up

On the other hand, it could be seen that the SOFC efficiency decreased as the power level increased. Although the operating temperature was maintained, the flow rate and current input to the system increased. Hence, the voltage loss increased as the current density increased, so that the efficiency decreased.

Nevertheless, the amount of heat remaining in the system has increased, which had the potential to increase the branching ratio to the engine, so it could be expected to increase the system efficiency through branching to the engine. Accordingly, a study was conducted to increase the engine branching ratio in following chapter.

4.5.3.1.3. Improvement in system performance

Engine branching at fuel utilization rate 68% of power level up case

It was confirmed that the amount of heat remaining in the system increased as the power level was increased. Accordingly, if the excess heat was not burned in the burner but branched to the engine, there was a possibility of obtaining additional system output and increasing the efficiency. In the same way as the method of increasing the engine branching ratio at the validation point earlier, the engine branching ratio was increased until the steam mixing temperature reached 100℃ while maintaining the SOFC operating temperature constant. At this time, the reference point with the branching ratio of 0% was set as the system maximum power level up point which is shown in Table 4.12 and the definition of fuel utilization rate is shown in Eq (4.10). In Figure 4.34, it can be seen that the temperature of the stack is maintained, and at this time, the temperature of the external reformer out (state 19) and steam mixing in (state 14) decreases, as shown in Figure 4.35-4.36.

$$Fuel\ utilization\ rate = 1 - \frac{LHV_{anode\ out}}{LHV_{anode\ in}} \quad (4.10)$$

Table 4.12. Reference point of engine branching of power level up

SOFC input condition	
NG input [lpm/kW]	35.42/20.8
SOFC current [A]	170.74
Fuel utilization rate [%]	68
Air flow rate [lpm]	2311.74

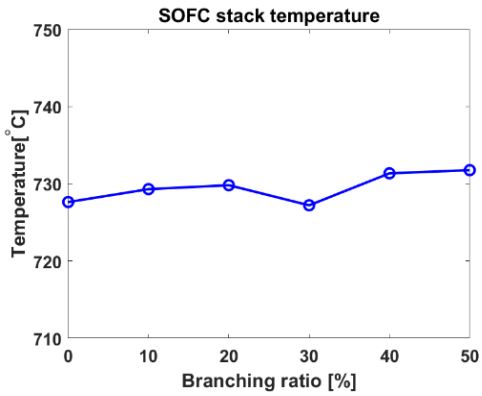

Figure 4.34. SOFC stack temperature with engine branching from power level up

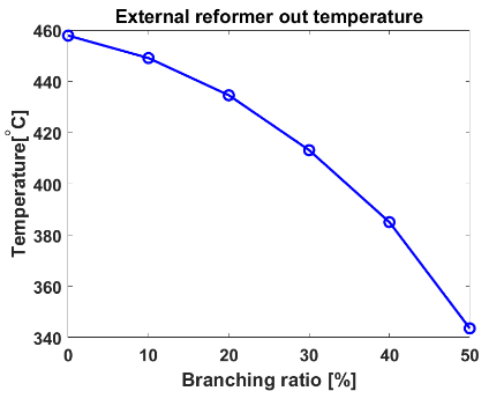

Figure 4.35. External reformer out (state 19) temperature with engine branching from power level up

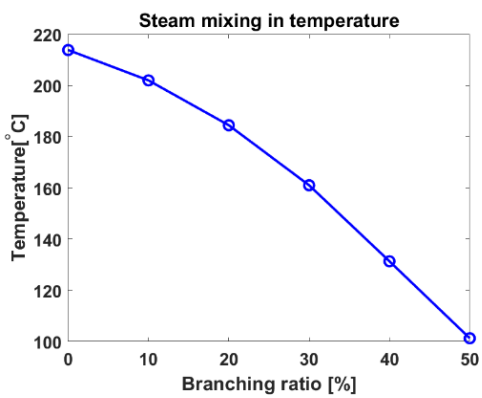

Figure 4.36. Steam mixing in (state 14) temperature with engine branching from power level up

As a result, the engine branching ratio was up to 50%, which is a 14%p increase compared to 5-kW system. Through this, it was confirmed that the branching ratio to the engine could be increased by increasing the remaining heat of the system by reducing the heat loss of the system.

As for the engine power output, the expected net power was calculated using the LHV value at the anode off-gas maximum branching ratio by fixing the engine efficiency to 25% as in the previous study. As a result, the engine was able to produce an output of 1.01 kW.

On the other hand, in SOFC, the rate of internal reforming increased as the temperature of the external reformer decreased, and voltage loss occurred due to concentration loss as the hydrogen fraction decreased. As a result, the power and efficiency of SOFC decreased as the engine branching ratio was increased. However, as a result, as the engine was branched, the increased power of the engine increased system total power output, so that the system efficiency was increased by 3.22%p. This is shown in Figure 4.37-4.39.

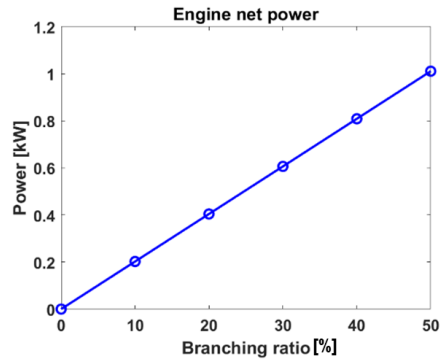

Figure 4.37. Engine net power expectation by engine branching from power level up

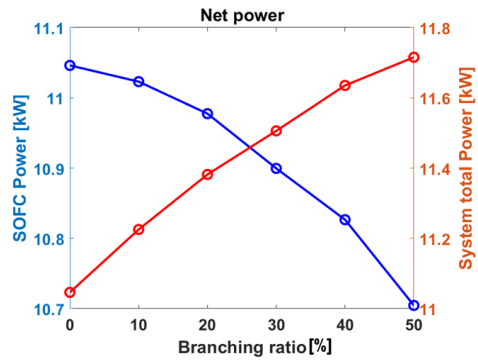

Figure 4.38. SOFC & system total power expectations by engine branching from power level up

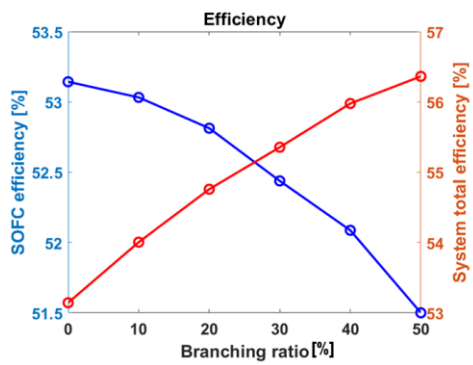

Figure 4.39. SOFC & system efficiency expectations by engine branching from power level up

Engine branching at fuel utilization rate 82.16% of power level up case

However, since the thermal efficiency of the SOFC is generally higher than that of the engine, it was necessary to increase the fuel utilization rate of the SOFC in order to further increase the system efficiency. In the experiment, SOFC operation was performed under the condition of a fuel utilization rate of 68% for stable operation of the SOFC. However, as shown in Figure 4.40-4.41, when the i-V curve and the efficiency curve of the simulation model simulating the SOFC stack used in the experiment were checked, the maximum efficiency of SOFC was shown at a fuel utilization rate of 82.16%. Therefore, it was necessary to check whether it was possible to branch to the engine even at the corresponding fuel utilization rate and how much the system efficiency could be increased. At a higher fuel utilization rate than 82.16%, a study was not conducted because the concentration loss due to fuel depletion in the anode rapidly increased and durability could be reduced.

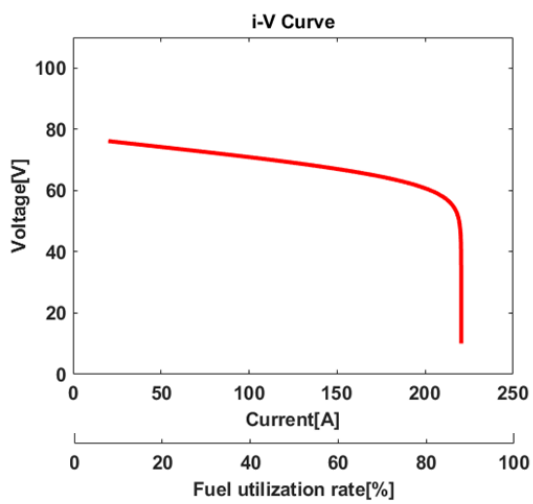

Figure 4.40. i-V curve of SOFC stack simulation model

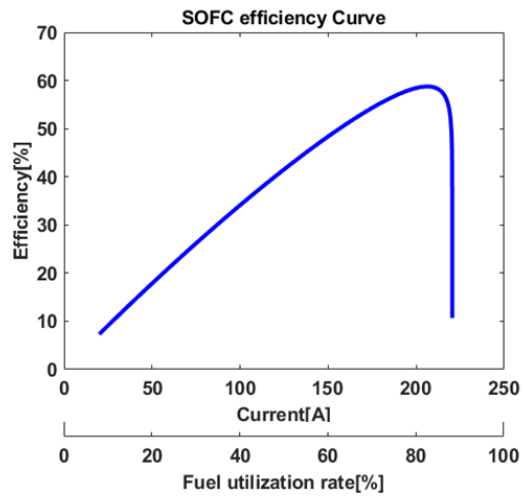

Figure 4.41. Efficiency curve of SOFC stack simulation model

Table 4.13. Reference point of engine branching of power level up at 82.16% fuel utilization rate

SOFC input condition	
NG input [lpm/kW]	35.42/20.8
SOFC current [A]	204.89
Fuel utilization rate [%]	82.16
Air flow rate [lpm]	1766.2

In the same way as the previous anode off-gas branching method, the anode off-gas was branched until the temperature of steam mixing in (state 14) reached 100°C while maintaining the temperature of the SOFC stack at 730 °C. This is

shown in Figure 4.42. As a result, the engine branching ratio was found to be 48%, which was lowered by 2%p compared to the case of the fuel utilization rate of 68%. However, as the SOFC produced more power output, the fuel component of the anode off-gas decreased and the LHV value of the anode off-gas flowing into the engine decreased. Therefore, the power output of the engine was reduced, and it could be predicted that the engine output of 550W would be produced when the net indicated efficiency of the engine was fixed at 25%. This is shown in Figure 4.43.

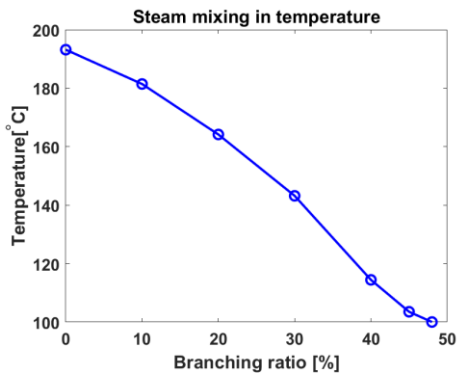

Figure 4.42. Steam mixing in (state 14) temperature with engine branching from power level up and maximum fuel utilization rate

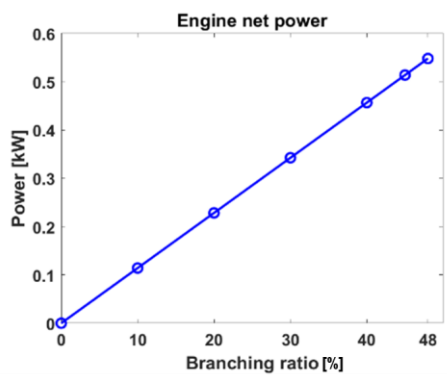

Figure 4.43. Engine net power expectation by engine branching from power level up and maximum fuel utilization rate

As before, as the engine branching ratio increased, the temperature of the external reformer out also decreased, and accordingly, the output of the SOFC decreased. This is shown in Figure 4.44. However, the power output of engine compensated for the SOFC power output reduction, and as a result, the system efficiency could be increased by 2.4%p by the engine. Additionally, the efficiency could be increased by 6.5%p compared to the case of the fuel utilization rate of 68%. Eventually, it was confirmed that branching to the engine is possible even at the maximum efficiency point of the SOFC, and the system efficiency could be increase through the engine. This is shown in Figure 4.45-4.46.

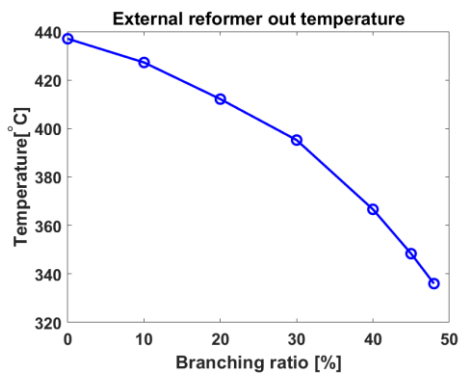

Figure 4.44. External reformer out (state 19) temperature with engine branching from power level up and maximum fuel utilization rate

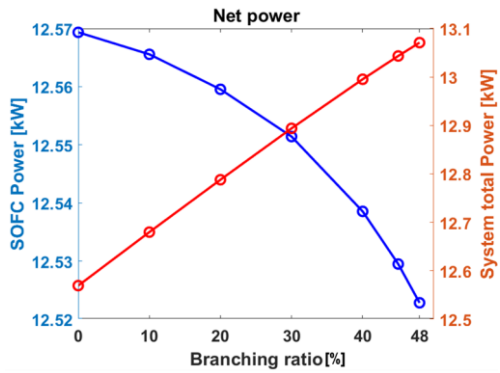

Figure 4.45. SOFC & system total power expectations by engine branching from power level up and maximum fuel utilization rate

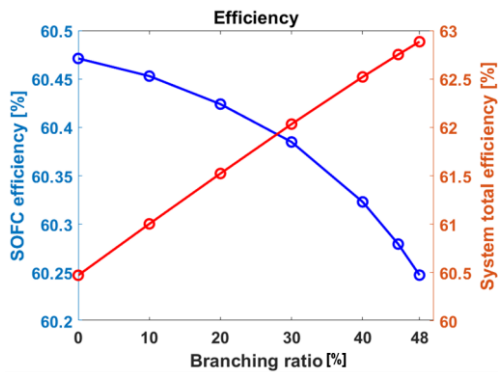

Figure 4.46. SOFC & system efficiency expectations by engine branching from power level up and maximum fuel utilization rate

4.5.3.1.4. Exergy analysis

In this chapter, the results of exergy analysis are presented for the case of power level up and the case of increasing engine branching ratio. First, the component where exergy destruction occurred the most in the system was shown in Figure 4.47. It can be seen that exergy destruction occurred most in HEX 1, HEX 3, and Burner. In HEX 1 and HEX 3, air and water at room temperature were entrained to the cold side, respectively. However, system exhaust gas of a very high temperature of about 500℃ was entrained to the hot side, so the temperature difference was large and exergy destruction was large. In the case of the burner, a high temperature gas of about 450 ~ 600℃ is entrained into the cold side, but exergy destruction occurred greatly because the temperature of the hot side for heat exchange was very high as the flame temperature.

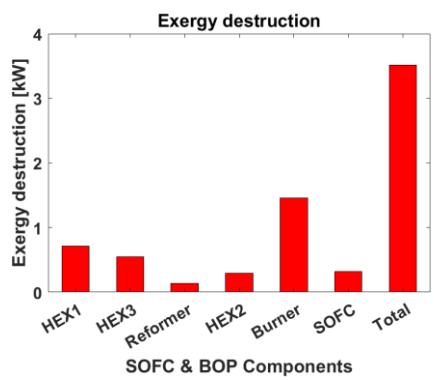

Figure 4.47. Exergy destruction of each component of SOFC system

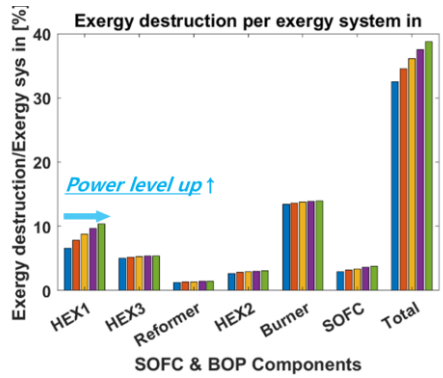

Figure 4.48. Exergy destruction of each component with respect to power level up

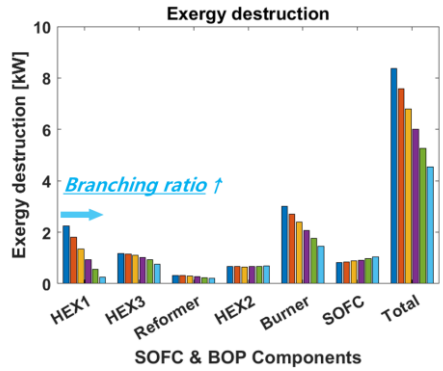

Figure 4.49. Exergy destruction of each component with respect to branching ratio

First, in the case of power level up, the temperature of both the hot side and the cold side of most heat exchangers increased, so that exergy destruction was kept constant. However, as for HEX 1, room temperature air was entrained into the cold side, but as the temperature of the system exhaust gas increased, the temperature difference between the high temperature part and the low temperature part of HEX 1 increased, confirming that exergy destruction increased. This is shown in Figure 4.48.

Second, as the engine branching ratio increased, exergy destruction decreased in HEX 1, HEX 3, and burner, where exergy destruction was significantly large. This is shown in Figure 4.49. In HEX 1 and HEX 3, as the engine branching ratio increased, the heat and temperature discharged to the system exhaust decreased. As a result, the temperature difference between the hot and cold side of the heat exchanger was reduced, and exergy destruction was reduced. On the other hand, in the case of burner, the external reforming rate decreased as the engine branching ratio increased, and it was confirmed that the specific heat of reformed gas flowing into the burner decreased. As a result, the temperature rise of the reformed gas in the burner was large, so the temperature of the anode in was maintained at a high temperature, and the temperature difference between the high and low temperatures of the burner was reduced, so that exergy destruction was reduced. Finally, it was confirmed that the thermal efficiency according to the first law of thermodynamics of the system could be increased through the additional power output of the engine by increasing the engine branching ratio, and at the same time, the efficiency according to the second law of thermodynamics could also be increased.

4.5.3.2. Scale up of system

4.5.3.2.1. Assumptions and methodology for system scale up

In the previous study, it was confirmed that the system efficiency could be increased by increasing the amount of heat remaining in the system through power level up and increasing the engine branching ratio. According to this, it was confirmed that if the load is increased while reducing the heat loss of the system, the amount of heat remaining in the system could be increased. Therefore, it could be predicted that the engine branching ratio and system efficiency could be increased by using this concept. Starting from this motivation, a study was conducted to increase the system efficiency by reducing the heat loss ratio per input LHV of the system through the scale-up of the system hot box and stack.

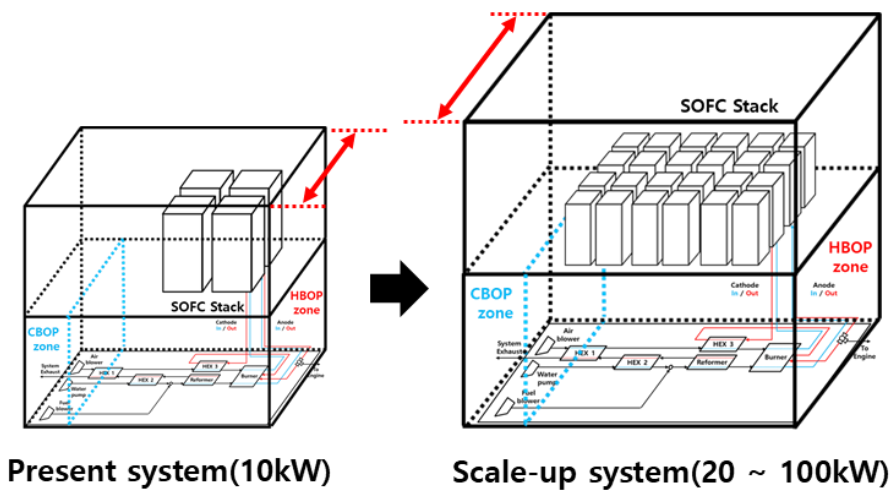

Figure 4.50. Simplified description of scale-up schematic of system

Accordingly, system scale-up modeling was performed by assuming some assumptions while maintaining the configuration and layout of the system. The reference point for scale-up was taken as the maximum power level up point of the present system, and the corresponding operating conditions are shown in Table 4.14. The assumption of system scale-up is as follows, and the method of scale-up is briefly described in Figure 4.50.

Table 4.14. Reference point of scale up model

SOFC input condition	
NG input [lpm/kW]	35.42/20.8
SOFC current [A]	170.74
Air flow rate [lpm]	2311.74

Assumptions of system scale-up

1) Scale-up ratio is 2.0 [20kW] ~ 10.0 [100kW]: Reference point – 1.0 [10kW]

2) Use only one hot box and increase only the dimension of the hot box.

3) The dimension of the hot box maintains the height and only changes the width and depth. Width and depth are scaled up in the same ratio, and [width x depth] is made equal to the scale up ratio.

4) Stack is scaled up in parallel with 4 stacks as 1 set. This is because, due to technical limitations, planar SOFCs have limitations in stacking in series.

5) Stack is connected in parallel by making face to face contact inside the hot box. Accordingly, the area between stacks is not exposed to the environment and only the outermost area of scaled-up SOFC stack is exposed to the hot box cavity gas and transfer heat.

6) Pipe length and diameter are scaled-up in the same ratio as the scale ratio.

7) LHV of fuel input and SOFC current are also scaled-up to the same scale ratio to maintain fuel utilization rate at 68% and S/C ratio is also fixed to 2.0.

8) The operating temperature of the SOFC is kept the same as the reference point, and this is controlled by the supplied cathode air flow rate. (Increasing by a larger ratio than the scale ratio.)

4.5.3.2.2. Improvement in heat loss

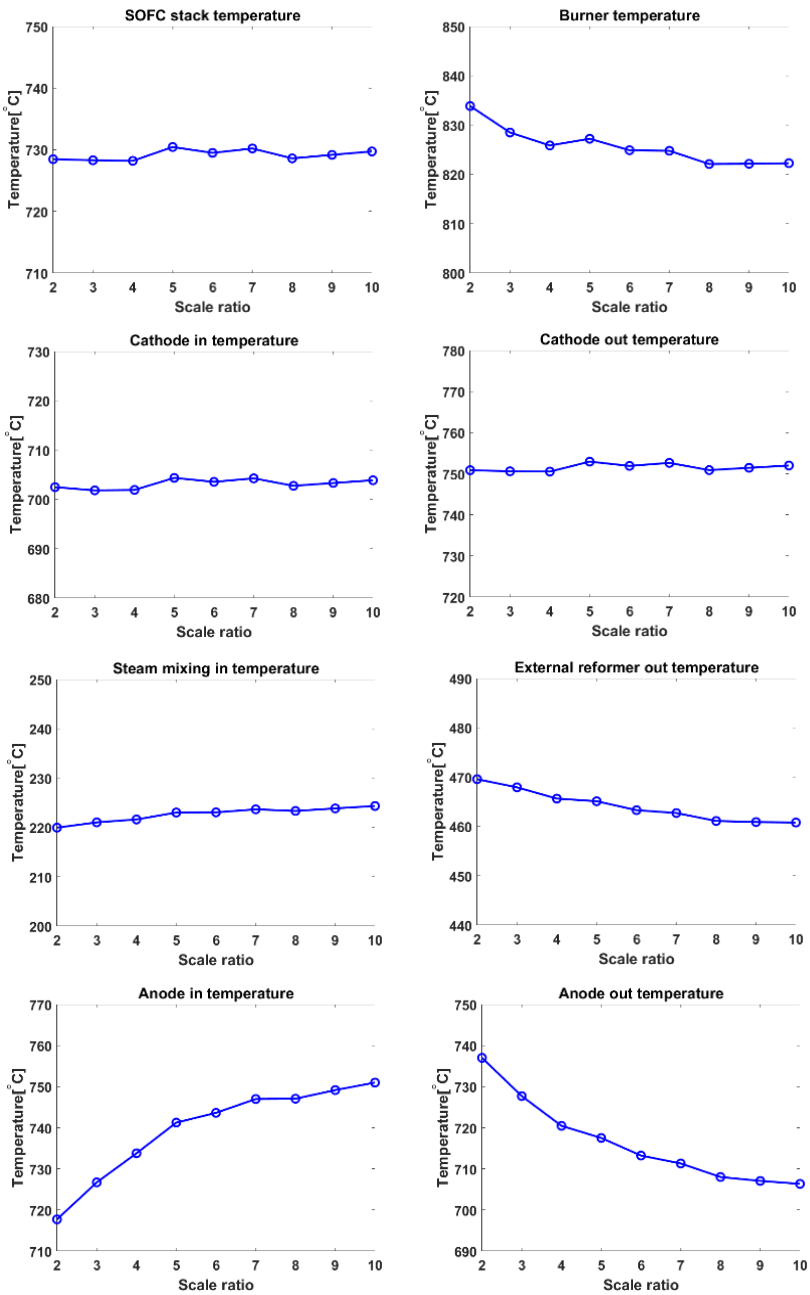

Figure 4.51. Temperature of each point with scale-up of system

As a result of scale-up, the temperature change at each point is shown in Figure 4.51. Except for changes in anode in and out, most of the temperatures were kept relatively constant.

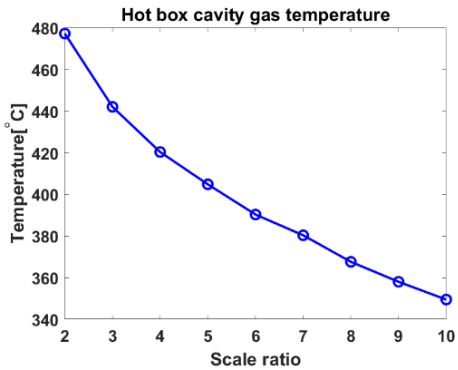

Figure 4.52. Hot box cavity gas temperature with scale-up

While the temperature at each point of the system was kept constant, the hot box cavity gas temperature decreased significantly as the system scaled up. This was because the amount of heat discharged to the system exhaust was increased rather than heat loss due to the increase in the amount of heat remaining in the system. Accordingly, the system total heat loss ratio to LHV fuel also decreased because the amount of heat transfer to the outside through the hot box wall decreased as the hot box cavity gas temperature decreased. Even considering the heat loss ratio to LHV fuel in the high temperature part where the main heat loss of the system occurred, the heat loss was reduced at most points. In the case of SOFC, the heat loss slightly increased, but the effect on the total heat loss was small. The heat loss ratio and hot box cavity gas temperature of the system are shown in Figure 4.52-4.54.

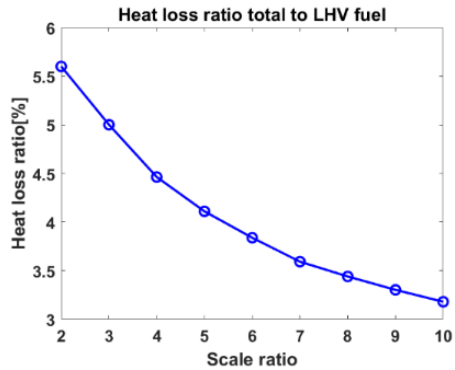

Figure 4.53. Total heat loss to LHV fuel with scale-up

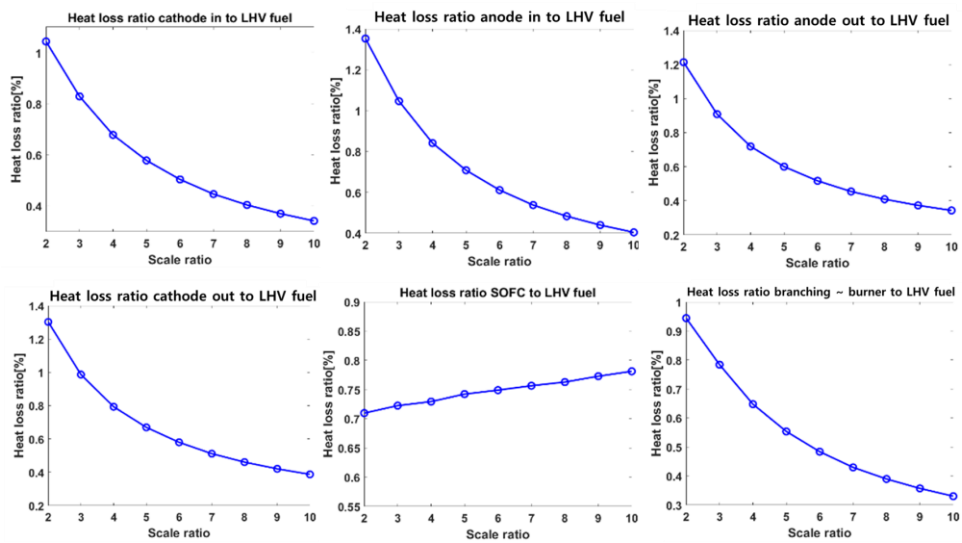

Figure 4.54. Heat loss ratio to LHV fuel of high temperature point with scale-up: heat loss decrease

In the end, it was confirmed that the amount of heat remaining in the system increased as the scale up increased, which means that there was a possibility to increase the branching ratio to the engine.

4.5.3.2.3. Improvement in system performance

The scale-up system also increased the amount of heat remaining in the system as the scale-up was performed. Accordingly, there was a possibility to increase the branching ratio to the engine, which might increase the system efficiency.

In the same method as the engine branching analysis performed previously, the anode off-gas was branched until the steam mixing in temperature reached 100°C while the operating temperature of the SOFC was fixed. The reference point for branching was taken as the maximum scale-up point, and the SOFC input condition of the reference point is shown in Table 4.15.

Table 4.15. Reference point of engine branching of scale up model

SOFC input condition	
NG input [lpm/kW]	354.2/208
SOFC current [A]	1700.74
Air flow rate [lpm]	6773.4

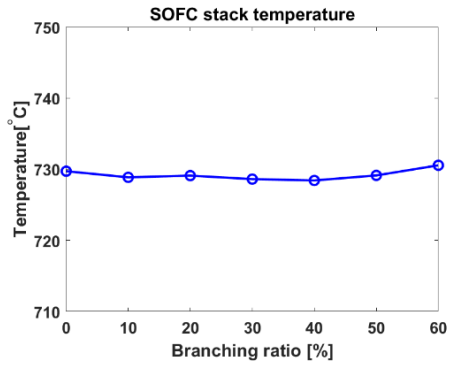

Figure 4.55. SOFC stack temperature with engine branching from scale-up point

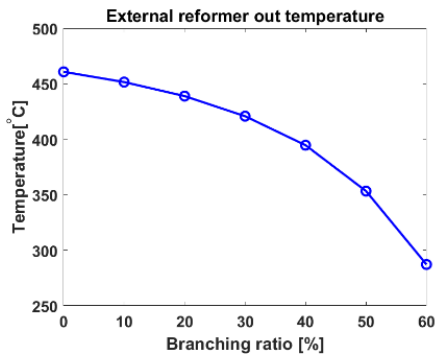

Figure 4.56. External reformer out temperature with engine branching from scale-up point

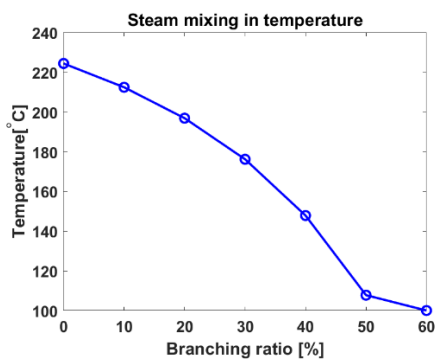

Figure 4.57. Steam mixing in temperature with engine branching from scale-up point

As the engine branching ratio was increased, the amount of heat remaining in the system was branched to the engine, and the amount of heat remaining gradually decreased. Before branching, heat was given to each BOP and then the remaining amount of heat was discharged to the system exhaust, but since the heat was divided and branched, the temperature of each BOP decreases. This is shown in Figure 4.56-4.57.

As a result, the maximum engine branching ratio of the scale up system was found to be 60% when the steam mixing in temperature became 100℃. This is 26%p higher than 5kW-class and 10%p higher than 10kW-class.

As the branching ratio increased, the temperature of the external reformer decreased, and accordingly, the internal reforming rate of SOFC increased and SOFC power decreased. However, when the engine efficiency was assumed to be 25%, the increase in engine power was found to be up to 12.13kW, which increased the total system power. As a result, the system efficiency increased by 3.46%p by the engine branching. This is shown in Figure 4.58-4.60.

Therefore, it was confirmed that the heat loss of the system could be reduced through power level up and scale-up, and the system efficiency could be increased by converting the reduced heat loss into the engine branching ratio.

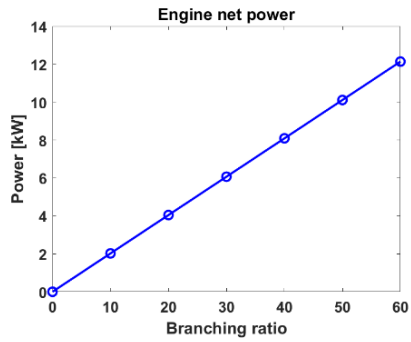

Figure 4.58. Engine net power expectation by engine branching from scale up point

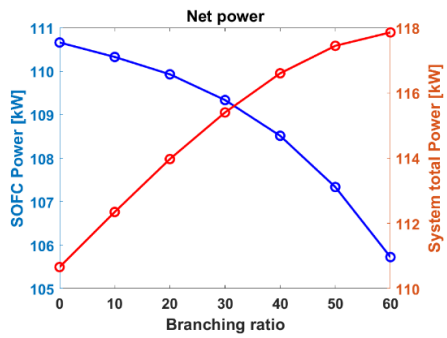

Figure 4.59. SOFC & system total power expectations by engine branching from scale up point

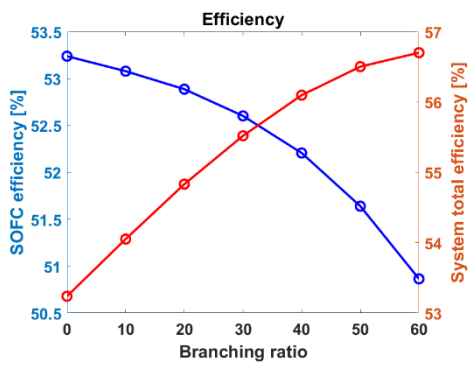

Figure 4.60. SOFC & system efficiency expectations by engine branching from scale up point

4.5.3.2.4. Exergy analysis

In this chapter, the results of exergy analysis are presented for the case of scale up and the case of increasing engine branching ratio.

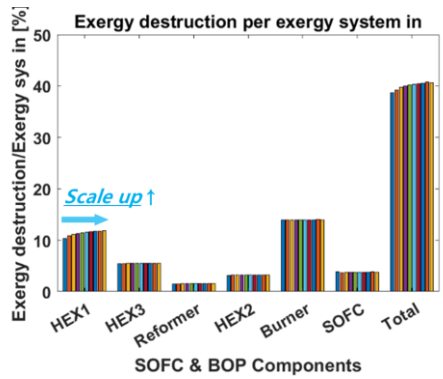

Figure 4.61. Exergy destruction of each component with respect to scale-up

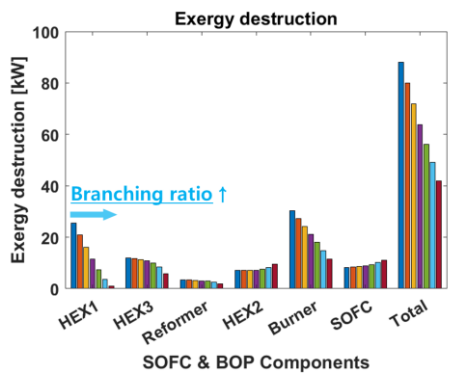

Figure 4.62. Exergy destruction of each component with respect to branching ratio

First, in the case of power level up, the temperature of both the hot side and the cold side of most heat exchangers increased, so that exergy destruction was kept constant. However, as for HEX 1, room temperature air was entrained into the cold side, but as the temperature of the system exhaust gas increased, the temperature difference between the high temperature part and the low temperature part of HEX 1 increased, confirming that exergy destruction increased. This is shown in Figure 4.48.

Second, as the engine branching ratio increased, exergy destruction decreased in HEX 1, HEX 3, and burner, where exergy destruction was significantly large. This is shown in Figure 4.49. In HEX 1 and HEX 3, as the engine branching ratio increased, the heat and temperature discharged to the system exhaust decreased. As a result, the temperature difference between the hot and cold side of the heat exchanger was reduced, and exergy destruction was reduced. On the other hand, in the case of burner, the external reforming rate decreased as the engine branching ratio increased, and it was confirmed that the specific heat of reformed gas flowing into the burner decreased. As a result, the temperature rise of the reformed gas in the burner was large, so the temperature of the anode in was maintained at a high temperature, and the temperature difference between the high and low temperatures of the burner was reduced, so that exergy destruction was reduced. Finally, it was confirmed that the thermal efficiency according to the first law of thermodynamics of the system could be increased through the additional power output of the engine by increasing the engine branching ratio, and at the same time, the efficiency according to the second law of thermodynamics could also be increased.

4.6. Discussion

In chapter 4, through the simulation model validated to the experimental results, heat loss, exergy, and performance prediction were analyzed by suggesting power level up, scale up, and increment of engine branching ratio as a method to improve system performance. In this process, it is necessary to discuss some of the validity and significance of this study, which are summarized as follows.

1. Are the simulation model validation results reasonable?
2. Is the assumption of 25% engine efficiency reasonable?
3. Is the system scale-up method reasonable?
4. When power level up and scale up, the total heat loss ratio to LHV fuel can be reduced by up to 50%, is it reasonable?

1. Simulation model validation results validity

It was difficult to obtain temperature data for more points due to security issues in the SOFC system, and accordingly, temperature validation was performed for only 8 points. In order to show a more accurate validation result, it is necessary to check the validating not only for temperature but also for heat transfer rate. Therefore, using the thermodynamic properties and power output of the input and output gas of the hot box, the system heat loss in the experiment and the simulation model were compared. As a result, it could be confirmed that both the direction of change and the absolute value were well validated as shown in Figure 4.63.

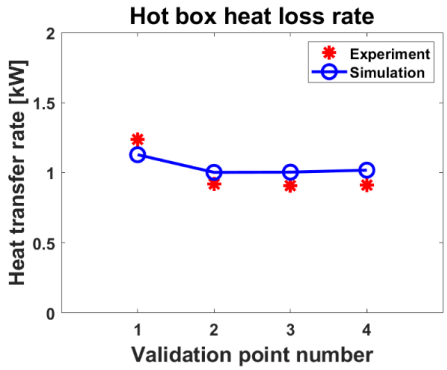

Figure 4.63. System heat loss rate validation results

2. Validity of assumption: Engine net indicated efficiency was fixed at 25%

In order to predict the engine performance while increasing the engine branching ratio in the case of power level up and scale up, the net indicated efficiency of the engine was fixed at 25%. Efficiency of an engine may vary depending on various conditions such as fuel composition and equivalence ratio, RPM, compression ratio, stroke to bore ratio, and intake temperature. Therefore, there is a limitation of this study in that it is necessary to verify through experiments in order to accurately predict the performance of the engine. However, due to the characteristics of the power generation system, the change in operating conditions was small compared to that of a vehicle, so that the operating conditions of the engine could be fixed through appropriate assumptions. Therefore, in predicting engine performance, the following assumptions were made to ensure validity of assuming that the engine efficiency was 25%.

1. The engine was scaled up with the same stroke to bore ratio as shown in Figure 4.64.

2. The engine RPM, compression ratio, equivalence ratio, and intake air temperature were assumed to be fixed under the same conditions as in the experiment.

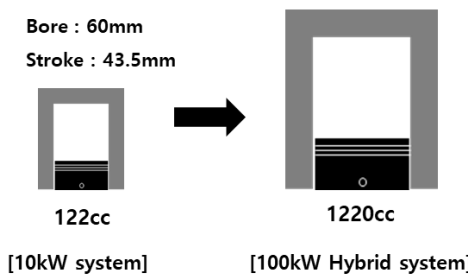

Figure 4.64. Engine displacement scale up method

Under the above assumptions, as the engine displacement increases, the surface to volume ratio of the engine decreases as shown in Figure 4.65, which generally means that the heat loss of the engine decreases. Therefore, there is a high possibility of increasing the thermal efficiency of the engine according to the scale up of the engine displacement. The actual engine efficiency needs to be confirmed through experiments, but for the realism of engine power prediction, the prediction was performed by fixing engine efficiency at 25%, which is the efficiency of the current engine, which is expected to have the lowest efficiency. Therefore, in actual system operation, a higher efficiency increase is expected than the simulation model results.

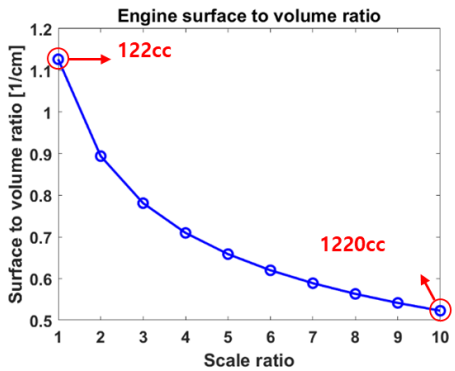

Figure 4.65. Engine surface to volume ratio according to engine displacement scale up

3. Validity of system scale up method

In this study, the maximum scale-up capacity with one hot box was assumed to be 100kW. In addition, as a method for system scale up, a method of stack scaling up by connecting the SOFC stack in parallel was used. Additionally, only the width and depth were scaled up according to the scale ratio in the current system, but it was necessary to confirm the validity of whether the appropriate hot box scale ratio was selected. Therefore, it was necessary to confirm the development direction of the actual SOFC manufacturers, and the validity of the scale-up used in this study could be confirmed through some data.

First, Bloom energy corporation developed a 1kW stack by stacking unit cells in series and connected them in parallel to make a module up to 50kW. In addition, it is aimed to scale up the stack module up to 75kW in the 2020s, so it was confirmed that the final goal of scale up in this study was realistically considered [33]. Second, the method of connecting the stack in parallel was confirmed as an

appropriate assumption because it has been studied not only by the bloom energy corporation, but also by Sunfire corporation [34] and Global thermoelectric corporation [35]. In general, when scaling up by increasing the cell size of the stack, the temperature gradient inside the cell increases, which can decrease the performance uniformity and durability. Additionally, when stacking stacks in series, there are technical difficulties due to sealing issues between cells [35]. Accordingly, it was found that a certain amount of stacked stack was developed as a unit stack and scaled up by connecting in parallel. Finally, it is necessary to verify the validity of the scale ratio used in the study. For this, the dimension of the 100kW system of Bloom energy corporation was investigated and compared with the dimension of the system scaled up to 100kW in this study. As a result, it was confirmed that the 100kW system scaled up according to the scale ratio used in this study had a dimension similar to that of the Bloom energy corporation's 100kW system, and the validity of the scale ratio was also confirmed. It is shown in Table 4.16.

Table 4.16. Dimension comparison of scaled up system with Bloom energy system

	Present system (MiCo hot box)	Scale-up system (100 kW)	Bloom energy 100 kW system [36]
Width [m]	1.845	5.83	5.69
Depth [m]	0.93	2.94	2.1336
Height [m]	1.86	1.86	2.0574

4. Validity of 50% decrement of total heat loss ratio to LHV fuel during power level up and scale up

(1) Power level up

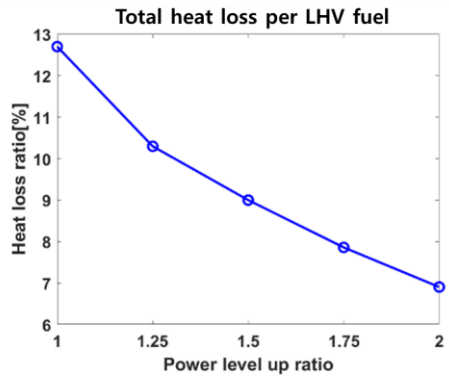

Figure 4.66. Total heat loss ratio to LHV fuel in case of power level up

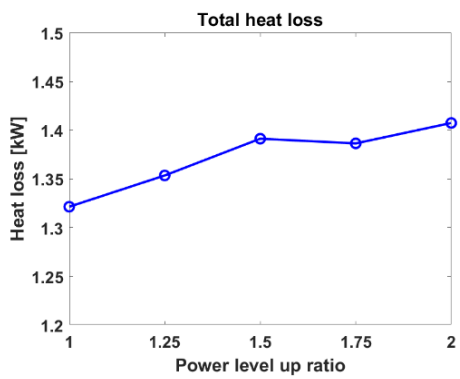

Figure 4.67. Total heat loss of system in case of power level up

As shown in Figure 4.66, if the power level was increased, the total heat loss ratio to LHV fuel was reduced up to 50% level. On the other hand, it can be seen in Figure 4.67 that the absolute value of the total heat loss for each power level slightly increased. In the same system component, if the fuel flow rate and the

SOFC loading current were increased, the heat production by exothermic reaction of the SOFC increased, so the temperature inside the system generally rose and the system heat loss increased. Accordingly, in case of power level up, total heat loss increased. However, since the temperature of the SOFC stack was fixed at 730°C, there was an effect that the maximum temperature of the system was limited, so there was a limit in the range of temperature increase compared to the amount of heat generated by the input fuel. Therefore, this led to the effect of reducing the heat loss compared to the LHV of fuel input, and the remaining heat was discharged to the system exhaust rather than the heat loss to the outside. This could be confirmed by increment of the mass flow rate and temperature of the system exhaust according to power level up in Figure 4.68. In this study, the performance improvement was predicted by increasing the branching ratio to the engine using this increasing system exhaust enthalpy.

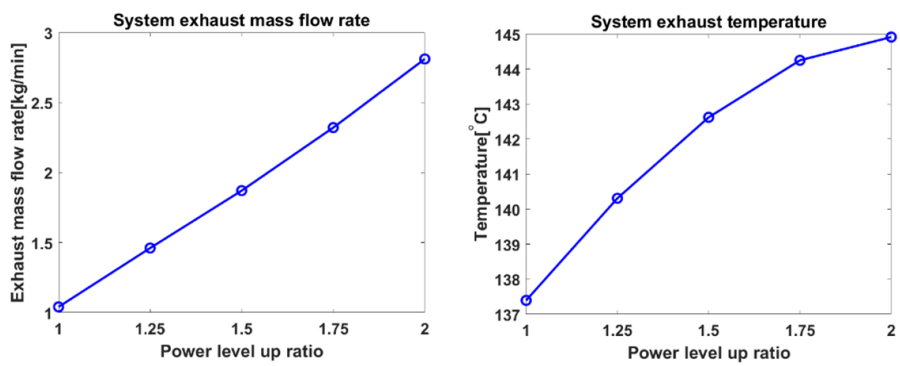

Figure 4.68. System exhaust mass flow rate and temperature in case of power level up

In addition, while the flow rate of the input fuel increased, the size of the hot box was maintained as it was, so the heat loss area of the hot box was maintained as it was. In other words, the hot box area per the input fuel flow was decreased, and it can be seen from Figure 4.69 that this value was reduced by about 50%. As a result, as the power level was increased, the amount of heat loss per input fuel flow could be reduced by up to 50%.

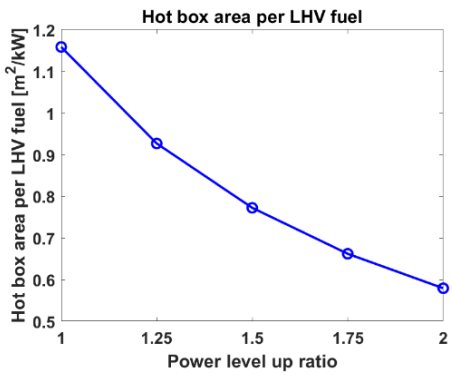

Figure 4.69. Hot box area per LHV fuel input in case of power level up

(2) Scale up

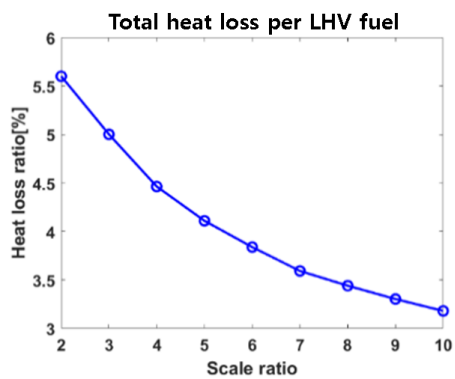

Figure 4.70. Total heat loss ratio to LHV fuel in case of scale up

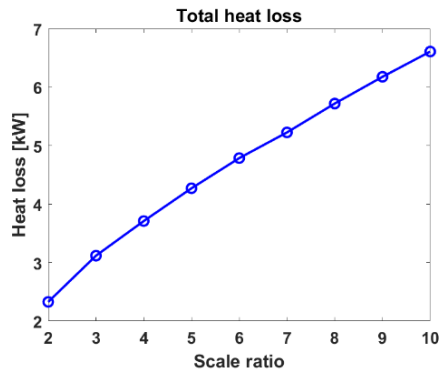

Figure 4.71. Total heat loss of system in case of scale up

As shown in Figure 4.70, if the scale ratio was increased, the total heat loss ratio to LHV fuel was reduced up to 50% level. On the other hand, it can be seen in Figure 4.71 that the absolute value of the total heat loss for each scale ratio increased. Similar to power level up case, if the fuel input and the SOFC loading current were increased, the heat generation of the SOFC increased, so the temperature inside the system rose and the system heat loss increased. Hence, the total heat loss increased. However, since the temperature of the SOFC stack was fixed at 730°C, there was an effect that the maximum temperature of the system was limited, so there was a limit in the range of temperature increase compared to the amount of heat generated by the input fuel. Therefore, this led to the effect of reducing the heat loss compared to the LHV of fuel input, and the remaining heat was discharged to the system exhaust rather than the heat loss to the outside. This could be confirmed by increment of the mass flow rate and temperature of the system exhaust according to scale up in Figure 4.72.

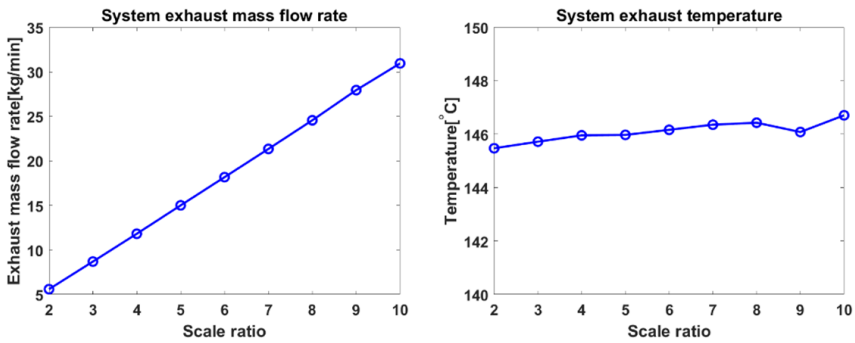

Figure 4.72. System exhaust mass flow rate and temperature in case of scale up

Unlike power level up, the size of the hot box increases according to the scale ratio in scale up of system. However, the hot box outer area increased smaller than the increment of the input fuel flow, which decreased the hot box area per the input fuel flow. As a result, the value of the hot box area per the input fuel flow was reduced by up to 50%, as shown in Figure 4.73. In addition, this meant that the system heat loss per the input fuel flow could be reduced by 50%. After all, this study is meaningful because it can increase the thermal efficiency of the system by reducing the heat loss area per unit fuel input when the stack is connected in parallel in the hot box and scaled up.

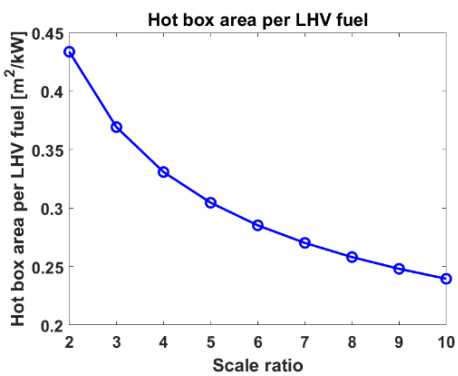

Figure 4.73. Hot box area per LHV fuel input in case of scale up

4.7. Conclusions

In chapter 4, through the simulation model validated to the experimental results, 1) Exploring the engine maximum branching ratio of the existing system, 2) System performance prediction, heat loss analysis, and exergy analysis through the power level up to 10kW power level and the maximum engine branching, 3) Suggesting a method for system scale up to 100kW power level, 4) System performance prediction, heat loss analysis, and exergy analysis through system scale up to 100kW power level and maximum branching of the engine were performed. As a result, a physics model that can simulate system was developed, a system design method to improve system performance was presented, and its validity was confirmed. A study was also conducted to predict the system performance in the improved system design and analyze the phenomenon to suggest an improvement method for the SOFC-Engine hybrid system capable of thermal self-sustainable operation. The detailed findings are summarized as follows.

1) It was possible to develop a simulation model that validated the results of the system integration experiment and considered the heat loss of system components and pipes, which was not considered in the previous SOFC-Engine hybrid system simulation studies.

2) The maximum engine branching ratio, which could not be confirmed through the system integration operation, could be confirmed through the simulation model, and the system efficiency improvement through the engine in the current system was predicted. The engine power output of 344W and system efficiency improvement of 2.2%p were predicted at the

maximum engine branching rate of 34%.

3) The amount of heat loss at each location was calculated through system heat loss analysis, and the main heat loss locations of the system were analyzed. Based on this, it was possible to suggest a method to reduce heat loss. In addition, it was confirmed that the heat loss decreased by about 50% in the case of power level up and scale up, and this could be explained by the 50% decrease in the heat loss area per system fuel input. As a result, a system design improvement method to reduce system heat loss was suggested.

4) A method for simulating system scale up was presented in a similar way to the actual system scale up method.

5) For the case of power level up and scale up, the maximum engine branching ratio of anode off-gas was searched, and the engine branching ratio was increased by 16%p and 26%p, respectively, compared to the 5kW system. Through this, it was confirmed that the efficiency of the system could be up to 56.7% at the present fuel utilization rate. In addition, branching to the engine was possible even at 82.16% of the fuel utilization rate where SOFC has the maximum efficiency point, and the system efficiency of 63% could be predicted through the engine branching ratio of 48%.

Chapter 5. Conclusions

In this study, two types of SOFC-Engine hybrid system were investigated to increase system efficiency and achieve thermal self-sustainable operation. First, an analysis of the demonstration operation of the SOFC-SAI engine hybrid system was performed. SAI engine has been analyzed in terms of operability, operable area, and performance through engine alone experiment and simulation studies in previous studies. In the previous study of Kim [24], system configuration optimization was proposed, but it was not carried out as a demonstration operation. Therefore, it was attempted to confirm the possibility of thermal self-sustainable operation of the SOFC-SAI engine hybrid system through a demonstration operation (chapter 3). Furthermore, in the SOFC-Engine hybrid system, since the demonstration operation considering the start-up operation was not performed in previous studies, the demonstration operation was performed to analyze the operating characteristics and performance of the system in the start-up operation and to secure the control strategy and data (Chapter 3). As a result, it was possible to confirm the system performance from start-up operation to the design point operation and establish a control strategy. Accordingly, a system configuration diagram capable of thermal self-sustainable operation was devised and research on a new system was conducted.

The new system configuration is composed of a hybrid system in which the SI engine is combined with the SOFC standalone system capable of thermal self-sustainable operation. It was called SOFC standalone system with SI engine hybrid system. Using the burner of the SOFC standalone system, a system in which the anode off-gas is partially branched by the engine was selected while the possibility of thermal self-sustainable operation of the system was already secured. There

were difficulties in analyzing various operating points and improvement methods through experiments, so a physics-based simulation model that simulates the experimental results was developed. In particular, a simulation model was developed considering the heat loss of the system component, which was not considered in the previous study, and the system performance considering the heat balance was predicted. As a result, the system efficiency was improved by suggested power level up and scale up methods and efficiency improvements of 3.22%p and 3.46%p was achieved through the additional power output of the engine, respectively. Finally, it can be said that it is meaningful as a study that suggests methods to improve system performance and design. The research objectives of Chapter 3 and Chapter 4 are as follows, and detailed findings are summarized below.

Guiding questions (Objectives)

(1) 5-kW SOFC-SAI engine hybrid system (in chapter 3)

1. Does the SOFC-SAI engine hybrid system be operated and controlled successfully from start-up to design point?

   Engine control:

   By determining the type and flow rate of supply gas suitable for each stage of the start-up operation, and controlling engine RPM in real time, the engine intervened in the entire start-up operation process and was successfully operated. Through engine RPM control, the engine was able to operate while maintaining the engine intake pressure at 1 bar and at a constant equivalence ratio (phi: ~0.85). In addition, the spark ignition timing that can produce the maximum indicated net power of the engine was found through spark ignition timing control, which can be utilized for spark control in the future.

2. What are characteristics of each process and performance?

   System performances:

   The undiluted fully reformed gas, which was not performed in the engine-alone experiment of previous study, was successfully combusted through the engine. It was confirmed that spark-assisted auto-ignition was possible to perform stable combustion with a COV of 3.55% or less, and it was confirmed that the engine could produce significant power of 660W with net indicated power and 28.7% with net indicated efficiency during the start-up process. In the SOFC loading process, as the fuel utilization rate increased, the engine spark ignition timing was advanced, so that the net

indicated power of the engine was constantly secured at 530W, and combustion stability was also secured at a certain level. However, it was confirmed that the COV of the engine increased from 2% to 12% as the dilution composition ratio of the anode off-gas increased, and the combustion stability of the engine was slightly decreased. Therefore, it is necessary to control the dilution composition ratio of the anode off-gas in order to secure combustion stability of the engine. As a result, the possibility of increasing the system efficiency by 5.05%p (based on engine net indicated power) was confirmed through the engine.

3. Does the SOFC-SAI engine hybrid system be operated thermally self-sustainable?

Limitation:

An electric furnace and heater, which was used to provide the thermal energy required for start-up operation, was also used for design point operation. As a result of calculation through the experimental data, it was confirmed that at least 3.39 kW of thermal energy was provided and considering all the heat loss not reflected in the calculation, it was confirmed that the thermal energy provided to the system was significantly large. This could lower the system efficiency from 54.6% to 41.3%, thus fading the meaning of system development. Nevertheless, the inlet temperature of the anode and cathode was lower than that of the SOFC stack by more than 100°C, possibly causing a temperature gradient inside the stack. As a result, it means that the thermal self-sustainable operation of the SOFC-SAI engine hybrid system is impossible, and the need to propose a new system configuration diagram capable of self-heat

operation was confirmed.

(2) SOFC standalone system with SI engine hybrid system (in chapter 4)

1. Does the simulation model be developed to emulate the physics of real system?

   Simulation model development

   Physics-based simulation model that validated the results of the system integration experiment and considered the heat loss of system components and pipes was developed, which was not considered in the previous SOFC-Engine hybrid system simulation studies. Almost all components were modeled based on zero dimension and steady state. Thermodynamic properties of each point were calculated by using Cantera [29] and GRI 3.0 mechanism [30] and MATLAB.

2. How much amount of anode off-gas can be branched to engine in the present system?

   Searching for maximum contribution of engine in the present system

   The maximum engine branching ratio, which could not be confirmed through the system integration operation, could be confirmed through the simulation model, and the system efficiency improvement through the engine in the current system was predicted. The engine power output of 344W and system efficiency improvement of 2.2%p were predicted at the maximum engine branching rate of 34%.

3. How to maximize the branching ratio to engine while maintaining thermally self-sustainable operation by reducing heat loss?

   For the case of power level up and scale up, the maximum engine branching ratio of anode off-gas was searched, and the engine branching ratio was increased by 16%p and 26%p, respectively, compared to the 5kW system. Through this, it was confirmed that the efficiency of the system could be up to 56.7% at the present fuel utilization rate. In addition, branching to the engine was possible even at 82.16% of the fuel utilization rate where SOFC has the maximum efficiency point, and the system efficiency of 63% could be predicted through the engine branching ratio of 48%.

4. How to design and operate the system to improve the system performance?

   Heat loss analysis and suggestion of reducing heat loss

   1) The amount of heat loss at each location was calculated through system heat loss analysis, and the main heat loss locations of the system were analyzed. Based on this, it was possible to suggest a method to reduce heat loss. In addition, it was confirmed that the heat loss decreased by about 50% in the case of power level up and scale up, and this could be explained by the 50% decrease in the heat loss area per system fuel input. As a result, a system design improvement method to reduce system heat loss was suggested.

   2) A method for simulating system scale up was presented in a similar way to the actual system scale up method.

Appendix A. SOFC simulation modeling based on steady state with considering heat transfer

Current density [5]

$$j = \frac{\dot{n}_{O_2}(2n_e)F}{n_{cell}A_{cell}} \quad \text{(A.1)}$$

Nernst equation [5]

$$V_{nernst} = E_0 + \frac{RT}{n_eF} ln \frac{(p_{an,H_2}/P_{atm})(p_{ca,O_2}/P_{atm})^{0.5}}{p_{an,H_2O}/P_{atm}} \quad \text{(A.2)}$$

Ohmic loss [37]

$$\rho_{ca} = 8.114 \cdot 10^{-5}\exp(^{600}/_{T_{SOFC}}) \quad \text{(A.3)}$$

$$\rho_{an} = 2.980 \cdot 10^{-5}\exp(^{1392}/_{T_{SOFC}}) \quad \text{(A.4)}$$

$$\rho_{el} = 2.940 \cdot 10^{-5}\exp(^{10350}/_{T_{SOFC}}) \quad \text{(A.5)}$$

$$\rho_{int} = 1.256 \cdot 10^{-3}\exp(^{4690}/_{T_{SOFC}}) \quad \text{(A.6)}$$

$$V_{ohm} = j(\rho_{ca}\delta_{ca} + \rho_{an}\delta_{an} + \rho_{el}\delta_{el} + \rho_{int}\delta_{int}) \quad \text{(A.7)}$$

Activation loss [5, 38]

$$V_{act} = -\frac{2RT_{SOFC}}{n_e F} sinh^{-1}(\frac{j}{2j_0}) \quad \text{(A.8)}$$

$$j_{0,an} = \gamma_{an}\left(\frac{p_{an,H_2}}{P_{atm}}\right)\left(\frac{p_{an,H_2O}}{P_{atm}}\right)\exp(-\frac{E_{act,an}}{RT_{SOFC}}) \quad \text{(A.9)}$$

$$j_{0,ca} = \gamma_{ca}\left(\frac{p_{ca,O_2}}{P_{atm}}\right)^{0.25}\exp(-\frac{E_{act,ca}}{RT_{SOFC}}) \quad \text{(A.10)}$$

Concentration loss [5, 39]

$$D_{K,i} = 97\gamma\sqrt{\frac{T_{SOFC}}{MW_i}} \quad \text{(A.11)}$$

$$D_{H_2,H_2O} = \frac{3.64\cdot 10^{-8}}{p_{an}/P_{atm}}\left(\frac{T_{SOFC}}{\sqrt{T_{c,H_2}T_{c,H_2O}}}\right)^{2.334}(\frac{(P_{c,H_2}P_{c,H_2O})^{\frac{1}{3}}}{(T_{c,H_2}T_{c,H_2O})^{-\frac{5}{12}}})(\frac{1}{MW_{H_2}}+\frac{1}{MW_{H_2O}})^{\frac{1}{2}} \quad \text{(A.12)}$$

$$D_{O_2,N_2} = \frac{2.745\cdot 10^{-8}}{p_{ca}/P_{atm}}\left(\frac{T_{SOFC}}{\sqrt{T_{c,N_2}T_{c,O_2}}}\right)^{1.823}(\frac{(P_{c,N_2}P_{c,O_2})^{\frac{1}{3}}}{(T_{c,N_2}T_{c,O_2})^{-\frac{5}{12}}})(\frac{1}{MW_{N_2}}+\frac{1}{MW_{O_2}})^{\frac{1}{2}} \quad \text{(A.13)}$$

$$D_{H_2}{}^{eff} = (\frac{1}{D_{H_2,K}^{eff}}+\frac{1}{D_{H_2,H_2O}^{eff}})^{-1} \quad \text{(A.14)}$$

$$D_{H_2O}{}^{eff} = (\frac{1}{D_{H_2O,K}^{eff}}+\frac{1}{D_{H_2,H_2O}^{eff}})^{-1} \quad \text{(A.15)}$$

$$D_{O_2}{}^{eff} = \left(\frac{1}{D_{O_2,K}^{eff}} + \frac{1}{D_{O_2,N_2}^{eff}}\right)^{-1} \quad \text{(A.16)}$$

$$D_{an}{}^{eff} = (p_{an,H_2O}/p_{an}) D_{H_2}{}^{eff} + (p_{an,H_2}/p_{an}) D_{H_2O}{}^{eff} \quad \text{(A.17)}$$

$$D_{ca}{}^{eff} = D_{O_2}{}^{eff} \quad \text{(A.18)}$$

$$\alpha_{O_2} = \frac{D_{O_2,K}{}^{eff}}{D_{O_2,K}{}^{eff} + D_{O_2,N_2}{}^{eff}} \quad \text{(A.19)}$$

$$V_{con,an} = \frac{-RT_{SOFC}}{n_e F} \ln\left(\frac{1 - j\left(\frac{RT_{SOFC}}{n_e F}\right)\frac{\delta_{an}}{D_{an}{}^{eff} p_{an,H_2}}}{1 + j\left(\frac{RT_{SOFC}}{n_e F}\right)\frac{\delta_{an}}{D_{an}{}^{eff} p_{an,H_2O}}}\right) \quad \text{(A.20)}$$

$$V_{con,ca} = \frac{-RT_{SOFC}}{2n_e F} \ln\left(\frac{\frac{p_{ca}}{\alpha_{o_2}} - \left(\frac{p_{ca}}{\alpha_{o_2}} - p_{ca,O_2}\right)\exp\left(\frac{RT_{SOFC}}{2n_e F}\left(\frac{\alpha_{o_2}\delta_{ca}}{D_{ca}^{eff} p_{ca}}\right) j\right)}{p_{ca,O_2}}\right) \quad \text{(A.21)}$$

Cell voltage [5]

$$V_{SOFC} = V_{nernst} - V_{act,an} - V_{act,ca} - V_{ohm} - V_{con,an} - V_{con,ca} \quad \text{(A.22)}$$

Table A.1. Specifications of the SOFC parameters [24]

Parameter		Value
Activation energy [J/mol]	$E_{act,an}$	$95*10^3$
	$E_{act,ca}$	$95*10^3$
Coefficients of exchange current density [A/m^2]	γ_{an}	$1*10^{11}$
	γ_{ca}	$1*10^{11}$
Thickness [μm]	δ_{an}	500
	δ_{ca}	50
	δ_{el}	10
	δ_{int}	20
Pore radius [μm]	r_{an}, r_{ca}	0.5
Porosity [%]	ε_{an}, ε_{ca}	9
Tortuosity [-]	τ_{an}, τ_{ca}	6

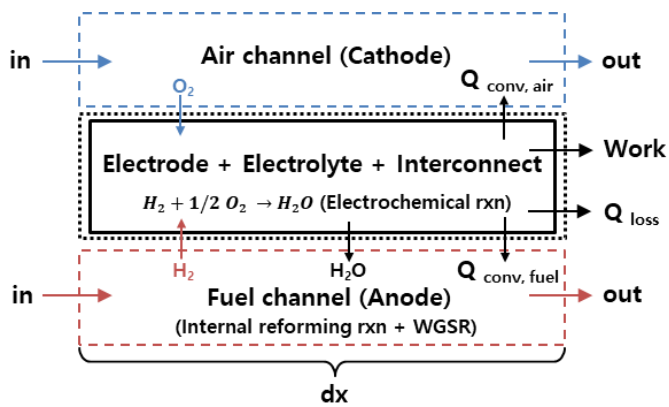

Figure A.1. SOFC model description

References

[1] Florides G, Christodoulides P. Global warming and carbon dioxide through sciences. Environment International. 2009;35:390-401.

[2] Anderson J, Rode D, Zhai H, Fischbeck P. Reducing carbon dioxide emissions beyond 2030: Time to shift U.S. power-sector focus. Energy Policy. 2021;148:111778.

[3] Annual Energy Outlook 2022. U.S. Energy Information Administration, 2022.

[4] Stambouli A, Traversa E. Solid oxide fuel cells (SOFCs): a review of an environmentally clean and efficient source of energy. Renewable and Sustainable Energy Reviews. 2002;6:433-55.

[5] O'hayre R, Cha S-W, Colella W, Prinz FB. Fuel cell fundamentals: John Wiley & Sons;2016.

[6] Wee JH. Contribution of fuel cell systems to CO_2 emission reduction in their application fields. Renewable and Sustainable Energy Reviews. 2010;14:735-44.

[7] Choi W. Simulation and Experiment for a Design of a Solid Oxide Fuel Cell-Homogeneous Charge Compression Ignition Engine Hybrid System: Mechanical and Aerospace Engineering of Seoul National University;2018.

[8] Kobayashi Y, Ando Y, Nishiura M, Kishizawa H, Iwata M, Matake N, Tomida K. Recent Progress of SOFC Combined Cycle System with Segmented-In-Series Tubular Type Cell Stack at MHI. ECS Transactions. 2013;57:53.

[9] Veyo S, Vora S, Litzinger K, Lundberg W. Status of Pressurized SOFC/Gas Turbine Power System Development at Siemens Westinghouse. ASME Turbo Expo 2002: Power for Land, Sea, and Air. 2002.

[10] Buonomano A, Calise F, d'Accadia MD, Palombo A, Vicidomini M. Hybrid solid oxide fuel cells-gas turbine systems for combined heat and power: a review. Applied Energy. 2015;156:32-85.

[11] Ahn KY, Lee YD, Kang SG, Lee SM, Kim HS, Cho JH, Kim MK, Park SH, Song SJ, Song HH. Fuel cell-engine hybrid system. Google patents. 2015.

[12] Park SH, Lee YD, Ahn KY. Performance analysis of an SOFC/HCCI engine hybrid system: System simulation and thermo-economic comparison. International Journal of Hydrogen Energy. 2014;39:1799-810.

[13] Lee YD, Ahn KY, Morosuk T, Tsatsaronis G. Exergetic and exergoeconomic evaluation of a solid-oxide fuel-cell-based combined heat and power generation system. Energy conversion and management. 2014;85:154-64.

[14] Lee YD. Thermodynamic, economic and environmental evaluation of solid-oxide-fuel-cell hybrid power-generation systems: Technische Universitat Berlin; 2015.

[15] Lee YD, Ahn KY, Morosuk T, Tsatsaronis G. Exergetic and exergoeconomic evaluation of an SOFC-Engine hybrid power generation system. Energy. 2018;145:810-22.

[16] Kang S, Ahn KY. Dynamic modeling of solid oxide fuel cell and engine hybrid system for distributed power generation. Applied Energy. 2017;195:1086-99.

[17] Choi W, Kim J, Kim Y, Kim S, Oh S, Song HH, Experimental study of homogeneous charge compression ignition engine operation fueled by emulated solid oxide fuel cell anode off-gas. Applied Energy. 2018;229:42-62.

[18] Choi W, Kim J, Kim Y, Song HH, Solid oxide fuel cell operation in a solid

oxide fuel-cell-internal combustion engine hybrid system and the design point performance of the hybrid system. Applied Energy. 2019;254:113681.

[19] Heywood JB. Internal combustion engine fundamentals. 1988.

[20] Choi W. Composition-considered Woschni heat transfer correlation: Findings from the analysis of over-expected engine heat losses in a solid oxide fuel cell-internal combustion engine hybrid system. Energy. 2020;203:117851.

[21] Kim YS, Lee YD. System integration and proof-of-concept test results of SOFC-engine hybrid power generation system. Applied Energy. 2020;277:115542

[22] Koo T, Kim YS, Lee YD, Yu S, Lee DK, Ahn KY. Exergetic evaluation of operation results of 5-k-W-class SOFC-HCCI engine hybrid power generation system. Applied Energy. 2021;295:117037.

[23] Hellström E, Stefanopoulou AG, Jiang L. Cyclic variability and dynamical instabilities in autoignition engines with high residuals. IEEE Transactions on Conrol Systems Technology. 2013;21:1527-36.

[24] Kim J. System Design and Optimal Operation for a Hybrid System of a Solid Oxide Fuel Cell and an Internal Combustion Engine Using Spark-assisted Ignition: Mechanical and Aerospace Engineering of Seoul National University;2019.

[25] Kim J, Kim Y, Choi W, Ahn KY, Song HH. Analysis on the operating performance of 5-kW class solid oxide fuel cell-internal combustion engine hybrid system using spark-assisted ignition. Applied Energy. 2020;260:114231.

[26] Kattke K, Braun R. Implementing Thermal Management Modeling Into SOFC System Level Design. ASME 2010 8th International Fuel Cell Science, Engineering and Technology Conference. 2010;2:295-308.

[27] Song H, Edwards C. Understanding chemical effects in low-load-limit extension of homogeneous charge compression ignition engines via recompression reaction. International Journal of Engine Research. 2009;10:231-50

[28] Korea Gas Corporation homepage; URL http://www.kogas.or.kr.

[29] Goodwin DG, Moffat HK, Speth RL. Cantera: An object-oriented software toolkit for chemical kinetics, thermodynamics, and transport processes. Caltech, Pasadena, CA. 2009.

[30] Smith GP, Golden DM, Frenklach M, Moriatry NW, Eiteneer B, Goldenberg M, Bowman CT, Hanson RK, Song S, Gardiner Jr W. GRI-Mech 3.0, 1999. URL http://www.me.berkeley.edu/gri_mech. 2011.

[31] Incropera FP, Dewitt DP, Bergman TL, Lavine AS. Fundamentals of heat and mass transfer: John Wiley & Sons; 2011.

[32] KCC Corporation homepage; URL http://www.kccworld.co.kr.

[33] A primer to understanding fuel cell power module life, bloom energy.

[34] Report on large scale manufacturing strategy for solid oxide fuel cells (SOFC), ComSos, 2019.

[35] Rastler D. Scale-up potential of solid oxide fuel cells technologies: An assessment of technical and economic factor, EPRI, 2005.

[36] Goodman B, Bosowski N, Sanford T. The bloom box: An investigation into the bloom box fuel cell, Worcester polytechnic institute, 2011.

[37] Bessette NF, Wepfer WJ, Winnick J. A mathematical model of a solid oxide fuel cell. Journal of the Electrochemical Society. 1995;142:3792-800.

[38] Costamagna P, Honegger K. Modeling of solid oxide heat exchanger integrated stacks and simulation at high fuel utilization. Journal of the Electrochemical Society. 1998;145:3995-4007.

[39] Chan S, Khor K, Xia Z. A complete polarization model of a solid oxide fuel cell and its sensitivity to the change of cell component thickness. Journal of power souces. 2001;93:130-40.

국문초록

고체산화물 연료전지(SOFC)-엔진 하이브리드 시스템은 SOFC의 애노드오프가스를 이용하여 엔진에서 연소함으로써 추가 출력을 얻고 시스템 효율을 향상시키는 것이 목적이다. 지금까지 SOFC-엔진 하이브리드 시스템은 SOFC-가스터빈 하이브리드 시스템의 연구 방향과 비슷하게 시스템의 구성도 제안, 다양한 운전점에서의 성능과 운전 영역 확인, 실증 운전의 순서로 연구가 수행되어 왔다. 이 과정에서 구성도 변경을 진행하고 엔진의 연소 방식을 변경하며 시스템의 운전 영역을 확장하고 성능을 개선하기 위한 방안들을 제시하며 선행 연구들이 수행되었다.

SOFC-엔진 하이브리드 시스템은 연구 초기 SOFC-HCCI 엔진 하이브리드 시스템으로 연구가 시작되었고, 시뮬레이션 분석, 실험적 분석, 하이브리드 시스템 통합 운전을 통한 실증의 순서로 연구가 진행되었다. 그러나 결과적으로 HCCI 엔진은 변화하는 운전점에 대응하여 엔진 연소를 제어하기 어려웠고, 동시에 실증 운전을 통해 시스템 자열 운전이 어렵다는 것이 확인되었다. 따라서 엔진의 연소 제어 용이성을 확보하고, 시스템의 열 활용도를 높이기 위해 엔진의 연소 방식을 HCCI에서 스파크-어시스트 점화(SAI) 방식으로 변경하였고, 엔진 단독 실험과 연료전지 시스템 시뮬레이션 모델을 통해 시스템의 설계점에서의 운전 가능성과 성능에 대한 선행 연구가 수행되었다.

이에 본 연구는 SOFC-SAI (Spark-assisted auto-ignition) 엔진 하이브리드 시스템을 이용하여 시동 운전에서부터 설계점까지의 성능과 운전 특성을 분석하고 시동 운전 전략을 수립하기 위한 실증 실험을 수행하였다. 또한 시스템의 한계점 (자열 운전의 불가능)을 분석하고, 새로운 시스템 구성도를 고안하여 자열 운전이 가능한 실증 운전을 수행하였고 이를 이용하여 시뮬레이션 모델 개발과 연구를 수행하였다. 최종적으로 시뮬레이션 연구를 통해 시스템의 열 손실 분석을 수행하고 시스템의 열 손실 및 성능을 개선할 수 있는 개선 방안을 제시하고 분석하는 것을 목표로 하였다.

연구의 첫 번째 단계로 SOFC-SAI 엔진 하이브리드 시스템의 통합 운전을 통한 실험적 연구가 수행되었다. 이는 스파크 어시스트 점화 방식을 이용한 최초의 SOFC-엔진 하이브리드 시스템 실증 운전으로, 실험은 실제 상용화 단계에서의 운전을 고려하여 시동 운전에서부터 운전 설계점까지 전과정에 대해 수행되었다. 엔진이 하이브리드 시스템의 중간에 위치하기 때문에 시스템의 상용화를 위해서는 시동 운전에서의 엔진의 성능과 운전 특성 그리고 제어 가능성을 모두 확인할 필요가 있었다. 결과적으로, 시스템은 약 35시간의 운전 시간 동안 SOFC, 엔진 모두 안정적인 작동을 하였다. 시동 운전 전 과정에 있어서 SOFC의 다양한 운전점에 대해 엔진으로 유입되는 부피 유량, 온도를 고려하여 엔진 흡기 압력을 상압 (1bar)로 유지할 수 있도록 엔진의 회전 속도 (RPM)를 실시간으로 대응할 수 있었다. 또한 다양한 운전점에 대해 엔진의 최대 출력 (Maximum brake torque)을 낼 수 있는 점화 타이밍 (Spark timing)으로 적절하게 제어할 수 있었다. 그리고 시동 운전 과정에서 SOFC의 부하 운전에 의해 희석되지 않은 개질 가스를 엔진에서 연소할 필요가 있는데, 이 과정에서의 연소도 안정적으로 (COV 5% 이하)

발생하는 것을 확인하였다. 이 과정에서 엔진의 배기 열과 애노드오프가스의 열 에너지를 이용한 2단계의 개질 과정을 통해 외부 개질율 12%를 달성할 수 있음을 확인하였다. 설계점에서의 운전에서는 SOFC는 5.2kW, 엔진은 530W (Indicated net power)로 기존 연구에서의 엔진 단독 실험 결과와 일치하는 결과를 보였고, SOFC의 부하를 증가시킴과 동시에 엔진으로 유입되는 연료의 불활성 가스 성분 (H_2O, CO_2)의 비율이 증가하여 엔진 연소 안정성을 의미하는 COV 값이 12%까지 증가하는 것을 확인하였다. 결과적으로 엔진을 통해 시스템의 열효율이 5%p 향상될 수 있음을 확인하였다. 이러한 성능을 확보할 수 있었지만 실험 결과 시스템에서 많은 열 손실이 발생하여, 이를 보상하고 안정적으로 운전하고자 스택 상하부에 전기로와 캐소드 공기 라인에 전기 히터를 추가하여 운전을 하였다. 결과적으로 설계점에서도 시스템 운전은 전기 히터와 전기로에 의존하여 3.4kW가 넘는 열량을 제공받았고, 애노드오프가스에서도 약 600W의 열 손실이 발생하였다. 결론적으로 해당 구성도의 실험 셋업으로는 시스템 자열 운전이 불가능함을 확인하였다.

연구의 두 번째 단계로 앞선 구성도의 한계점을 해결하고자 자열 운전이 가능하도록 변경된 시스템 구성도를 제안하였다. 기존 SOFC 단독 시스템의 구성도를 유지하고, 애노드 후단에 분기 밸브를 추가로 설치하여 엔진과 버너로 애노드오프가스가 분기되어 공급되도록 하였다. 새롭게 고안한 구성도를 이용해 하이브리드 시스템을 구축하고 실증 운전을 수행하여 자열 운전이 가능한 시스템을 개발하였다. 그러나 시스템 운전 안정성을 위해 추가한 스택 (기존 시스템 대비 2개의 스택 추가)만큼 추가 전력을 생산하지 못하였고, 엔진으로의 분기율 또한 23%에서 제한되어 운전이 수행되었다.

이에 따라 엔진으로의 최대 분기율을 예측하고 시스템의 개선 방안을 분석하기 위해 실증 운전의 다양한 운전점을 기반으로 하이브리드 시스템을 모사할 수 있는 시뮬레이션 모델을 개발하였다. 특히 이전의 연구들은 모든 배관과 장비들을 단열로 가정하고 시뮬레이션 모델을 개발하였는데, 본 연구에서는 SOFC와 배관에서의 열 손실을 계산할 수 있도록 열전달 모델을 포함한 시뮬레이션 모델을 개발하였다. 또한 이렇게 개발한 시뮬레이션 모델을 실증 운전의 4개의 운전점에 정합하여 모델의 신뢰도와 확장성을 확보하였다. 시뮬레이션 모델에 적용된 열전달 모델을 통해 시스템 핫박스와 외부와의 대류 열전달, 복사 열전달을 고려할 수 있었다. 핫박스 내부에서는 "Cavity 가스" 라는 개념을 도입하여 cavity 가스와 시스템 내부의 배관 및 SOFC가 대류 열전달을 수행하도록 하였다. 또한 모든 배관에서 시스템에 투입되는 연료 및 공기의 유량, 열역학적 물성치를 고려하여 Re, Pr, Nu 수가 계산이 되도록 하였다. 이를 통해 변화하는 운전 조건에 대해 배관 내부 유동의 대류 열전달 계수가 변화할 수 있도록 모델링을 하여 실제 열전달 물리 현상을 최대한 모사할 수 있도록 하였다.

마지막으로, 개발한 시뮬레이션 모델을 통해 열 손실 분석을 수행하였고, 열 손실을 줄이고 시스템 성능을 개선하기 위한 방안을 제시하여 시스템 성능 향상에 대해 분석을 하였다. 몇 가지 가정과 제한 조건을 통해 현재 시스템에서의 최대 엔진 분기율을 계산하여 34%의 분기율이 계산되는 것을 확인하였다. 그리고 최대 엔진 분기율에서 시스템 효율이 2.32%p 증가할 수 있음을 확인하였다. 열 손실을 줄이고 시스템 성능을 향상하기 위한 방안으로 현재 시스템에서의 power level을 올리는 방법과 시스템 scale-up 방법을 제안하였고, 결과적으로 투입 연료 발열량 대비 열 손실은 감소하였고 각각

50%, 60%의 엔진 분기율을 확보할 수 있음을 확인하였다. 그리고 엔진으로의 분기를 통해 시스템 효율이 각각 3.22%p, 3.46%p 상승할 수 있음을 확인하였다. 따라서 본 연구에서 개발한 모델을 통해 시스템 확장성을 연구할 수 있었고, SOFC-엔진 하이브리드 시스템의 실질적 개선 및 개발 방향을 제시하여 상용화 및 효율 개선에 기여할 것으로 기대된다.

주요어: 고체산화물 연료전지, 스파크 점화 엔진, 고체산화물 연료전지-엔진 하이브리드 시스템 통합 운전, 엔진 분기율, 시스템 수준 열 전달 모델 및 분석, 시스템 스케일업

학 번: 2015-20719